BIO-FUEL PRODUCTION FROM WASTE COOKING OIL USING PYROLYSIS TECHNIQUE

BY

WARINTORN BANCHAPATTANASAKDA

A DISSERTATION SUBMITTED IN PARTIAL FULFILLMENT OF THE REQUIREMENTS FOR THE DEGREE OF DOCTOR OF PHILOSOPHY IN (ENERGY AND ENVIRONMENTAL TECHNOLOGY MANAGEMENT)
DEPARTMENT OF CHEMICAL ENGINEERING FACULTY OF ENGINEERING
THAMMASAT UNIVERSITY
ACADEMIC YEAR 2023

BIO-FUEL PRODUCTION FROM WASTE COOKING OIL USING PYROLYSIS TECHNIQUE

BY

WARINTORN BANCHAPATTANASAKDA

A DISSERTATION SUBMITTED IN PARTIAL FULFILLMENT OF THE REQUIREMENTS FOR THE DEGREE OF DOCTOR OF PHILOSOPHY IN (ENERGY AND ENVIRONMENTAL TECHNOLOGY MANAGEMENT)

DEPARTMENT OF CHEMICAL ENGINEERING FACULTY OF ENGINEERING
THAMMASAT UNIVERSITY

ACADEMIC YEAR 2023

THAMMASAT UNIVERSITY

FACULTY OF ENGINEERING

DISSERTATION

BY

WARINTORN BANCHAPATTANASAKDA

ENTITLED

BIO-FUEL PRODUCTION FROM WASTE COOKING OIL
USING PYROLYSIS TECHNIQUE

was approved as partial fulfillment of the requirements for the degree of
Doctor of Philosophy in Energy and Environmental Technology Management

on July 12, 2024

Chairman _____
(Professor Cattaleeya Pattamaprom, Ph.D.)

Member and Advisor _____
(Associate Professor Malee Santikunaporn, Ph.D.)

Member _____
(Associate Professor Channarong Asavatesanupap, Ph.D.)

Member _____
(Associate Professor Sakon Klongboonjit, Ph.D.)

Member _____
(Anurak Winitsorn, Ph.D.)

Dean _____
(Professor Sanya Mitaim, Ph.D.)

Dissertation Title	BIO-FUEL PRODUCTION FROM WASTE COOKING OIL USING PYROLYSIS TECHNIQUE
Author	Warintorn Banchapattanasakda
Degree	Doctor of Philosophy
Major Field/Faculty/University	Energy and Environmental Technology Management Faculty of Engineering Thammasat University
Dissertation Advisor	Associate Professor Malee Santikunaporn, Ph.D.
Academic Year	2023

ABSTRACT

In this study, the activated carbon (AC) was used as a catalyst in a lab-scale pyrolysis process to convert the waste cooking oil (WCO), which was produced in a large amount each year and causes many environmental issues, into more valuable hydrocarbon fuels. The pyrolysis process was performed with WCO and AC in an oxygen-free batch reactor at room pressure. The effects of process temperature and activated carbon dosage (AC to WCO ratio) on the yield and composition are discussed systematically. Direct pyrolysis experimental results showed that WCO pyrolyzed at 425 ^{o}C yielded 81.7 wt.% bio-oil. When AC was used as a catalyst, a temperature of 400°C and 1:40 AC:WCO ratio were the optimum conditions for the maximum hydrocarbon bio-oil yield of 83.5 and diesel like fuel of 45 wt.%, investigated by boiling point distribution. Compared to biodiesel and diesel properties, bio-oil has a high calorific value (40.20 kJ/g) and density at 899 kg/m^3, which are within the bio-diesel standard range, thus demonstrating potential use as a liquid bio-fuel after certain upgradation processes. To understand the effect of AC on liquid bio-oil more, the BET surface area of AC was also studied. The optimum energy conversion operating conditions were determined for liquid bio-oil production from waste cooking oil (WCO) pyrolysis using activated carbon (AC) as the catalyst. Liquid bio-oil was produced by thermo-cracking activation in the pyrolysis process using technique of response surface

methodology (RSM). The most influential factor in each experimental design response was identified by analysis of variance (ANOVA). A second-order polynomial equation was developed based on the central composite design (CCD) to correlate the variable factors for one response as the yield of liquid bio-oil. RSM based on a three-variable CCD was used to determine the impacts of process temperature (375-425 ^{o}C), proportion of AC:WCO ratio (1:40, 1:30, 1:20) and BET surface area (500-1,000 m^2/g). The optimum condition for producing liquid bio-oil with highest energy conversion from catalytic WCO pyrolysis based on RSM equation was process temperature 425 ^{o}C, AC:WCO 1:40 and BET surface area 757.58 m^2/g, giving maximum energy conversion 93.41%. While, the experiment results showed the optimum condition at 425 ^{o}C, AC:WCO 1:40 and BET surface area 1000 m^2/g, giving maximum energy conversion 88.14% with diesel-like fuel 40 wt.%. The study revealed that the major impact on yield of liquid bio-oil was determined as the process temperature, optimum AC dosage and BET surface area promoted the thermal cracking of WCO but defined as non-significant parameter on liquid bio-oil yield in terms of energy conversion.

Keywords: Pyrolysis, Waste cooking oil, Activated Carbon, Liquid bio-oil, catalysts, Response Surface Methodology

ACKNOWLEDGEMENTS

Undertaking a Ph.D. study has been a transformative and challenging journey that has spanned a significant portion of my life. Throughout this academic way, I have encountered numerous obstacles and faced the discouraging task of balancing my research alongside my permanent work commitments, with time being the most prominent hurdle. Nevertheless, I am proud to present this dissertation, which stands as a testament to the unwavering determination and support of many individuals who have been instrumental in making this achievement possible.

First and foremost, I extend my heartfelt gratitude to my advisor, Associate Professor Dr. Malee Santikunaporn, for her invaluable guidance, unwavering patience, and unyielding belief in my capabilities. Her expertise and mentorship have been indispensable in shaping this research and guiding me towards the right path.

Furthermore, I am also grateful to Associate Professor Dr. Cattaleeya Pattamaprom for serving as chairman, her thoughtful comments, encouragement, and kind guidance, together with Associate Professor Dr. Channarong Asavatesanupap, Associate Professor Dr. Sakon Klongboonjit and Dr. Anurak Winitsorn as my dissertation committee. Their constructive guidance and comments are instrumental contributions to this dissertation.

I would like to express my sincere appreciation to my lab-colleagues for providing an intellectually stimulating environment and resources that facilitated my academic growth. I also wish to thank my friends, who have been a constant source of support, motivation, and encouragement which has enriched my research journey in ways beyond measure. Furthermore, I would like to thank the Faculty of Engineering, Thammasat University for partly funding a Graduate Thesis Grant.

Finally, I would like to express my deep gratitude to my family for encouraging and supporting me in my Ph.D. study.

Warintorn Banchapattanasakda

TABLE OF CONTENTS

	Page
ABSTRACT	(1)
ACKNOWLEDGEMENTS	(3)
LIST OF TABLES	(10)
LIST OF FIGURES	(12)
LIST OF ABBREVIATION AND SYMBOLS	(15)
CHAPTER 1 INTRODUCTION	1
1.1 Backgrounds information	1
1.2 Research objectives	5
1.3 Research scope	5
CHAPTER 2 REVIEW OF LITERATURE	7
2.1 Overview of the biofuels production	7
2.1.1 First-generation (Conventional biofuels)	7
2.1.2 Second-generation (Biomass residues and waste)	8
2.1.3 Third-generation (Algae biofuels)	8
2.2 Overview of the feedstocks for biofuels production	9
2.2.1 Agricultural and industrial waste biomass	9
2.2.2 Waste cooking oil (WCO)	10
2.2.3 Algae biomass	11

2.3 Overview of the energy conversion techniques for biofuels production 11
2.3.1 Combustion 11
2.3.2 Biochemical conversion 13
2.3.2.1 Anaerobic Digestion 13
2.3.2.2 Fermentation 13
2.3.3 Thermochemical conversion 13
2.3.3.1 Pyrolysis 13
2.3.3.2 Gasification 14
2.3.3.3 Liquefaction 14
2.3.4 Transesterification 17
2.4 Pyrolysis 17
2.4.1 Pyrolysis principle 18
2.4.2 Pyrolysis classification 20
2.4.3 Pyrolysis products 21
2.4.3.1 Pyrolysis oil 21
2.4.3.2 Pyrolysis gas 21
2.4.3.3 Solids (char) 22
2.4.4 Pyrolysis reaction mechanism 22
2.4.4.1 Reaction mechanism of biomass pyrolysis 22
2.4.4.2 Reaction mechanism of triglyceride pyrolysis 23
2.5 Catalysts 25
2.5.1 Non-activated carbon catalysts 25
2.5.1.1 Zeolite catalysts 25
2.5.1.2 Silica-alumina catalysts 27
2.5.1.3 Solid-state basic catalysts 27
2.5.2 Activated carbon catalysts 27
2.6 Overview of the liquid fuel types from crude oil fractional distillation 29
2.6.1 Process of fractional distillation 29
2.6.2 Types of liquid fuel from crude oil fractional distillation 31

2.6.2.1 Light distillate fractions 31
2.6.2.2 Medium distillate fractions 31
2.6.2.3 Heavy distillate fractions 31
2.7 Overviews of response surface methodology (RSM) for experimental design 32
2.7.1 Full factorial design (FFD) 33
2.7.2 Central composite design (CCD) 35
2.7.3 Box-Behnken design (BBD) 36
2.7.4 Taguchi's contribution to experimental design 37
2.8 Literature review 38
2.8.1 Triglycerides/WCO pyrolysis over non-AC catalysts 38
2.8.2 Triglycerides/WCO pyrolysis over AC catalysts 42
2.8.3 Response surface methodology (RSM) for experimental design 46

CHAPTER 3 RESEARCH METHODOLOGY 48

3.1 The catalytic conventional pyrolysis of waste cooking oil 48
3.1.1 Materials 48
3.1.2 Catalytic pyrolysis setup 49
3.1.3 AC and WCO characterization and product analysis 51
3.1.3.1 Elemental analyzer 51
3.1.3.2 Gas chromatography-mass spectrometry (GC-MS) 52
3.1.3.3 Scanning electron microscope (SEM) 53
3.1.3.4 Fourier transform-infrared (FT–IR) spectroscopy 53
3.1.3.5 Thermogravimetric analysis (TGA) 53
3.2 The optimization of waste cooking oil catalytic pyrolysis using RSM 56
3.2.1 Materials 56
3.2.2 Design of Experiment (DOE) 56
3.2.3 Pyrolysis experiment setup and characterization techniques 59
3.3 The catalytic supercritical ethanol liquefaction of *Saccharina Japonica Seaweed* 28

3.3.1 Materials 60
3.3.2 Catalyst 60
3.3.3 Catalytic liquefaction in supercritical ethanol experiment 61
3.3.4 Design of experiment (DOE) 62
3.3.5 Heating value of bio-oil analysis 64

CHAPTER 4 CONVERSION OF WASTE COOKING OIL INTO BIO-FUEL VIA PYROLYSIS USING ACTIVATED CARBON AS A CATALYST 65

4.1 Introduction 65
4.2 Experimental setup 66
4.3 Results and discussion 51
4.3.1 Characterization of WCO as pyrolysis feedstock 67
4.3.2 Characterization of AC as a catalyst 70
4.3.3 Pyrolysis of WCO in the absence of AC 72
4.3.4 Pyrolysis of WCO in the presence of AC 76
4.3.4.1 Effect of reaction temperature and AC 76
4.3.4.2 Effect of AC:WCO ratio 77
4.3.5 The Bio-oil characteristics 82
4.3.5.1 GC-MS analysis 82
4.3.5.2 FT-IR analysis 84
4.3.6 Fuel Properties of Liquid Bio-oil 86
4.3.7 Energy recovery 90
4.4 Conclusions 90

CHAPTER 5 OPTIMIZATION AND CHARACTERIZATION OF BIO-OIL PRODUCTION FROM CATALYTIC PYROLYSIS OF WASTE COOKING OIL OVER LOW-COST CARBONACEOUS CATALYST USING RESPONSE SURFACE METHODOLOGY 92

5.1 Introduction 92
5.2 Experimental setup 94
5.3 Results and discussion 95
5.3.1 Changes in percentage compound distribution of liquid bio-oil and WCO 95
5.3.2 Experimental design and optimum condition based on RSM 97
5.3.3 Experimental design and optimum condition for energy conversion of bio-oil 97
5.3.4 Regression model, statistical analysis, and response surface contour plots of energy conversion from liquid bio-oil production 99
5.3.5 Effect of process parameters on energy conversion 101
5.3.5.1 Effect of temperature on energy conversion of bio-oil yield 101
5.3.5.2 Effect of AC:WCO ratio on energy conversion of bio-oil yield 102
5.3.5.3 Effect of BET surface area on energy conversion of bio-oil Yield 102
5.5 Liquid bio-oil characterization 104
5.5.1 GC-MS Analysis 104
5.5.2 FT-IR Analysis 105
5.5.3 Fuel properties of liquid bio-oil 107
5.5.4 GC-SIMDIS Analysis 109

CHAPTER 6 BIO-OIL PRODUCTION VIA CATALYTIC SUPERCRITICAL ETHANOL LIQUIDFACTION OF SACCHARINA JAPONICA SEAWEED 112

6.1 Introduction 112
6.2 Experimental setup 114
6.3 Results and discussion 114
6.3.1 Polynomial equation of liquefaction 114
6.3.2 Effect of process parameters on bio-oil yield 117
6.3.3 The optimized condition for maximized bio-oil production 120
6.3.4 Heating value of liquid bio-oil 121

CHAPTER 7 CONCLUSIONS AND RECOMMENDATIONS 123

7.1 Conclusions 123
7.2 Recommendations 124

REFERENCES 126

APPENDICES 144

APPENDIX A PRODUCT EXPERIMENT DATA 145
APEENDIX B WCO OIL AND BIO-OIL CHARACTERIZATION DATA 147

BIOGRAPHY 154

LIST OF TABLES

Tables		Page
2.1	Pyrolysis types and parameters	20
2.2	Boiling point ranges and carbon number ranges of different products from crude oil fractional distillation	32
2.3	Summary of triglycerides pyrolysis studies over non-AC catalyst	39
2.4	Summary of triglycerides pyrolysis studies over AC catalyst	45
3.1	Summary of pyrolysis experiment conditions	49
3.2	Analytical techniques for AC, WCO and liquid bio-oil characterization	51
3.3	Variable parameters in WCO pyrolysis experiment	58
3.4	The coefficient values of the three variables used in Minitab 17 software for the experiment 16 runs.	59
3.5	The coefficient values of the three variables used in Minitab 17 software for the experiment 15 runs.	63
4.1	Characteristics of WCO	68
4.2	FT-IR Functional group of WCO	69
4.3	Characteristics of activated carbon	70
4.4	Group of organic compounds investigated by GC-MS analysis of bio-oil	82
4.5	Fuel properties of WCO, liquid bio-oil, diesel, and biodiesel	87
5.1	Experimental design and results of the energy conversion of liquid bio-oil yields from WCO pyrolysis	98
5.2	Estimated the regression coefficients for regression model	99
5.3	ANOVA for the response surface model	101
5.4	The fuel properties of liquid bio-oil obtained at the optimum condition compared to ASTM and EN biodiesel standards	107
6.1	Experimental design and results of liquid bio-oil yields	115
6.2	ANOVA for the response surface model	116
6.3	Estimated regression coefficients for regression model	117
6.4	Heating value of liquid bio-oil	122

A-1 Product yield (% & gram), calorific value and energy conversion 145

B-1 Chromatogram peak list from GC-MS analysis of WCO 147

B-2 Chromatogram peak list from GC-MS analysis of bio-oil obtained from WCO pyrolysis at processes temperature 400 °C with 1:40 AC:WCO ratio 148

LIST OF FIGURES

Figures		Page
2.1	Diagram of the different generation of biofuels production	8
2.2	Stages in a solid biomass combustion process	12
2.3	Reaction pathways of biomass hydrothermal liquefaction	15
2.4	Pyrolysis process diagram	18
2.5	Reaction mechanisms of biomass pyrolysis	23
2.6	Reaction mechanisms of triglycerides pyrolysis	24
2.7	Basic zeolite structure	26
2.8	Pore structure of activated carbon	28
2.9	Diagram of crude oil fractional distillation	30
2.10	Example of three-dimensional response surface and contour plot Represents the interaction between temperature and biomass-to-solvent ration on green diesel yield	33
2.11	A 3^3 full factorial design for 27 points of conditions	34
2.12	A 3-level and 3-variable CCD design for 15 points of conditions	35
2.13	An experimental design of 3-level and 3-variable by Box-Behnken model	36
2.14	Taguchi design of experiment	37
3.1	Materials in this study: (a) WCO as a feedstock and (b) AC as a catalyst	49
3.2	Schematic diagram of the WCO pyrolysis experiment	50
3.3	Elemental analyzer (CHN628/O628, LECO Instruments, Thailand)	52
3.4	Gas Chromatography-Mass Spectrometer (GC-MS)	53
3.5	Thermogravimetric analysis (TGA, Mettler Toledo, Greifensee, Switzerland)	54
3.6	Bomb calorimeter (IKA C600 Global Standard Bomb Calorimeter)	55
3.7	Saccharina Japonica Seaweed as a feedstock	60
3.8	Catalytic liquefaction in supercritical ethanol experiment setup	62
3.9	Bomb Calorimeter (Parr 6400 Calorimeter)	64
4.1	FT-IR profile of WCO used in this study	69
4.2	SEM analysis of activated carbon used in this study	71

4.3	FT-IR profile of AC used in this study	71
4.4	Influence of temperature on product yields of pyrolysis reaction	72
4.5	TGA and DTG curve of WCO pyrolysis	74
4.6	Boiling temperature distribution of liquid bio-oil obtained from pyrolysis	75
4.7	Influence of reaction temperature on products yields	76
4.8	Product yields distribution obtained from pyrolysis at various AC:WCO mass ratio at the process temperature	78
4.9	Boiling temperature distribution of liquid bio-oil obtained from pyrolysis of WCO at various AC:WCO mass ratio at 350 °C	80
4.10	Boiling temperature distribution of liquid bio-oil obtained from pyrolysis of WCO at various AC:WCO mass ratio at 400 °C	81
4.11	The proposed reaction scheme for the pyrolysis of triglycerides over activated carbon	84
4.12	FT-IR spectra of liquid bio-oil obtained at the optimum operating condition	85
4.13	Energy recovery of liquid bio-oil obtained from WCO pyrolysis	91
5.1	Compounds distribution of liquid bio-oil obtained from catalytic WCO pyrolysis at various temperatures	96
5.2	Comparison between actual and predicted energy conversion from Bio-oils	100
5.3	3-D and 2-D surface response plots showing the effect of (a) temperature and AC:WCO ratio, (b) temperature and BET, and (c) BET and AC:WCO ratio on liquid bio-yield produced from WCO pyrolysis.	103
5.4	Major group of organic compositions in liquid bio-oil obtained from the optimum condition of WCO pyrolysis	106
5.5	FT-IR spectra of liquid bio-oil obtained at the optimum operating Condition	107
5.6	The fractionated compounds of liquid bio-oil according to the boiling temperature distribution by GC-SIMDIS analysis	111

6.1 3-D and 2-D surface response plots showing the effect of (a) how temperature and catalyst dosage per feedstock, (b) temperature and EtOH: feedstock, and (c) %catalyst dosage and EtOH: feedstock ratio on liquid bio-yield produced from WCO pyrolysis. 119

6.2 The optimal condition results in the highest yield of bio-oil through the Response Optimizer function 120

A-1 Bio-oil product of WCO pyrolysis at 1:40 AC:WCO ratio 146

B-1 Chromatogram profile from GC-MS analysis of WCO 148

B-2 Chromatogram profile from GC-MS analysis of bio-oil obtained from WCO pyrolysis at processes temperature 400 oC with 1:40 AC:WCO ratio 149

B-3 TGA and DTG curves of WCO 149

B-4 Simulated distillation profile of liquid bio-oil obtained from pyrolysis of WCO at 350 ^{o}C without AC 150

B-5 Simulated distillation profile of liquid bio-oil obtained from pyrolysis of WCO at 350 ^{o}C with 1:40 AC:WCO ratio 150

B-6 Simulated distillation profile of liquid bio-oil obtained from pyrolysis of WCO at 350 ^{o}C with 1:30 AC:WCO ratio 151

B-7 Simulated distillation profile of liquid bio-oil obtained from pyrolysis of WCO at 350 ^{o}C with 1:20 AC:WCO ratio 151

B-8 Simulated distillation profile of liquid bio-oil obtained from pyrolysis of WCO at 400 ^{o}C without AC 152

B-9 Simulated distillation profile of liquid bio-oil obtained from pyrolysis of WCO at 400 ^{o}C with 1:40 AC:WCO ratio 152

B-10 Simulated distillation profile of liquid bio-oil obtained from pyrolysis of WCO at 400 ^{o}C with 1:30 AC:WCO ratio 153

B-11 Simulated distillation profile of liquid bio-oil obtained from pyrolysis of WCO at 400 ^{o}C with 1:20 AC:WCO ratio 153

LIST OF ABBREVIATIONS AND SYMBOLS

Symbols/Abbreviations	Terms
℃	Degree(s) Celsius
%	Percent
AC	Activated Carbon
WCO	Waste Cooking Oil
GC-MS	Gas Chromatography-mass spectrometry
FTIR	Fourier Transform Infrared Spectroscopy
GC-SIMDIS	Gas Chromatography-Simulated Distillation
SEM	Scanning Electron Microscope
TGA	Thermogravimetric Analysis
RSM	Response Surface Methodology
CCD	Central Composite Design
BBD	Box-Behnken Design
EtOH	Ethanol

CHAPTER 1
INTRODUCTION

1.1 Background information

The demand for fossil fuels has significantly increased due to rapid industrialization, global economic growth, and population rise. However, the depletion of fossil fuel reserves has driven researchers to seek alternative sources and suitable technologies to convert them into more valuable alternative energy which have high efficiency and are environmentally friendly. One such promising option is biofuels, which are gaining popularity worldwide as they can be blended with or even replace fossil fuels (Zhang et al., 2014).

In the first period of biofuels production studies, a first-generation of biofuels, biomass residues from agricultural farming, industrial processes byproducts such as wood scraps, coffee husks, sugarcane bagasse, etc. (Lu et al., 2009) were studied the feasibility to be used as alternative sources of biofuels production. Then, a second-generation of biofuels, researchers continued to study the various types of biomasses and various methods to convert those of biomass into biofuels. Biofuels from biomass could be produced from different techniques, including combustion, biochemical conversion, and thermochemical conversion (Bridgwater, 1999). Among these technologies, pyrolysis, which is one of the thermochemical conversion techniques, is a kind of efficient biomass conversion method (Schaefer, 1975; Malkow, 2004; Abnisa et al., 2014; Zhou et al., 2017).

Biomass pyrolysis has emerged as a prominent area of research recently. This process involves heating biomass in the absence of oxygen to produce solid, liquid, and gaseous products (Kim and Kim, 2000). Pyrolysis stands out from biochemical methods due to its ability to generate a wide range of complex products, including alkanes, olefins, aromatics, alcohols, aldehydes, and acids, all within a shorter reaction time (Wang et al., 2012; Zhou et al., 2017). Despite the pyrolysis oil is an environmentally friendly biofuel, the yield of biofuels from pyrolysis remains relatively

low, typically ranging from 35% to 50% at moderate temperatures around 500°C (Khanday et al., 2016; Zhou et al., 2017). Additionally, the properties of the biofuels produced through pyrolysis are still inferior to those of fossil fuels, especially in terms of combustion efficiency. The primary issue leading to this discrepancy is the high concentration of oxygenated compounds present in pyrolysis oil. It has been observed that pyrolysis oil generally contains a significant oxygen content, typically ranging from 20% to 55% (Parihar et al., 2007; Khanday et al., 2016; Zhou et al., 2017). The elevated oxygen level contributes to a low caloric value, corrosion problems, and instability in the resulting biofuels (Lu et al., 2009).

In addition to utilizing biomass as a feedstock for biofuel production through the pyrolysis process, there has been a growing interest among researchers in investigating waste cooking oil (WCO) as an alternative feedstock. WCO holds significant potential as a valuable bioresource in the pyrolysis-based production of liquid biofuels. This interest stems from its economic viability and widespread accessibility, as it offers a cost-effective and abundant source for such biofuel production endeavors. In Thailand, WCO was approximately produced up to 580,000 ton per year (Thushari and Babel, 2022). This suggests that the generation of WCO can be considerable. However, the management of WCO is currently not conducted optimally, and there is a lack of well-defined guidelines for its proper disposal, resulting in various socioeconomic and environmental issues. Furthermore, it should be noted that these WCO feedstocks are not economically viable when compared to their use in human consumption or agricultural activities. However, their potential valorization presents an opportunity to address the environmental challenges arising from their disposal (Xu et al., 2016).

The direct utilization of WCO as fuel in a diesel engine can lead to combustion issues and air pollution, particularly the deposition of particulate matter (Graboski and Cormick, 1998). To improve the properties of these WCO and make them more like Diesel properties, various treatment methods have been suggested. Transesterification with catalyst involves converting WCO into biodiesel using alcohol, resulting in glycerol as a byproduct. However, transesterification has its drawbacks, such as high alcohol consumption, acidic biodiesel, solid content, and the need for biodiesel treatment (Demirbas, 2008). Thus, thermochemical conversion via pyrolysis

emerges as an effective solution to transform WCO into biofuels, given the abundant organic molecules with long hydrocarbon chains (fatty acids, triglycerides, and their derivatives) present in these waste materials (Chiaramonti et al., 2016).

The pyrolytic product yield and properties from waste cooking oil pyrolysis depends on various parameters such as reaction temperature, heating rate, residence time, catalysts, catalyst dosage, and inert gas flow rate (Basu, 2010). Among these, the reaction temperature and catalysts including catalyst dosage are the key parameters that affect the yield and properties of pyrolytic product especially for liquid bio-oil (Chiaramonti et al., 2016; Wang et al., 2017; Ben Hassen Trabelsi et al., 2018). This dissertation also includes a discussion of these parameters.

The catalytic pyrolysis process can be performed with low-cost catalysts such as activated carbons. From the reviews of literature, activated carbon (AC) has been extensively studied as a catalyst in biomass pyrolysis (Suprianto et al., 2021; Han et al., 2019; Aswie et al., 2021; Rangel et al., 2023) but very few in WCO pyrolysis as a catalyst (Heil et al., 2013; Chiaramonti et al., 2016). AC was found to be used as absorbent in the microwave-assisted pyrolysis of WCO. By acting as an absorber, AC facilitates the heating of triglyceride materials to attain high temperatures through microwave radiation, resulting in the production of components that can be utilized as diesel fuel (Lam et al., 2016; Lam et al., 2017; Echaroj et al., 2021). But the main limitation of AC as an absorbent in microwave pyrolysis works was the large amount of AC use about 1:1 of AC to feedstock mass ratio and could not be recovered to be reused as catalyst caused the mass amount of waste by products.

However, compared to the studies of WCO catalytic pyrolysis, there are very few reports of using AC as a catalyst. Most research has been to develop the WCO process and upgrade the bio-oil in WCO catalytic pyrolysis in using zeolites and aluminosilicates catalysts (Li et al., 2016; Ngo et al., 2010; Chiaramonti et al., 2016). In addition, AC has been studied as just a heat-transferring agent in microwave-assisted pyrolysis studies (Lam et al., 2016; Lam et al., 2017). Moreover, the primary attribute of AC is its porosity, which can augment the reactivity during the pyrolysis process. This property makes it a viable candidate for utilization as a catalyst in the conventional pyrolysis of WCO as investigated in this research.

Apart from catalytic waste cooking oil pyrolysis, which is a second-generation feedstock to produce biofuel, we are also interested in a third-generation biofuel production, particularly from seaweed. Besides being used as food, seaweed can also be converted into energy. *Saccharina Japonica Seaweed* is well known as Kombu seaweed which is the one of the Phaeophyceae (brown algae) family. Within this seaweed, two significant compounds, alginate, and fucoidan, have attracted considerable attention in the scientific community in recent years. Alginate is a linear polysaccharide abundant in free hydroxyl and carboxyl groups, while fucoidan is a sulfated polysaccharide containing fucose. These natural polysaccharides are highly valued for their potential applications in the medical and pharmaceutical fields.

Several methods exist for converting seaweed/macro-algae into bioenergy for various applications. In the past, researchers have primarily focused on biochemical conversion techniques like fermentation and anaerobic digestion to transform seaweed into bioenergy (Adam et al., 2009; Adam et al., 2011; Gurung et al., 2012). However, more recently, attention has shifted towards thermo-chemical processes such as combustion (Wang et al., 2009), pyrolysis, hydrothermal liquefaction (Anastasakis and Ross, 2011; Anastasakis et al., 2011), and gasification (Adam et al., 2011; Onwudili et al., 2013) as potential alternatives. However, to the best of our knowledge, there hasn't been any prior report on the optimization of catalytic liquefaction parameters while producing bio-oil from *Saccharina Japonica Seaweed*.

To study the influence of these process parameters on the maximum yield of bio-oil production, optimization techniques on the yield of bio-oil during pyrolysis of various feedstock materials such as Design Expert, Super Pro Designer (SPD) and Response Surface Methodology (RSM) have been reported (Abnisa et al., 2011; Abnisa et al., 2014; Mabrouki et al., 2015; Zhuang et al., 2022). Among these, RSM is a genuine simplified technique to optimize and predict the yield of different pyrolytic products as a mathematical and statistical method to evaluate interactions of multiple process parameters and analyze possible process reactions. RSM also allows selecting the optimum conditions giving highest liquid yields with a smaller dataset of experiments (Nayak and Vyas, 2019; Nayak and Vyas,2022). Analysis of variance (ANOVA) was employed to determine the significance and suitability of the model suggested by RSM.

1.2 Research objectives

1.3.1 To upgrade the WCO pyrolysis process in terms of bio-oil yield and diesel-like fuel fraction in bio-oil using AC as a catalyst to enable effective waste management with energy saving.

1.3.2 To investigate the effects and relationship of operating conditions including the reacting temperature, the catalyst dosage (AC:WCO ratio), and the BET surface area of AC on the liquid bio-oil obtained from waste cooking oil pyrolysis in terms of the yield and energy conversion based on heating value.

1.3.3 To study the effect of temperature, percentage of catalysts to feedstock, and ethanol (EtOH) per feedstock ratio on liquid bio-oil yield obtained from catalytic supercritical ethanol liquefaction of *Saccharina Japonica Seaweed*.

1.3 Research scope

In this research, we investigated the conventional pyrolysis of waste cooking oil to produce the target product which can be applied in diesel-like fuel. This work can be divided into four main parts including:

Part 1. WCO pyrolysis in the absence of AC, a lab-scale pyrolysis of WCO focuses on the investigation of the effects of the reacting temperature in the thermal pyrolysis of WCO as feedstock without catalyst to produce liquid bio-oil with diesel-like fuel fraction. These reactions were performed with various temperatures from 350 ^{o}C to 450 ^{o}C.

Part 2. WCO pyrolysis in the presence of AC, a lab-scale pyrolysis of WCO focuses on the investigation of the effects of the reacting temperature with the various catalyst dosage (AC:WCO ratio) in the thermal pyrolysis of WCO as feedstock to produce liquid bio-oil with diesel-like fuel fraction. These reactions were performed with various temperatures from 350 ^{o}C to 450 ^{o}C.

Part 3. Over the reacting temperature and AC dosage (AC:WCO ratio), the effects of the BET surface areas of AC on liquid bio-oil from WCO pyrolysis in terms of the yield and energy conversion based on the heating value were also investigated.

The relationship between the reacting temperature, AC dosage, and various BET surface areas of AC were statistical estimate and experimental designed via a central composite design (CCD) with Response Surface Methodology (RSM) by three variables factors and three levels.

Part 4. Reacting temperature, percentage of catalysts to feedstock, and EtOH per feedstock ratio in the bio-oil production via catalytic supercritical ethanol liquefaction of Saccharina Japonica Seaweed were investigated to study the relationship of those three parameters on the liquid bio-oil yield using Box-Behnken Design (BBD) with RSM to design the experiment and analyzed the effect of those parameters.

CHAPTER 2
REVIEW OF LITERATURE

This chapter presents theories, principles, and relevant literature concerning the catalytic pyrolysis of waste cooking oil. It begins by exploring energy conversion techniques, focusing on transforming biomass and waste cooking oil into biofuels or higher-value chemical compounds. Subsequently, it delves into the fundamental principles of pyrolysis techniques and reviews studies related to this dissertation.

2.1 Overview of the biofuels production

Biofuels can be produced through various methods, and the composition and yields of different products depend on the feedstock and the production processes applied. The names of the process may vary depending on the techniques used, as they have been developed over different generations. They can be broadly categorized into three major generations (Lee et al., 2019) as shown in Figure 2.1.

2.1.1 First-generation (Conventional biofuels)

This is the first period of studying biomass residues, which are left over from various processes, starting from the beginning of the production line, farming, and harvesting. There will be leftovers such as branches, leaves, or dried remains like rice straw due to the modern agricultural practices that involve increased crop rotation, resulting in leftover plant residues before continuing the production process. Then, the agricultural products that undergo industrial processes will be transformed into finished products, and there will be residues left behind. For example, wood scraps, rise husks, sugarcane bagasse, and the leftovers from the manufacturing process, some of which cannot be properly managed. Therefore, various studies have been conducted to find suitable ways to manage and utilize this biomass for beneficial purposes (Naik et al., 2010).

Figure 2.1

Diagram of the different generation of biofuels production

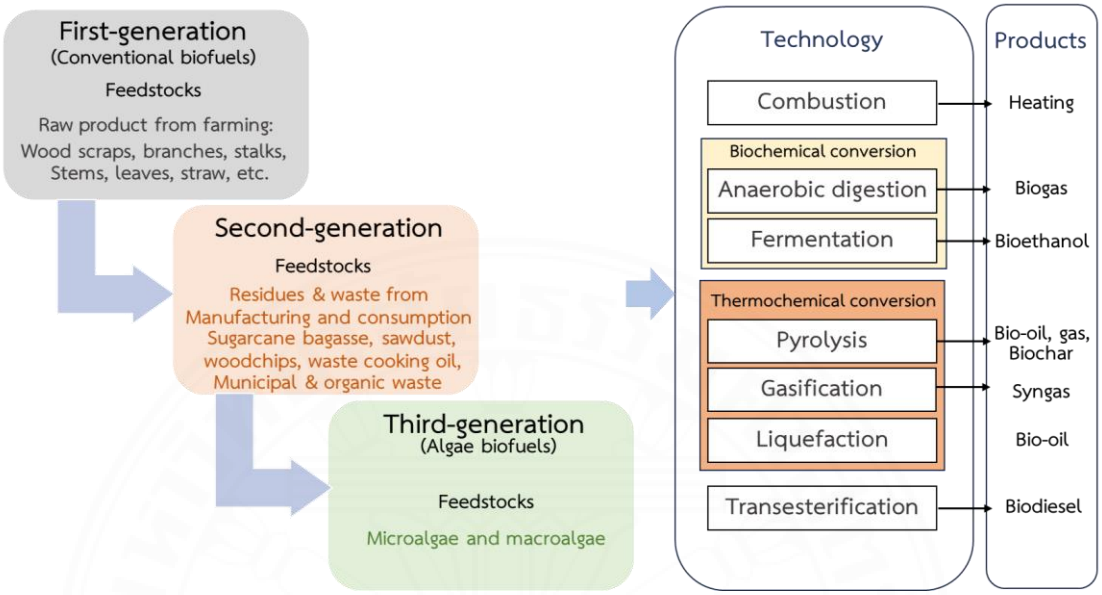

Note. Adapted from "Waste to bioenergy: a review on the recent conversion technologies," by S.Y., Lee, R., Sankaran, K.Y., Chew, C.H., Tan, R., Krishnamoorthy, D.T., Chu, and P.L. Show, 2019, *BMC Energy*, 1, 4.

2.1.2 Second-generation (Biomass residues and waste)

It is a period of continuous development until the present. Various types of biomasses, especially for wastes and residues from manufacturing and consumption have been converted into energy through various methods and products. Energy can be produced in different forms, including thermal energy, and fuels (Sims et al, 2010). The methods of converting biomass into energy include combustion, pyrolysis, gasification, liquefaction, transesterification and biochemical conversions as shown in Figure 2.1.

2.1.3 Third-generation (Algae biofuels)

This generation is the utilization of microalgae and macroalgae for biofuel production through transesterification, which is a chemical conversion of the biomass of microalgae (small algae) into biodiesel. This can be achieved by using

triglycerides of fatty acids and converting them into biodiesel, reaching up to 98% efficiency. This is an improvement from the previous method of separating biodiesel from methanol and then converting glycerol to glycerol carbonate. In the transesterification process, triglycerides will combine with monohydric alcohol using suitable catalysts, which can be acids, bases, or enzymes, to produce Fatty Acid Methyl Esters (FAME) and glycerol. This process is highly efficient, but the cost of enzymes is significantly high. The resulting glycerol, a by-product of the Transesterification process, is used in the pharmaceutical and cosmetic industries.

2.2 Overview of the feedstocks for biofuels production

Biofuels can be produced using different types of raw materials, and the quality and quantity of the resulting products are influenced by the characteristics of these materials. This review provides current information on feedstocks categorized as second and third generation for biofuel production. The main types of feedstocks discussed are agricultural and industrial waste biomass, waste cooking oil, and algae.

2.2.1 Agricultural and industrial waste biomass

In contrast to intentionally grown biomass for biofuels production, biomass residues and waste are produced incidentally as by-products during the cultivation, processing, and consumption of desired raw materials (Speight and Singh, 2014).

The remains of wood manufacturing, such as sawdust, wood chips, and unused logs produced during sawmill and lumber operations, have the potential to serve as valuable resources for the production of biofuels (Ragauskas et al., 2006). For instances, the wood residues and sawdust generated from saw and paper mills industry can be applied as boiler fuels and feedstocks for ethanol production. Moreover, transforming the cellulose, hemicellulose, and lignin present in sawdust into valuable high-added products through pyrolysis holds significant importance (Wang et al., 2017).

The straw pertains to the remains or secondary products generating from the harvesting of food crops like rice, wheat, corn, beans, cotton, and sugar crops (Zeng et al., 2007). Corn stover, comprising stalks, cobs, and leaves, has demonstrated promising capabilities in being transformed into fermentable sugars, which can be utilized for the production of bio-butanol (Qureshi et al., 2010; Cai et al., 2016).

In agricultural manufacturing, sugarcane residues, notably bagasse and leaves, present a promising option for economically utilizing residual materials in the production of bioethanol (Krishnan et al., 2010; Chandel et al., 2012) and other biofuels like biochar (Inyang et al., 2010). Palm kernel press cake, which is a byproduct of palm oil extraction, has been shown to be utilizable in the production of bioethanol using a fermentation process (Cerveró et al., 2010; Jørgensen et al., 2010). And oil palm fruit press fiber for the biofuels production by supercritical liquefaction also reported (Mazaheri et al., 2010)

2.2.2 Waste cooking oil (WCO)

Waste cooking oils (WCO) are generated by frying at temperatures ranging from 160 ^{o}C to 200 ^{o}C in households, restaurants, catering businesses and food manufacturing industries. During frying, the oil can undergo various chemical reactions such as polymerization, hydrolysis, and oxidation which possibly form many different chemical components such as a dimer, polymer, triglycerides, diglyceride, and fatty acids (Sharma et al., 2012). The production of waste cooking oil has been increasing each year throughout the world. The simple way to get rid of WCO is dumping on the ground, landfilling and even in water directly without any treatments which cause environmental and human health issues.

Since waste cooking oil is mainly composed of triglyceride, it was widely used in biodiesel production through transesterification (Lopresto et al., 2015; Ghoreishi and Moein, 2013). According to reports, the incorporation of waste oils is expected to result in a significant reduction of 60 to 90% in the production cost of biodiesel (Telebian-Kiakalaieh et al., 3013). Additionally, the high extraction expenses associated with glycerol-recovery during the transesterification process further compound the issues. (Li et al., 2016). There is no significant reported in quality

between used cooking oils and unused cooking oils. By employing basic pre-treatment techniques like filtration and heating, it is possible to eliminate water and undesired solid particles before the subsequent transesterification process (Jacobson et al., 2008). Hence, there remains a significant research focus on finding a cost-effective and productive method to convert waste cooking oil into high quality fuels.

2.2.3 Algae biomass

In an initial assessment, algae can be divided into two main groups: macroalgae, commonly known as seaweeds, and microalgae. Macroalgae refer to large, multicellular algae typically found in ponds, while microalgae are unicellular and tiny, often suspended in water-bodies. Macroalgae contain a diverse range of bioactive compounds, but they have lower potential for biofuel production compared to microalgae (Bansemir et al., 2006). Thus, microalgae offer a promising alternative as a source of oil due to their high lipid accumulation and rapid growth rates. Furthermore, microalgae have the advantage of not competing for agricultural land or large freshwater resources. Similar to biomass residues and waste, the leftover microalgae biomass can be converted into biofuels after extracting target products such as oils or other valuable compounds from the microalgae biomass.

2.3 Overview of the energy conversion techniques for biofuels production

Biofuels can be produced through various methods, and the composition and yields of different products depend on the feedstock and the production processes applied. The names of the process may vary depending on the techniques used, as they have been developed over different generations. They can be broadly categorized into three major generations.

2.3.1 Combustion

This technique is a heat dissipating reaction coupled with high temperature, heat, and light generation. This phenomenon occurs continuously as heat is generated from the reaction when using biomass as fuel. The oxidation reaction generates heat by burning carbon, hydrogen, oxygen, sulfur, and nitrogen in biomass

with oxygen, which is called combustion. The combustion process occurs through gas-phase reactions, surface reactions, or both, followed by melting, vaporization, and pyrolysis. In actual combustion, various complex phenomena take place, such as vaporization, devolatilization, diffusion, conduction, radiation, and high-temperature ignition (Sims et al., 2010; Speight and Singh, 2014). Direct combustion of fuel occurs in the gas phase as shown in Figure 2.2. Combustion can be of two types: premix combustion and diffusion combustion. Liquid fuels can be burned as gas after vaporization during gas-phase reactions. After vaporization on the surface, which is called surface combustion, solid fuels will be burned as diffusion combustion.

Figure 2.2

Stages in a solid biomass combustion process.

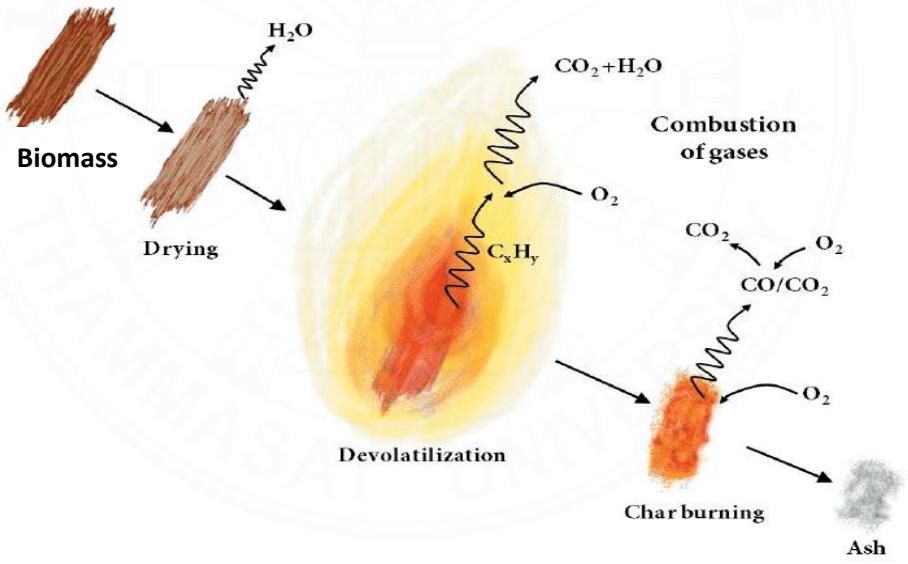

Note. From "Fate of Fuel-Bound Nitrogen and Sulfur in Biomass-Fired Industrial Boilers," by E. Vainio, 2014, Doctoral thesis, Åbo Akademi University (https://www.researchgate.net/publication/260243997)

2.3.2 Biochemical conversion

The biochemical processes can be divided into two methods:

2.3.2.1 Anaerobic Digestion

Anaerobic digestion is a process of decomposing organic substances in the absence of air or oxygen. It involves the fermentation of waste materials in the form of liquids, resulting in biogas production. Biogas contains mainly methane (CH_4) and carbon dioxide (CO_2) (Cantrell et al., 2008).

2.3.2.2 Fermentation

Fermentation is a process that converts complex organic molecules, such as starch, sucrose, and cellulose from agricultural crops like sugarcane, cassava, corn, sweet sorghum, sugarcane bagasse, and agricultural residues like rice straw, sugarcane leaves, corn stalks, rice bran, sawdust, paper waste, and wood shavings, into simpler molecules. This process is carried out by microorganisms like yeast and fungi and results in the production of alcohol, which can be used as fuel in gasoline engines (Naik et al., 2010; John, et al., 2011).

2.3.3 Thermochemical conversion

Thermochemical conversion is the process of transforming heat into chemical changes. It involves converting biomass through processes of decomposition, breaking down biomass and reforming of organic matter into biochar (solid), synthesis gas and highly oxygenated bio-oil (liquid). Thermochemical conversion can be categorized into three sub-processes: pyrolysis, which involves burning without oxygen; gasification, which converts biomass into gas or syngas; and liquefaction.

2.3.3.1 Pyrolysis

Pyrolysis is a thermal chemical process. When biomass encounters a hot environment, it undergoes decomposition and transforms into combustible gas and char. Pyrolysis is the process of breaking down high-molecular-weight substances through a heat-driven reaction. This occurs in the absence of air at temperatures ranging from 450 to 600 $^{\circ}C$ (Dhyani and Bhaskar, 2018). The pyrolysis products are gas, solid, and liquid. The gas composition includes methane (CH_4) to

propane (C_4H_{10}), while the liquid portion, commonly referred to as bio-oil, has similar properties to heavy oil (Chiaramonti et al., 2016). The liquid portion is the most desired product from the process. As for the solid component, it is charcoal (char), a fine powder of small-sized carbon molecules produced from the decomposition reaction. The ratio of the products depends on the temperature, heat input rate, feedstock rate, and the type of feedstock introduced into the process.

2.3.3.2 Gasification

Gasification is a technology that converts biomass into energy in the form of fuel gases, using the thermal chemical process of combusting fuel in a limited oxygen environment to create a controlled condition with less oxygen than required for complete combustion. This process breaks down the biomass into hydrocarbon compounds, both in solid and gas forms, which include carbon monoxide (CO), hydrogen (H_2), methane (CH_4), carbon dioxide (CO_2), nitrogen (N_2), and other gases (Ahmad et al., 2016). This resulting gas mixture is called producer gas. The gasification process of biomass is an incomplete combustion process, making the chemical reactions complex and resulting in various types of products or gases depending on the type of biomass and other factors. The products obtained from this process include fuel gases, solid char, ash, tar, and non-combustible impurities.

2.3.3.3 Liquefaction

Liquefaction is the process of transforming a substance into a liquid state by breaking down the molecular structure of biomass through heat and using a liquid solvent such as water or other solvents to produce bio-oil. During the liquefaction of biomass, the biomass is converted into stable liquid hydrocarbon compounds under controlled temperature and pressure conditions, and hydrogen gas may be used as a catalyst in the process.

(1) Hydrothermal liquefaction

This is a process that utilizes high-temperature and high-pressure conditions ranging from 250 to 374 $^{\circ}C$ and 4 to 22 MPa (Diitriadis and Bezergianni, 2016). The significant advantage of hydrothermal conversion is that it doesn't require a drying process for the starting materials, allowing it to be used with high-moisture content feedstocks such as biomass, waste, organic residues, and others.

In hydrothermal biomass conversion, the biomass is transformed into solid products called biochar, liquid products known as bio-oil, and gas products by controlling variables like reaction temperature, reaction time, and pressure in the process.

Moreover, various reactions can occur at different temperatures. The reaction that occurs in a system with high pressure and temperature, approximately 100 °C, can dissolve substances in the system, suitable for the extraction of materials above the temperature of 150 °C (Diitriadis and Bezergianni, 2016). Hydrolysis and biomass materials such as cellulose, hemi-cellulose, proteins, and others will be degraded from polymers into monomers at temperatures around 200°C and a pressure of 1 MPa. The biomass materials will be treated to become a slurry at approximately 300 °C and a pressure of 10 MPa (Kumar and Gupta, 2008). Under certain reaction conditions, the reaction time, and the main products will also undergo changes. Hydrothermal liquefaction involves both decomposition and polymerization reactions as shown in Figure 2.3. In the initial step, biomass is decomposed into liquid substances. These liquid substances then undergo polymerization to form biochar. With prolonged reaction times, the biochar formed further transforms into graphite (Kumar and Gupta, 2008).

Figure 2.3

Reaction pathways of biomass hydrothermal liquefaction

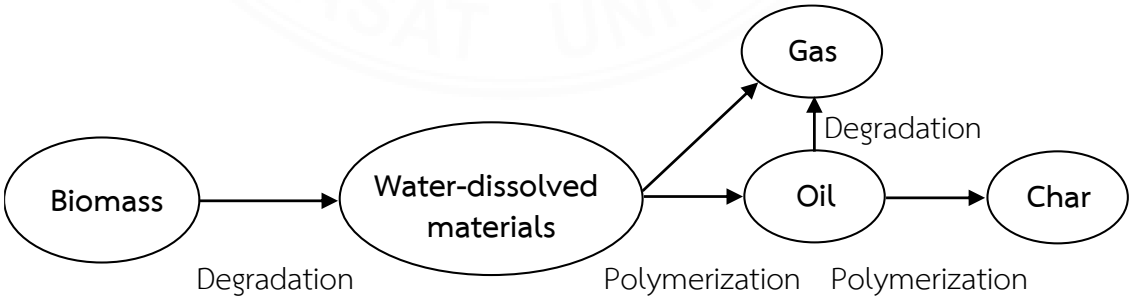

Note. Adapted from "An overview of OPS from oil palm industry as feedstock for bio-oil production," by S.S. Qureshi, S. Nizamuddin, H.A. Baloch, M.T.H. Siddiqui, N.M. Mubarak, and G.J. Griffin, 2019, *Biomass Conversion and Biorefinery*, 9, 827-841.

(2) Supercritical liquefaction

Supercritical liquefaction refers to an extraction method employing supercritical carbon dioxide as the solvent. This technique is highly beneficial for enhancing yield and selectivity when extracting organic compounds from plants (Azevedo et al., 2008). Supercritical liquefaction offers several advantages over conventional extraction techniques. These benefits encompass enhanced selectivity, reduced processing duration, and the utilization of non-toxic solvents. Other supercritical solvents suitable for the process include ethanol, methanol, propanol, and acetone. Once these solvents reach the supercritical state, their hydrogen bonds significantly decrease, resulting in reduced polarity and dielectric constant. This change enables the solvent molecules to act as independent monomers. Consequently, these supercritical solvents have the ability to homogeneously dissolve non-polar triglycerides, leading to the production of diglycerides in a uniform liquid phase (Lee et al., 2019).

Supercritical alcohols, including supercritical methanol, have displayed promising outcomes in biodiesel production. By adjusting temperature and pressure, the solvent polarity of these supercritical fluids can be controlled. Under supercritical conditions, the hydrogen bond network in methanol breaks, promoting a stronger direct nucleophilic attack by methanol on the carbonyl group. Additionally, the dielectric constant of methanol decreases in the supercritical state, leading to an accelerated reaction rate (Hoang et al., 2013; Lee et al., 2019). However, the choice of alcohol is crucial in assessing both cost and performance. Ethanol, obtained easily from agricultural renewable feedstock, is preferred over methanol. Ethanol exhibits higher dissolving power for oils and is better suited for the transesterification of vegetable oils. Moreover, alcohols with higher or branched structures can produce fuels with improved properties. The extra carbon atom provided by ethanol results in a slight increase in heat content and cetane number (Hoang et al., 2013; Lee et al., 2019).

2.3.4 Transesterification

Producing biofuels from potential biomass, particularly cellulosic biomass, presents a more intricate process as the extracted oil must be tailored to match the properties of hydrocarbon-based fuels. The main challenge lies in efficiently converting the oils and fats obtained from these biomasses into suitable biofuels, which can effectively replace conventional fuels. Biomass-derived biofuels, like those from lignocellulosic materials, often encounter issues with high viscosity, low energy content, and polyunsaturated characteristics. To address these challenges, various pretreatment methods can be employed, with transesterification being the most promising approach. Transesterification is a reaction that converts fats and oils into esters and glycerol in the presence of catalysts (Lee et al., 2019). The resulting fatty acid methyl ester (FAME) exhibits physical properties comparable to commercial petroleum fuels, making it a suitable substitute. Additionally, the by-product glycerol holds commercial value, further enhancing the economic viability of the process.

The Transesterification process with the most potential for biodiesel production uses algal species such as Spirogyra and Oedigonium (Hossain et al., 2008), with small-sized microalgae. They can achieve a high FAME conversion rate of up to 90% (Hossain et al., 2008; Khan et al., 2017) when using aliphatic alcohol as a catalyst. The Transesterification process can be carried out in two ways: Transesterification from an external source of triglycerides and Transesterification within the microalgae source itself or in situ.

2.4 Pyrolysis

Pyrolysis techniques have been considered as an economic and environmentally friendly treatment process for many kinds of wastes because they have the potential to recover the energy and generate valuable products (oil and gas) which can be used as a feedstock in the petroleum refinery and petrochemical industries. Also, the solid char produced can be utilized as a substitute for activated carbon (Kim and Kim, 2000).

2.4.1 Pyrolysis principle

Pyrolysis is a thermal process where the raw material is degraded under high temperatures (250 °C-700 °C) together with an absence of oxygen condition. This reaction changes the chemical composition and physical properties into three different types of end products including liquids (oil), gases and solids (char) (Qi et al., 2007; Naves et al., 2011; Lee et al., 2019) which can be illustrated in Figure 2.1.

Figure 2.4

Pyrolysis process diagram

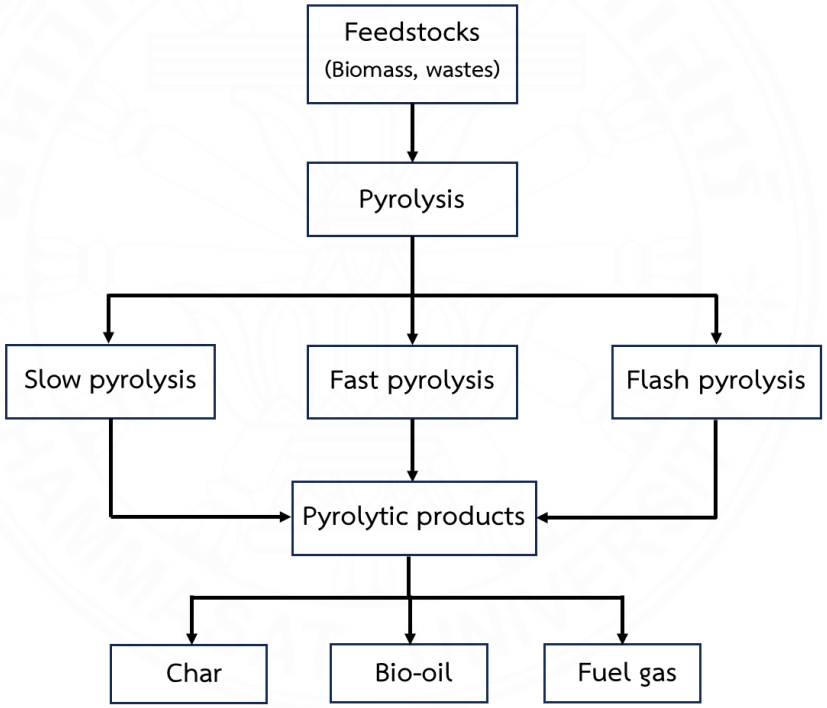

Note. Adapted from "*Waste to bioenergy: a review on the recent conversion technologies*," by S.Y. Lee, R. Sankaran, K.W. Chew, C.H. Tan, R. Krishnamoorthy, D.T. Chu, and P.L. Show, 2019, BMC Energy, 1, 4.

The product of pyrolysis varies based on the thermal conditions and the desired temperature. At low temperatures, below 450 °C with gradual heating, the primary result is bio-char. However, at high temperatures exceeding 800 °C with fast

heating rates, the main output is gases. When intermediate temperatures and relatively high heating rates are applied, the predominant product is bio-oil.

The pyrolysis of waste cooking oil and biomass results in three primary products: bio-char or residue, bio-oil, and gas, all of which have wide-ranging applications as energy sources. Bio-char, a solid carbon-rich by-product created through the thermal stabilization of biomass or organic matter, possesses considerable energy content, comparable to coal used as fuel in industries. Its high carbon content makes it valuable for various industrial uses. In agriculture, bio-char serves as a soil amendment, enhancing plant growth yield by increasing available nutrients, water retention, and reducing the need for fertilizers, preventing nutrient leaching. Additionally, it curtails methane and nitrous oxide emissions from soil, thereby contributing to reduced greenhouse gas (GHG) emissions. Moreover, pyrolysis bio-char can be utilized as an energy source due to its high heating value (Sanahuja-Parejo et al., 2018). As for bio-oil produced during the pyrolysis process, it serves as an excellent feedstock for power generation, as it contains high energy, comparable to fossil fuels when upgraded (Tripathi et al., 2016). Alternatively, the bio-oil can be upgraded to a specialized engine fuel or converted through gasification processes into syngas and then further processed into biodiesel or bio-fuel (Bok et al., 2012; Kader et al., 2013; Soysa et al., 2015).

For the pyrolysis reaction, it can be concluded that there are two stages in the process including primary pyrolysis and secondary pyrolysis (Conesa et al., 1998). The primary pyrolysis involves the devolatilization, dehydration, dehydrogenation, or decarboxylation reactions of the waste materials where different reaction zones can appear conforming to the thermal decomposition of the Mai dehydrogenation, for example, biomass is generally decomposed during the primary stage to form solid char at 200–400^{o}C, which is the largest degradation of biomass (Fisher et al., 2002). For secondary pyrolysis, it mainly comprises of the decomposition reaction of the solid components such as thermal or catalytic cracking where heavy compounds are broken into gases, while char residue is also converted into gases.

In previous pyrolysis research field, the heating source for pyrolysis process has been conducted by a conventional heating source, for example, electrical gas heater, blast furnace in tubular or fixed bed reactor which is well known as conventional pyrolysis. In this type of pyrolysis technique, the thermal energy will be applied to the reactor from the outside and heats all the materials in the reactor. In this technique, thermal energy is not focused on the materials directly but loss to the environment which causes the inefficient performance of the pyrolysis process.

2.4.2 Pyrolysis classification

Basically, the pyrolysis process can be classified into three types: slow, fast, and flash pyrolysis, which depend on several factors such as heating rate, residence time, reaction temperature, raw material feed rate and others. In most cases, slow pyrolysis is conducted in a temperature range of 250-600 °C whereas 500-700 °C and 750-1100 °C for fast and flash pyrolysis *(Onwudili et al., 2009)*, respectively as shown in Table 2.1.

Table 2.1

Pyrolysis types and parameters

Pyrolysis Type	Residence time (s)	Heating rate (°C/s)	Temperature (°C)	Products
Slow	450-550	0.1-1	250-650	Solids (Char)
Fast	0.5-10	10-200	500-700	Liquids, gases
Flash	<0.5	>1000	750-1100	Liquids, gases

From Table 2.1, it can be noticed that the products from the pyrolysis process can be designed by controlling parameters while conducting the process such as temperature, heating rate and residence time (Onwudili, 2002). For example, a high temperature and extremely high heating rate with low residence time called flash pyrolysis leads to increase the liquid or oil yield while the fast pyrolysis which conducted under the moderate temperature and residence time results in elevated yield of gas products, whereas, if solid or char yield is most required a low temperature

and heating rate with high residence time is needed for pyrolysis process (slow pyrolysis) (Dominguez et al., 2007).

2.4.3 Pyrolysis products

The products from the pyrolysis process can be divided into three products including oil, gas, and char, all of them have the potential to be improved for further use especially in the petroleum refinery process. Each product, the yields, and characteristics can vary depending upon the type of feedstock and the pyrolysis conducting conditions.

2.4.3.1 Pyrolysis oil

Pyrolysis oil is a primary product of interest from the process which is a complex mixture of organic compounds and sometimes together with inorganic components. In order to get the high yield of oil fraction, fast or flash pyrolysis is the optimum condition for the process (Bridgwater and Peacocke, 2000). The fast pyrolysis of biomass conducting with a medium temperature in the range of 450-650oC and very short residence time (0.5-10 seconds), oil fraction (bio-oils) is found to be a major fraction about 50-70 wt% and 13-16 wt% and 14-37 wt% for gas and char, respectively (Bridgwater, 1999; Isahak et al., 2012). The pyrolysis oil products can be used in many kinds of industries such as power plants, additives in chemical production, binder, diesel engine fuel etc (Fernandez et al., 2011). But bio-oil fraction from biomass pyrolysis consists of highly oxygenated compounds and are not in a stable condition to be used as fuels directly (Demirbas, 2002). Hence, the upgrading and removing of any residues from the bio-oil products is needed.

2.4.3.2 Pyrolysis gas

The gas fraction released in a pyrolysis process primarily consists of combustible gases, including carbon monoxide (CO), carbon dioxide (CO_2), hydrogen (H_2), methane (CH_4), ethane (C_2H_6), ethylene (C_2H_4), propane (C_3H_8), ammonia (NH_3) and other pollutant gases, such as nitrogen oxides (NO_x) and sulphur oxides (SO_x), etc (Kan et al., 2016). Practically, the gas yield of pyrolysis process would be increased when the reaction temperature is raised because of the heavy compounds thermal cracking (Dominguez et al., 2008). Besides, the increasing of heating rates also

influences the acceleration of gas yield production (Menendez et al., 2007). In some applications, the pyrolysis gas can be used as a fuel directly i.e., direct burning in boilers for heat production and for electricity generation in the gas turbine process (Motasemi and Muhammad, 2013). And in some applications, for example, syngas production process, the pyrolysis gas which contains H_2 and CO might be separated prior to the process.

Pyrolysis char is a carbonaceous residue mainly consisting of elemental carbon generated from the pyrolysis process which must be focused on. Because it contains the mineral content of the original feed material, relevant to specific catalytic processes (Raveendran et al., 2013). The importance of the char cannot be understated as it may be involved as a reactive in heterogeneous or catalytic heterogeneous reactions (Menendez et al., 2007). Solid char can be used in many industries such as solid fuel for boilers directly and can be a feedstock to produce activated carbon and make carbon nanofilaments. In some applications, solid char can be used as a catalyst in the chemical reaction for the electrochemical process (Fernandez et al, 2011).

2.4.4 Pyrolysis reaction mechanism

2.4.4.1 Reaction mechanism of biomass pyrolysis

Figure 2.5 illustrates the reaction mechanism of catalytic pyrolysis of three main components of woody biomass (cellulose, hemicellulose and lignin) proposed by Zadeh et al., (2020). The literature has extensively investigated the pathway of catalytic pyrolysis for cellulose, and findings indicate that cellulose was predominantly transformed into anhydrosugars and other light substances like acetal, gas, char, and coke (Saraeian et al., 2019; Stephanidis et al., 2011). In the case of lignin catalytic fast pyrolysis (CFP), outcomes have demonstrated diminished liquid and gas yields but elevated char production. To elaborate, during the initial stages, lignin underwent decomposition resulting in oxygenate compounds like phenol, achieved through the cleavage of **β**–O–4, **α**–O–4 bonds as well as other C-C and C-O bonds Zadeh et al., (2020). This was succeeded by the re-polymerization of lignin leading to

the formation of char. The creation of aromatic compounds ensued through a sequence of reactions encompassing dehydration, decarboxylation, decarbonylation, and oligomerization (Nguyen et al., 2013). A multitude of researchers have explored the catalytic pyrolysis pathway for hemicellulose, focusing on xylan decomposition due to its abundance within cellulose. Predominant compounds arising from the catalytic pyrolysis of hemicellulose comprise furan compounds (Carlson et al., 2011).

Figure 2.5

Reaction mechanisms of biomass pyrolysis

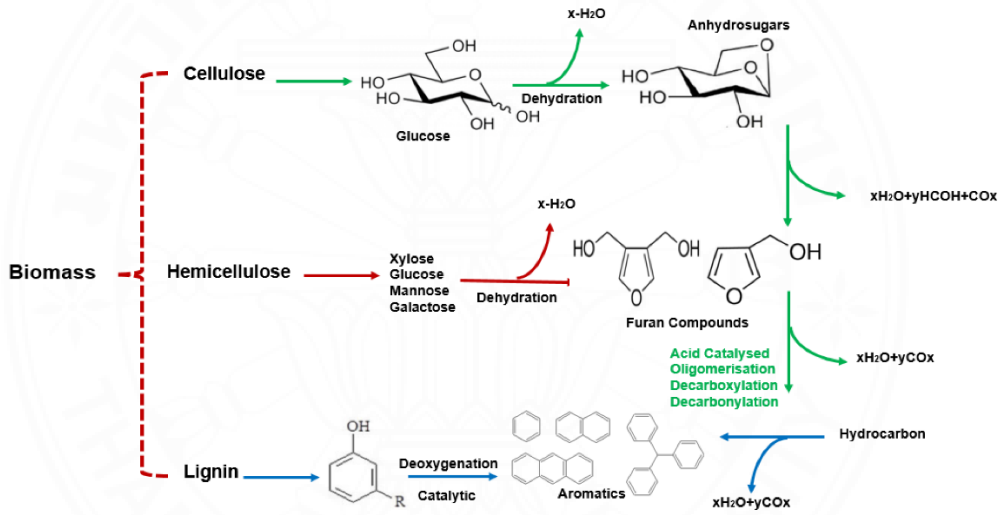

Note. From "*Recent insights into lignocellulosic biomass pyrolysis: A critical review on pretreatment, characterization, and products upgrading*," by Z.E. Zadeh, A. Abdulkhani, O. Aboelazayem, and B. Saha, 2020, Processes, 8(7), 799.

2.4.4.2 Reaction mechanism of triglyceride pyrolysis

Since the pyrolysis process in triglyceride involves many highly complex organic reactions, there is no definite solution to the resulting reactions that will be obtained in each execution. Figure 2.6 presents the reaction scheme for triglyceride pyrolysis proposed by Wiggers et al. (2017). The process (1) begins with the breakdown of the triglyceride molecule, yielding heavily oxygenated hydrocarbons. Some of the resulting saturated fatty acids may remain unchanged without further

reactions. (2) Decarboxylation and decarbonylation reactions are promoted by unsaturated compounds and compete with the cleavage of C-C bonds (3). The deoxygenation reactions in (2) and (4) produce CO and CO_2. Isomerization, polymerization, dehydrogenation, and cyclization are responsible for the formation of dienes, acetylenes, cycloparaffins, and polyolefins (5). Additionally, the Diels-Alder addition of dienes to olefins generates cyclo-olefins (8) and releases hydrogen. The hydrogenation of cyclo-olefins to cycloparaffins and the reverse reaction occurs in steps (6) and (7). Hydrogen is also produced in steps (9) and (10). The solid product coke is directly produced from triglycerides (12) through the polycondensation of heavy hydrocarbons, saturated fatty acids (11), and aromatics (10). Furthermore, the polymerization of olefins can also lead to the formation of coke (13) Wiggers et al. (2017).

Figure 2.6

Reaction mechanisms of triglycerides pyrolysis

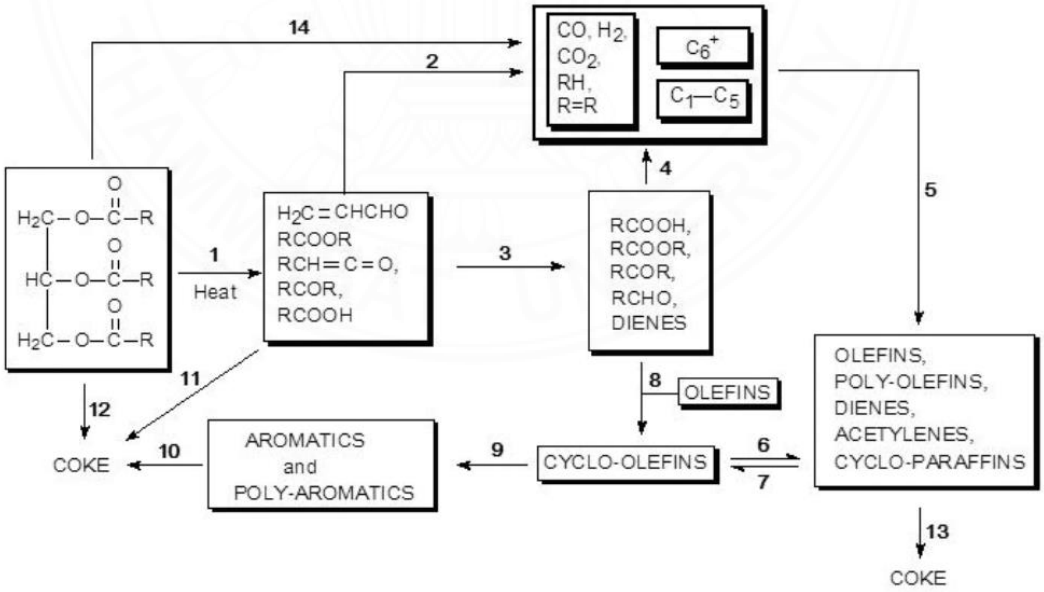

Note. From "Renewable Hydrocarbons from Triglyceride's Thermal Cracking," by V.R. Wiggers, R.F. Beims, L.E. Ender, E.L. Simionatto, and H.F. Meier. 2017, In Jacob-Lopes, E. & Zepka, L.Q. (Eds.), Frontiers in Bioenergy and Biofuels (pp. 407-424). Intech Open. https://doi.org/10.5772/65498

2.5 Catalysts

Catalyst is a substance that modifies the speed of a chemical reaction without undergoing any chemical changes itself. While most catalysts accelerate the rate of chemical reactions, there are some that decelerate the reaction rate. Positive catalysts, also known as promoters, are the most common type of catalysts and speed up chemical reactions. On the other hand, negative catalysts, referred to as inhibitors, slow down chemical reactions. In this section, we divide into two parts: non-activated carbon and activated carbon catalysts.

2.5.1 Non-activated carbon catalysts

From the previous research, there are 3 major types of catalysts that are used in the catalytic pyrolysis process including zeolite-form catalysts, silica-alumina catalysts, and solid-state basic catalysts. In addition to the three main types of catalysts mentioned earlier, there is an increasing focus on the use of carbonaceous materials as catalysts in the pyrolysis process. The utilization of carbonaceous materials with a high surface area, such as activated carbon, as a catalyst in pyrolysis, has not been extensively documented. Activated carbon is a type of carbonaceous material that possesses a porous structure and excellent adsorption properties. It is primarily composed of carbon atoms and exhibits a complex arrangement of pores within a rigid framework of disordered carbon layers. Activated carbons can be derived from various sources, including coconut shells, peat, hard and soft wood, lignite coal, bituminous coal, olive pits, biomass, and other carbon-rich materials. The production of activated carbon from these raw materials typically involves chemical activation or high-temperature steam activation mechanisms.

2.5.1.1 Zeolite catalysts

Zeolite catalysts are crystalline alumino-silicates with a molecular sieve structure. They consist of a three-dimensional framework composed of eight tetrahedrally coordinated silicon (or aluminum) atoms and eight oxygen atoms (Chiaramonti et al., 2016). This framework contains large open pores and channels that can accommodate cations, as illustrated in Figure 2.7. The key features of these

catalysts are their ion exchange capabilities and the presence of open pores. Zeolites exhibit remarkable stability as solids, being resistant to temperatures exceeding 1,000°C, high pressures, and they do not dissolve in water or other inorganic solvents. Additionally, they do not undergo oxidation in the presence of air.

Figure 2.7

Basic zeolite structure

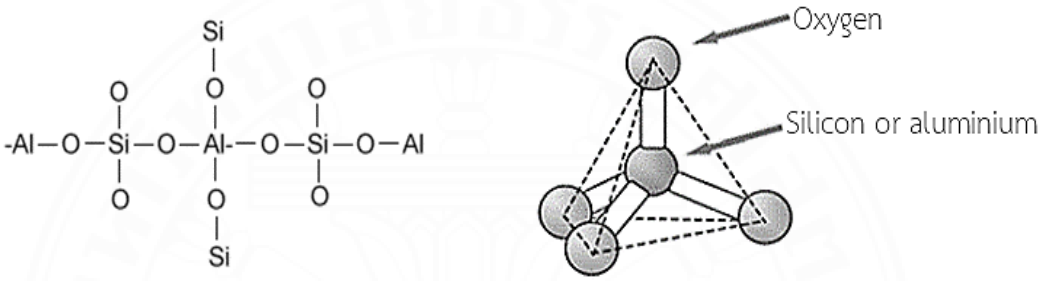

Note. From "Synthesis zeolites-structure, classification, current trends in zeolite synthesis," by D. Geogiev, B. Bogdanov, K. Angelova, I. Markovska, and Y. Hristov. 2009, [Paper presentation]. International Science Conference. Stara Zagora, Prof. Dr. Assen Zlatarov University, Bulgaria, June 4-5, 2009).

Zeolites can be categorized into two primary types: natural zeolites and synthetic zeolites. Natural zeolites comprise approximately 40 different types, with the most commonly utilized ones being chabazite, clinoptilolite, and mordenite. Synthetic zeolites, on the other hand, are specifically designed to meet particular requirements. Among the well-known synthetic zeolites are zeolite A, often used in laundry detergents, and zeolites X and Y, which belong to the Faujasite family and are utilized in catalytic cracking processes. One of the most commonly employed zeolites as a catalyst in pyrolysis is H-ZSM5, extensively utilized in the petrochemical industry for its high selectivity in hydrocarbon isomerization reactions. The intriguing feature of zeolites lies in their porous structure, resembling a cage. Within this structure, numerous pores of fixed sizes and shapes act as millions of tiny test tubes, effectively trapping shape-selective hydrocarbon molecules. Chemical reactions occur readily

within these confined spaces, leading to the breakdown of large hydrocarbon molecules into various products such as gasoline, diesel, kerosene, and waxes.

Zeolite catalysts play a crucial role in pyrolysis by affecting the stability of bio-oil's chemical compositions and the properties of fuels produced from triglyceride pyrolysis. The level of acidity in zeolites, determined by the Si/Al ratio, is responsible for reducing the oxygen content in bio-oil, thereby enhancing its energy density.

2.5.1.2 Silica-alumina catalysts

Silica-alumina catalysts known as amorphous catalysts (Chiaramonti et al., 2016) possess Lewis acid sites, which act as electron acceptors, as well as Bronsted acid sites that contain ionizable hydrogen atoms. The acidity of these catalysts plays a significant role in influencing the generation of liquid oil during the pyrolysis process. Among these catalysts, MCM-41 is a commonly utilized catalyst in pyrolysis.

2.5.1.3 Solid-state basic catalysts

Solid-state basic catalysts refer to amorphous catalysts that possess larger pore sizes and lower surface areas compared to zeolites and aluminosilicate catalysts like calcium oxide and magnesium oxide. These catalysts can effectively inhibit the formation of stable chemical structures in products and weaken C-C bonds through an oxygen transfer mechanism. Consequently, they reduce the activation energy required for the complex pyrolysis reaction (Chiaramonti et al., 2016).

2.5.2 Activated carbon catalysts

In addition to the three main types of catalysts mentioned earlier, there is a growing focus on carbonaceous materials as catalysts in the pyrolysis process. The use of carbonaceous materials with a high surface area, such as activated carbon, as catalysts in pyrolysis has not been extensively documented. Activated carbon is a type of carbonaceous material that possesses a highly porous and adsorptive structure consisting primarily of carbon atoms. The porous network within activated carbons comprises channels formed within a rigid framework of unordered carbon atom layers. Activated carbons can be derived from various raw materials, including coconut shells,

peat, hard and soft wood, lignite coal, bituminous coal, olive pits, biomass, and other carbonaceous sources. The production of activated carbons from these raw materials involves chemical activation or high-temperature steam activation mechanisms.

Activated carbon primarily serves the purpose of adsorption, where it captures atoms, ions, and small molecules (referred to as adsorbates) from gases, liquids, or solutions by drawing them into its porous structure, as depicted in Figure 2.8. The porosity of activated carbon enables a substantial surface area for effective adsorption. This process transpires within pores that are marginally bigger than the molecules being adsorbed. Essentially, there are two classifications of adsorption: physical adsorption and chemical adsorption.

The primary characteristic of activated carbon is its distribution of pore sizes, which varies for each carbon type. These pores are categorized as micropores (with a radius less than 1 nm), mesopores (with a radius between 1 nm and 25 nm), and macropores (with a radius greater than 25 nm). It is crucial to select an activated carbon with a pore size that aligns with the size of the molecule we aim to adsorb, emphasizing the significance of this matching process.

Figure 2.8

Pore structure of activated carbon

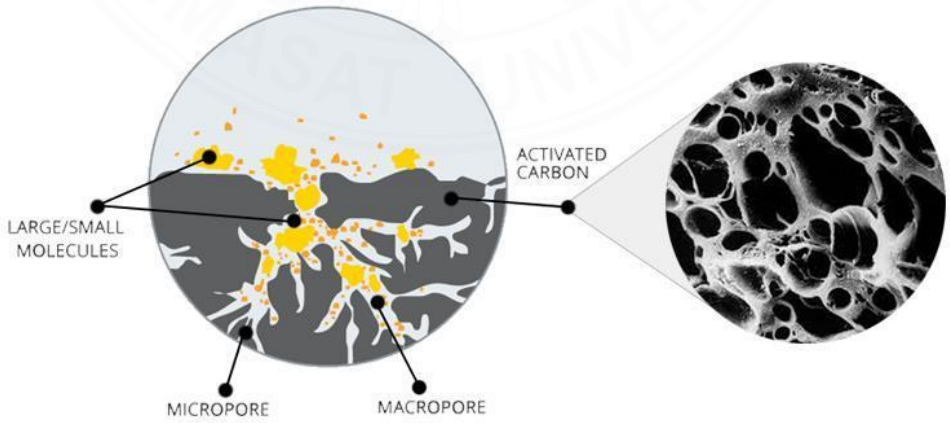

Note. From "Functionalized Metal-Organic Frameworks as Selective Metal Adsorbents," by D.D. Jeroen, 2017 Doctoral dissertation, Ghent University. (https://www.researchgate.net/publication/317577477)

Additionally, in the process of triglyceride pyrolysis, activated carbon has been utilized as a substance to absorb and transfer heat to materials that do not readily absorb microwaves. This allows for the attainment of high temperatures through microwave heating. Activated carbon serves as both an intermediary for energy transfer, enabling the heating of triglyceride materials, and a catalyst for the pyrolysis of triglycerides, resulting in the production of components suitable for diesel fuel.

2.6 Overview of the liquid fuel types from crude oil fractional distillation

Fractional distillation involves the separation of crude oil into various hydrocarbon products of greater utility, based on their differing molecular weights, within a distillation tower at oil refineries. This marks the primary stage in crude oil processing, serving as the fundamental separation method that initiates the differentiation of distinct fuels (Kraushaar and Ristinen, 2006). The components segregated in this procedure are termed "fractions," encompassing gasoline, kerosene, diesel, kerosene, and fuel oil among others. Through fractional distillation, a diverse array of valuable products can be derived from crude oil, but the utilization of these beneficial products carries significant environmental implications.

2.6.1 Process of fractional distillation

The concept of fractional distillation is relatively straightforward, yet it holds significant potency in its ability to segregate the various intricate constituents of crude oil. Initially, the crude oil undergoes heating to transform it into vapor, which is then introduced into the lower section of a distillation tower. Subsequently, the resulting vapor ascends within the vertical column. During this ascent, the temperature progressively declines, causing specific hydrocarbons to undergo condensation and drain away at distinct levels. Each condensed fraction, located at a particular tier, encompasses hydrocarbon molecules with a comparable count of carbon atoms. These separations based on boiling points facilitate the simultaneous isolation of multiple hydrocarbons (Boyle et al., 2012). The process of separation is enabled by the cooling effect that correlates with the tower's height as shown in Figure 2.9.

Figure 2.9

Diagram of crude oil fractional distillation

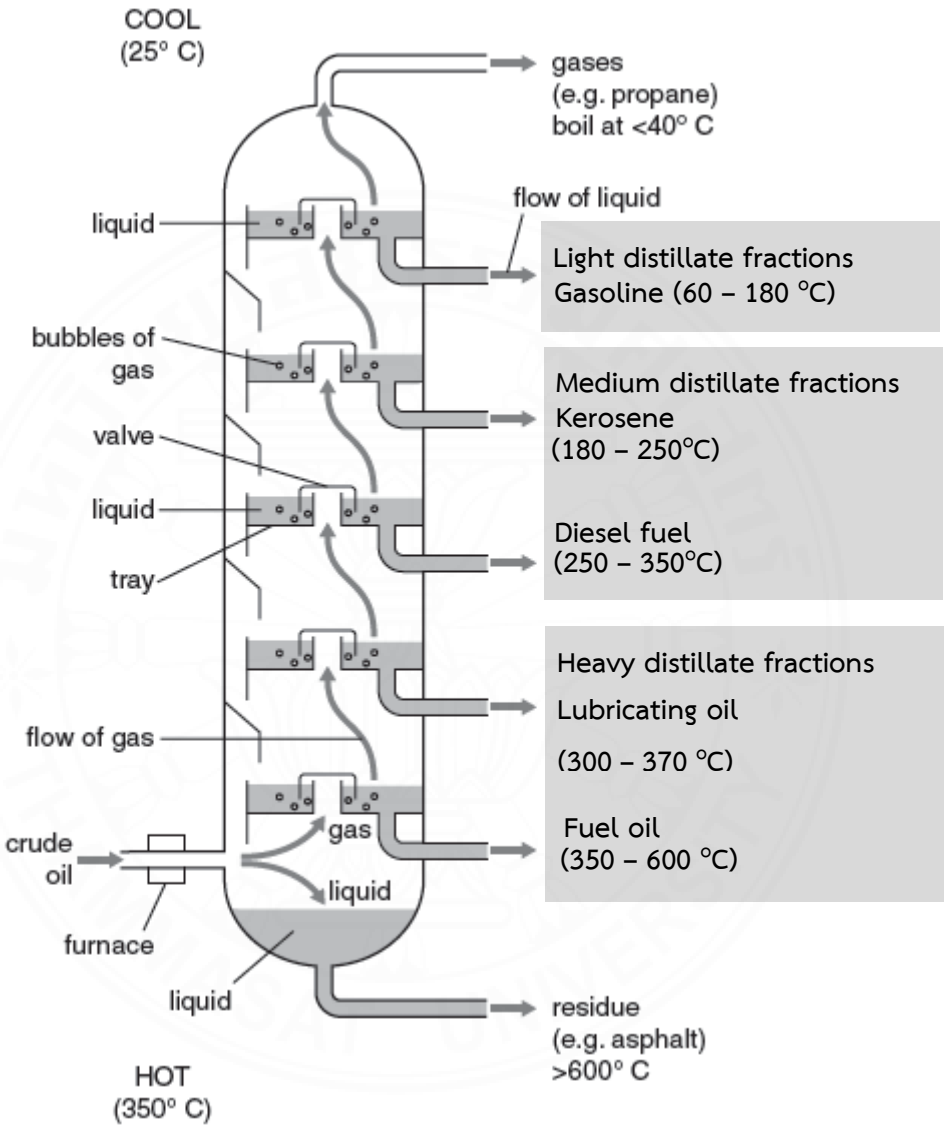

Note. Adapted from "Distillation process of crude oil," by A. Ashraf, 2012 Bachelor Thesis, Qatar University (https://www.researchgate.net/publication/261551891)

2.6.2 Types of liquid fuel from crude oil fractional distillation

There are multiple methods to categorize the valuable components obtained through distillation of crude oil. One common approach involves dividing them into three main groups: light, intermediate, and heavy fractions in accordance with the boiling point range distributions (Ashraf, 2012). The heavier elements are collected at the lower end of the distillation column due to their tendency to condense at higher temperatures. On the other hand, the lighter fractions ascend the column and are cooled until they reach their condensation point, which permits their extraction at somewhat elevated levels as shown in Figure 2.8 and Table 2.2. Moreover, these fractions exhibit the subsequent characteristics:

2.6.2.1 Light distillate fractions

Light distillate constitutes a significant portion within petroleum fractions, with its products exhibiting boiling points approximately within the range below 180 ^{o}C with the carbon number from C4 to C10 (Heil, 2008; Ashraf, 2012, Al-Dahhan, 2016). Hydrocarbons of value in this bracket encompass gasoline. These substances possess notable volatility, consist of compact molecules, display low boiling points, exhibit smooth flow characteristics, and readily undergo ignition.

2.6.2.2 Medium distillate fractions

Medium distillate pertains to products characterized by boiling points range of 180-350 ^{o}C. Examples of items in this category encompass kerosene with the boiling point range of 180-250 ^{o}C and diesel fuel in the boiling point range of 250-350 ^{o}C. Kerosene serves as both aviation fuel and a heating source in certain regions around the world. Diesel is employed within diesel engines, which provide propulsion for trucks, buses, and certain automobiles.

2.6.2.3 Heavy distillate fractions

Constituting the group of heavy distillates are products with the least volatility, distinguished by boiling points surpassing 350 ^{o}C. These fractions might exist in solid or semi-solid states, often necessitating heating to facilitate flow. This fraction gives rise to fuel oil. These commodities feature substantial molecules, possess low volatility, exhibit poor flow properties, and demonstrate limited

combustibility. This fraction is utilized to manufacture lubricating oils and more viscous fuels.

Table 2.2

Boiling point ranges and carbon number ranges of different products from crude oil fractional distillation.

Fuel products	Status	Boiling point	Number of carbon	Applications
Petroleum gas *(methane, ethane, propane, butane)*	Gas	< 40 °C	C1-C4	Heating, cooking, industrial
Gasoline	Liquid	60-180 °C	C4-C10	Engine fuel
Kerosine	Liquid	180-250 °C	C11-C14	Aviation fuel, jet engines, lamp fuel
Diesel	Liquid	250-350 °C	C15-C20	Diesel fuel, motor fuel, heating oil
Lubricating oil	Liquid	300-370 °C	C20-C50	Lubricant, motor oil
Fuel oil	Liquid	> 350 °C	C20-C70	Industrial fuels
Residues	Solid	> 600 °C	>C70	Asphalt, tar, coke,

2.7 Overviews of response surface methodology (RSM) for experimental design

RSM, which stands for Response Surface Methodology, serves as a valuable tool for examining the relationships between multiple variables. It encompasses a blend of mathematical and statistical techniques employed for the purpose of experiment design, constructing numerical models, assessing the impacts of variables, and seeking optimal conditions. The response can be visually depicted using graphs, either in three-dimensional graphs or two-dimensional as contour diagrams, which aid in visualizing the form of the outcome's representation. Contour diagrams consist of lines representing consistent values of the response, illustrated in the xi, xj plots while

holding other factors constant. Each contour signifies a specific level of the response's height, as illustrated in Figure 2.10.

Figure 2.10

Example of three-dimensional response surface and contour plot represents the interaction between temperature and biomass-to-solvent ration on green diesel yield.

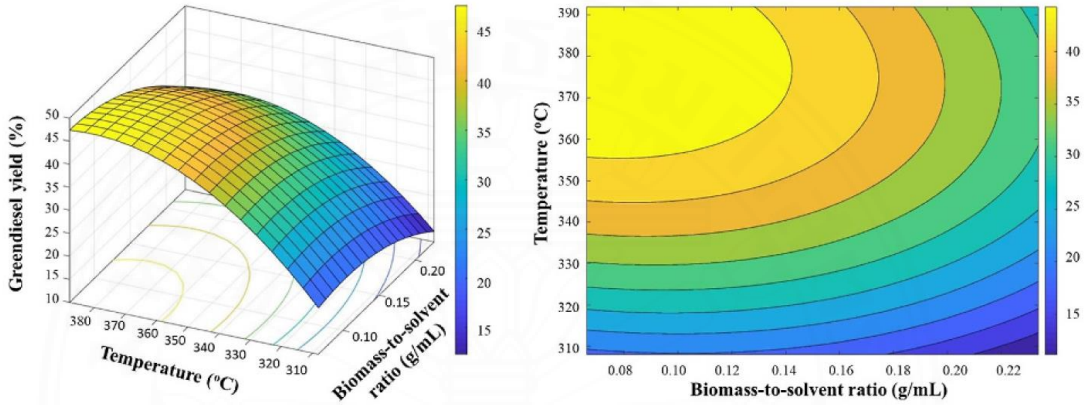

Note. From *"Supercritical ethanol liquefaction of bamboo leaves using functionalized reduced graphene oxides for high quality bio-oil production,"* by S. Echaroj, M. Santikunaporn, and A.N. Phan, 2023, Renewable Energy, 204, 848-857.

A key element of RSM is the utilization of Design of Experiments (DOE), which involves strategic approaches to determine the locations where the response needs to be assessed. Originally developed for fitting models in physical experiments, these strategies can also be applied to numerical experiments. The primary aim of DOE is the thoughtful selection of evaluation points for the response.

RSM encompasses various techniques, including Full factorial design (FFD), Central composite design (CCD), Box-Behnken design (BBD), D-optimal design (DOD), and Taguchi's contributions to experimental design. (Laougé et al., 2020).

2.7.1 Full factorial design (FFD)

FFD is a common technique widely used approach in experimental design. In this method, all input parameters are established at two different levels. FFD encompasses every conceivable combination of variables involving multiple levels. This comprehensive approach enables the identification of primary effects and minor interaction effects with flexibility and efficiency. Nevertheless, employing this design, according to Khatree and Rao (2003), can lead to challenges in fitting polynomial models of second or higher orders. To address this limitation, the integration of a second-order model can notably enhance the optimization process. This is particularly applicable in scenarios involving three-level factorial designs called 3^N full factorial, *N* stands for the design variables in the optimization problem which needs to be defined. In case, there are three variables which need to be observed the experimental design of 3^3 full factorial offers 27 points or 27 conditions for the study as depicted in Figure 2.11.

Figure 2.11

A 3^3 full factorial design for 27 points of conditions.

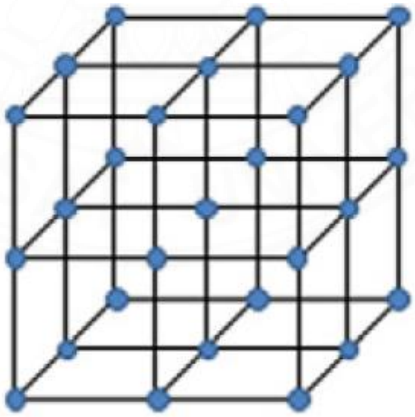

Note. From *"Application of response surface methodology and artificial neural network methods in modelling and optimization of biosorption process,"* by A. Witek-Krowiak, K. Chojnacka, D. Podstawczyk, A. Dawiec, K. Bubala, 2014, Bioresource Technology, 160, 150-160.

2.7.2 Central composite design (CCD)

CCD is widely acknowledged as a recognized design for Response Surface Methodology (RSM) due to its exceptional usefulness and efficiency in handling the impact of experimental parameters on the final output. It achieves this by recommending the minimum number of test runs required. (Hossain et al., 2016; Gupta and Mondal, 2019).

The central composite design offers equivalent information to the 3^N full factorial design. Nevertheless, this approach necessitates a reduced quantity of experimental runs compared to FFD. Furthermore, CCD offers accurate forecasts for both linear and quadratic interaction impacts of variables influencing the procedure. The CCD encompasses the complete factorial or fractional factorial layout at two levels (2^N), alongside central points (cp) that signify the midpoint of the factors, and axial points (2N), which are determined by the specific design objectives and the number of associated parameters as $2^N + 2N + cp$ (Myers and Montgomery, 2002). Figure 2.12 shows the CCD for 3 design variables [$(2^3 + 2(3) + 1) = 15$ runs].

Figure 2.12

A 3-level and 3-variable CCD design for 15 points of conditions.

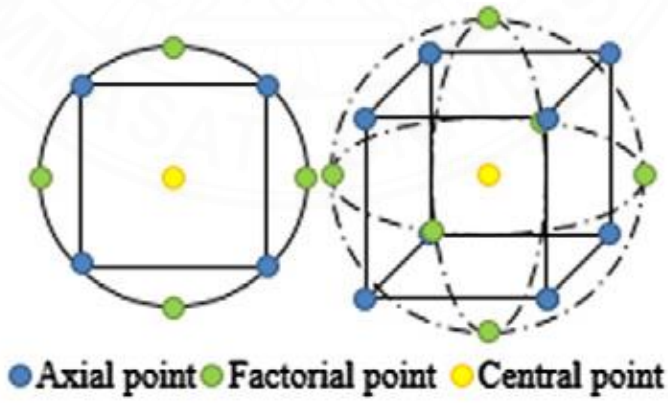

Note. From *"Application of response surface methodology and artificial neural network methods in modelling and optimization of biosorption process,"* by A. Witek-Krowiak, K. Chojnacka, D. Podstawczyk, A. Dawiec, K. Bubala, 2014, Bioresource Technology, 160, 150-160.

2.7.3 Box-Behnken design (BBD)

Box and Behnken (1960) introduced a 3-level incomplete factorial design as a viable alternative to the more labor-intensive full factorial design. In order to effectively capture linear, quadratic, and interaction effects, they employed a second-order polynomial for modeling purposes. This design by Box and Behnken aimed to minimize the need for extensive experimentation, particularly when fitting quadratic models. They constructed experimental matrices using two-level factorial designs (+1, -1) combined with incomplete block designs. To enhance precision, the final matrix incorporated multiple replications of the central point. Notably, this design omitted experimental points where all factors reached extreme values, which could prove advantageous in scenarios involving unwanted phenomena under extreme conditions. The Box-Behnken design demonstrated slightly greater labor efficiency compared to the Central Composite Design (CCD) and significantly higher efficiency than the Full Factorial Design (FFD). However, two significant constraints accompanied this approach: the design required a minimum of three experimental factors, and it was only suitable for fitting second-order polynomial equations, precluding its application for other equation types as shown in Figure 2.13.

Figure 2.13

An experimental design of 3-level and 3-variable by Box-Behnken model.

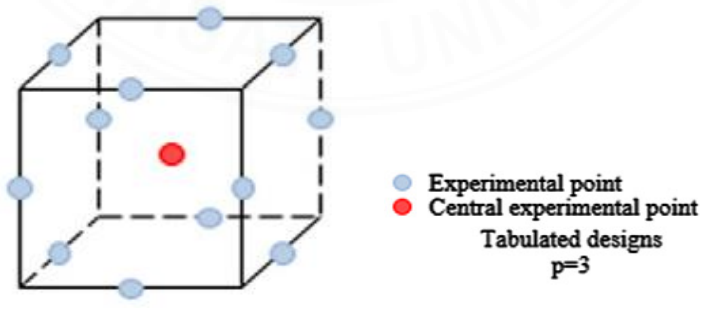

Note. From *"Application of response surface methodology and artificial neural network methods in modelling and optimization of biosorption process,"* by A. Witek-Krowiak, K. Chojnacka, D. Podstawczyk, A. Dawiec, K. Bubala, 2014, Bioresource Technology, 160, 150-160.

2.7.4 Taguchi's contribution to experimental design

Taguchi's techniques (as discussed by Montgomery in 2003) explore the parameter range using fractional factorial arrays obtained from Design of Experiments (DOE), specifically utilizing orthogonal arrays. Taguchi's viewpoint suggests that there's no need to explicitly account for the interaction between two design variables. Consequently, he devised a set of pre-arranged designs that curtail the required number of experiments when compared to a complete factorial design.

Figure 2.14 shows a diagram of the experimental design by Taguchi method with 4 x 4 = 16 experimental runs. One could also note that all the results manifest at the edges of the design 'boundary', implying that the interior of the boundary remains concealed. An optimal point could potentially lie within this boundary, and we can seek out such a point through the utilization of contour plots. An asset of this approach is its capability to manage discrete variables, though a drawback lies in Taguchi's omission of considering interactions among parameters.

Figure 2.14

Taguchi design of experiment

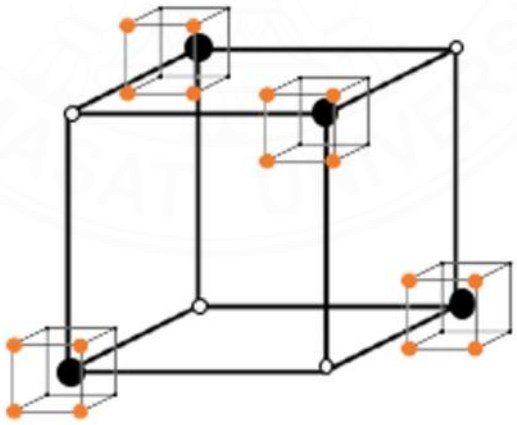

Note. From *"The role of machine learning and design of experiments in the advancement of biomaterial and tissue engineering research,"* by G. Al-Kharusi, N.J. Dunne, S. Little, and T.J. Levingstone, 2022, Bioengineering, 9(10), 561.

2.8 Literature review

Recently, many researchers have investigated the factors the effect to the triglyceride pyrolysis over various types of catalysts divided into two groups: non-activated carbon and activated carbon as catalysts aimed to enhance the pyrolysis process together with upgrading the quality of bio-oil.

2.8.1 Triglycerides/WCO pyrolysis over non-AC catalysts

Pyrolysis is regarded as an alternative way to produce biofuels from triglyceride-based materials. Many previous authors investigated pyrolysis of triglycerides and fatty acids materials, conducting the process in different conditions which reported and summarized in Table 2.3. Thermal cracking of vegetable oils was originally studied by Chan and Wang (1947) in the serious shortage of fuel situation after World War II in 1947. They used a Chinese wood oil namely tung oil which mainly composed of fatty acid chain with C18 Carbon chain as a feedstock to produce biodiesel. In the past decade, several studies revealed that pyrolyzing triglyceride-based materials can obtain high-quality bio-oil with the advantages of low viscosity, low freezing point and cold filter plugging point, and high cetane number (Wang et al., 2012).

Wiggers et al. (2009) studied the soybean oil continuous pyrolysis at a temperature ranging from 450°C to 600°C in a pilot plant and obtained biofuels similar to fossil fuels. Then, Lappi and Alén (2011) investigated the thermochemical behaviors by gas chromatography together with mass selective and flame ionization detection (Py-GC/MSD and FID) of bio-oil from saponified, palm, olive, rapeseed, and castor oil pyrolysis at the temperature of 750°C for 20 s. It was reported that bio-oils mainly contained linear alkenes (up to C19) and alkanes (up to C17) both like those found in gasoline (C4-C10) and diesel fuel (C11-C22) boiling range fractions of petroleum, while in the case of castor oil, a significant amount of undesired oxygen-containing products (e.g., ketones and phenols) were formed.

Table 2.3

Summary of triglycerides pyrolysis studies over non-AC catalyst.

Feedstock	Catalyst	Working conditions	Process temperature	Reaction time	Liquid yield (%)	Compositions	References
Vegetable oil	None	Continuous	450 – 600 °C	10-36 s	34-74	Mainly diesel compounds	Wigger et al. (2009)
Vegetable oil	None	Batch	750 °C	20 s	N/A	Gasoline and diesel	Lappi and Alén (2011)
Vegetable oil	Zeolites	Batch	350 – 450 °C	0.33–2 h	47-92	Mainly gasoline	Buzetzki et al. (2011)
Vegetable oil	Zeolites	Continuous	400 – 550 °C	1 hr	77.4	High gasoline compounds	Saxena and Viswanadham (2014)
Vegetable oil	Zeolites	Continuous	420 – 450 °C	N/A	75	Mainly aromatic	Ngo et al. (2010)
WCO	None	Batch	550 – 800 °C	N/A	80	Mainly carboxylic acid and high acidity	Ben Hassen Trabelsi et al. (2018)
Vegetable oil	Alumino silicates	Continuous	380 – 400 °C	2-5 h	47 -80	Oxygenated compounds	Phung et al. (2015) Pardo et al. (2009) Twaiq et al. (2003)
WCO	Solid base	Batch	350 – 450 °C	N/A	66-83	High HCs and low acidity	Dandik & Aksoy (1998) Junming et al. (2009) Romeo et al. (2016)

Recently, Ben Hassen Trabelsi et al. (2018) investigated the biofuels production from waste cooking oil via pyrolysis process in lab-scale fixed-bed reactor by varying the temperature in the range of 550°C to 800°C and heating rate of 5°C/min, 15°C/min, 20°C/min, 25°C/min. The bio-oil yield of 80 wt% has been obtained at 800°C and 15°C/min. The bio-oil fuel properties show that this pyrolytic oil has high calorific value (HHV around 8834 kg/Kcal) promoting its use as a liquid fuel but some other properties such as acidity and viscosity were high (126.8 mg KOH/g sample and 8.95 cSt, respectively) which need to be upgraded. The GC/MS characterization of the bio-oil highlights its high molecular complexity allowing it to be used as source of chemical products and of active molecules. The syngas heating value (reaching 8 MJ/kg) is suitable for its application as source of energy for the pyrolysis reactor. The remaining biochar is suitable for application as fertilizer since it is rich in iron and organic carbon.

After that, to improve the bio-oil quality and quantity, catalysts have been an important role in pyrolysis process studies. Zeolites-form catalyst is one of the most attractive ones for pyrolysis. Ngo et al. (2010) pyrolyzed soybean oil with various catalysts including H-ZSM5 catalysts (molar ratio SiO_2/Al_2O_3 = 28, 40, and 180) and 2 wt.% (Ga, Al or Cu) impregnated MCM41 in a fix-bed reactor at 420°C and 450°C under N_2 flow. It was found that the gas products in all experiments were mainly methane, ethane, and propylene. The liquid products in the presence of H-ZSM5 catalysts were mainly aromatic components while those with metal/MCM41 catalysts were a mixture of alkanes, alkenes, alkadienes, aromatic and carboxylic acids. Buzetzki et al. (2011) studied the influence of zeolite catalysts on the pyrolysis products from rapeseed oil thermal cracking in a batch reactor with the temperature of 350 °C-440 °C together with 1:10 of catalyst to oil ratio. Liquid yields were found up to 90-93 wt.% with a large amount of diesel range hydrocarbons and their properties such as density and viscosity were close to those of diesel fuel properties. Sirajudin et al. (2013) investigated the conversion of palm oil to biofuel by catalytic cracking under the temperature of 450oC with H-ZSM5 catalyst for 2 hours, observing yields up to 46.8 wt% in mass of hydrocarbons which is mainly in the gasoline characteristics range. Chew and Bhatia (2009) obtained the liquid yields up to 49.2 wt% from the palm oil cracking in a fixed bed reactor at 450°C with zeolites catalyst under WHSV of 2.5 h^{-1}.

Another relevant study was investigated by Saxena and Viswanadham (2014) on the conversion of Jatropha oil to green gasoline, using zeolites at temperature of 550°C and WHSV of 1.5 h^{-1}. This study achieved a total hydrocarbon yield of 65.3 wt% on total mass feed, with a larger fraction of aromatics (up to 70%) and high gasoline selectivity (about 77.4%) with Octane number fully comparable to commercial gasoline. Products in the range of gasoline boiling points, with high fractions of aromatics, were observed. Generally, zeolites, that favor secondary cracking reactions, combined with the typical reaction temperature and WHSVs, produce a large fraction of gaseous products.

Except zeolites, alumina and aluminosilicates-based catalysts have also been studied in triglyceride-based materials pyrolysis. Most general types of alumina catalysts comprise of mesoporous materials, such as MCM-41. Prado et al. (2009) and Phung et al. (2015) conducted multiple sequential tests exploring catalytic pyrolysis on bauxite and alumina around 400°C. Their findings revealed substantial conversion of vegetable oil into a hydrocarbon-rich bio-oil; however, the liquid also included oxygenated compounds.

Twaiq et al. (2003) examined the impact of catalytic cracking using MCM-41 to convert palm-derived oil into bio-oils containing hydrocarbons. Employing a reactor setup similar to zeolite cracking experiments, they observed a greater proportion of hydrocarbons, particularly heavier compounds in the diesel range. Meanwhile, Yu et al. (2013) conducted significant research on catalytic pyrolysis of soybean oil utilizing Al-MCM-41 catalysts at 450°C, with reduced catalyst mass (WHSV at 6 h^{-1}). This approach resulted in increased fractions of hydrocarbons in the diesel range (constituting 28.3% of the total feed mass) but led to decreased liquid yield. The higher pyrolysis temperature between 600 °C to 650 °C of rape oil as a feedstock was investigated by Kirszensztejn et al. (2009). The experiment was carried out in a lab-scale with WHSV of 2.44 h^{-1} by observing the higher aliphatic to aromatic hydrocarbons ratio (from 1.48 to 3.83) and higher reaction time (passing from 3 to 9 hrs.). In conclusion, the experimental investigations of the process on alumina and MCM-41-based catalysts generally showed a lower level of catalytic cracking than zeolites, leading to the formation of heavier compounds.

Several research works investigated the base catalysts, such as calcium oxide and magnesium oxide for catalytic pyrolysis of triglyceride-based materials. In comparison to zeolites and aluminosilicates, base catalysts possess larger pore sizes, resulting in a lower surface area. Dandik and Aksoy (1998) studied batch catalytic pyrolysis of used sunflower oil over sodium carbonate at various percentages, observing at 420°C and 0.1 g g^{-1} of CTO a maximum hydrocarbons mass fraction of 47.3%. Increasing the catalyst mass, the reaction temperature, and the length of the packed column resulted in a reduction in the carbon chain length of the hydrocarbons present in the product. Using the same setup, Dandik and Aksoy (1998) conducted a comparative analysis, examining the pyrolysis of used sunflower oil with sodium carbonate, silica-alumina, and H-ZSM-5 catalysts. The utilization of sodium carbonate resulted in the highest conversion yield in terms of mass fraction (73.2%), concurrently yielding the highest proportion of hydrocarbons (32.8%) within the gasoline boiling range. Romero et al. (2016) studied catalytic cracking utilizing base catalysts within a pressurized pyrolysis reactor operating at 400°C and a maximum pressure of 11 MPa. They achieved a liquid biofuel composed of 81% hydrocarbons from the total mass feed, falling within the range of C8-C15. In a separate study, Junming et al. (2009) investigated sodium and potassium carbonate in a small-scale reactor operating at temperatures up to 400°C. They measured a total liquid product ranging from 73.3% to 75.6% by mass, and notably, they observed an extremely low content of acids, with the absence of carboxylic acids. In general, these catalysts play a pivotal role in enhancing the deoxygenation process of fatty acids, aligning with the framework outlined by Tani et al. (2011). Additionally, these same authors investigated continuous pyrolysis over MgO and noted the prevalence of olefins in the collected liquid product, corroborating the reaction mechanism they proposed.

2.8.2 Triglycerides/WCO pyrolysis over AC catalysts

In addition to zeolites catalysts, silica-alumina catalysts, and solid-state basic catalysts, there have been limited investigations on the use of activated carbon as catalysts in studies related to the pyrolysis of waste cooking oil (WCO).

Fraunhofer Institute (Germany) (2008) proposed the Greasoline process, in which animal fat and/or vegetable oil are converted into hydrocarbons at 450 °C to 600 °C, over a fixed bed of activated coal. This work focused on catalytic cracking by an inert catalyst (referred to acidity), to reduce the oxygenated compounds. They achieved up to 55% of diesel range components in terms of mass fraction, calculated based on the raw material feed. However, many unidentified compounds were also observed, even in the boiling range of detected hydrocarbons, because of unknown cracking and polymerization reactions. In a recent work (Heil et al., 2013), the same group investigated the catalytic cracking over activated carbon and other microporous catalysts with the aim of maximizing the yield of kerosene, obtaining similar yields of previous work. The production of alkylated benzene (that makes those compounds a key-additive for aviation fuels) was observed by adopting different plant oil such as jatropha and waste oils. Other experiment, Chiaramonti et al. (2016) used activated carbon as a catalyst in pilot plant waste cooking oil and fatty acids pyrolysis at the temperature of 500°C. It was reported that the total observed hydrocarbon yield mass fraction on waste cooking oil and fatty acid increased from 23% (UWHSV = 4 h^{-1}) to 35% (WCO, WHSV = 2.5 h^{-1}) and finally to 40% (FA, WHSV = 2.5 h^{-1})

Furthermore, activated carbon has been employed to elevate the temperature in the triglyceride pyrolysis procedure, particularly when dealing with substances that have low microwave-absorbing capabilities. By acting as an absorber, activated carbon facilitates the heating of triglyceride materials to attain high temperatures through microwave radiation. Additionally, activated carbon serves as an energy transfer agent, aiding in the heating process of triglyceride materials. Moreover, it also functions as a catalyst, promoting the pyrolysis of triglycerides, resulting in the production of components that can be utilized as diesel fuel.

AC was also employed as an absorbent in the microwave pyrolysis of used frying oil (Lam et al., 2016; Lam et al., 2017; Echaroj et al., 2021). The results showed that AC acted as both a medium (heat-transferring agent) and a catalyst for heating, and pyrolyzed WCO to yields of up to 73 wt.% bio-oil products. However, compared to the studies of WCO catalytic pyrolysis, there are very few reports of using AC as a catalyst. Most research has been to develop the WCO process and upgrade

the bio-oil in WCO catalytic pyrolysis in using zeolites and aluminosilicates catalysts (Li et al., 2016; Ngo et al., 2010; Chiaramonti et al., 2016). In addition, AC has been studied as just a heat-transferring agent in microwave-assisted pyrolysis studies (Lam et al., 2016; Lam et al., 2017).

Activated carbon (AC) has been extensively studied as a catalyst in triglyceride pyrolysis, because of AC's large surface area and high porosity, which are the most important properties of solid catalysts (Rachid et al., 2019). These properties of AC affect reactivity in the decomposition process, including pyrolysis, by allowing the efficient contact time between the pyrolytic feedstock and the active sites (Suprianto et al., 2021; Han et al., 2019; Aswie et al., 2021; Rangel et al., 2023). Therefore, AC helps the thermal cracking of pyrolytic feedstock into lighter molecules, giving higher amounts of gaseous products (Han et al., 2019; Suprianto et al., 2021). Not only the surface area and porosity properties but also the functional groups and acidic sites of AC greatly affect the AC reactivity in the pyrolysis process (Suprianto et al., 2021; Rangel et al., 2023). The acidic properties of AC are associated with the surface functional groups. The acid surfaces are presented by carboxylic, phenolic, lactone, carboxylic anhydride and peroxide groups (Rangel et al., 2023), which depend on the type of feedstock material and the modified activation process in the AC production. The acidic character of AC makes AC a hydrophilic substance, which is potentially expected to convert the feedstock into the aromatic hydrocarbons by the pyrolysis process (Yang et al., 2020; Chen et al., 2018; Nejati et al., 2020). Moreover, due to the carbon structure of AC, the benzene rings on AC's surface can accelerate the cracking process of hydrocarbon molecules by increasing the length of C–C of hydrocarbons (Suprianto et al., 2021).

Table 2.4

Summary of triglycerides pyrolysis studies over AC catalyst.

Feedstock	Catalyst	Working conditions	Process temperature	Reaction time	Liquid yield (%)	Compositions	References
Animal fat Vegetable oil	AC	Batch	450 – 600 °C	N/A	55	Mainly diesel range	Fraunhofer (2008)
Vegetable oil	AC	Batch	450 – 550 °C	N/A	60	Mainly jet-fuel range	Heil et al. (2013)
WCO and fatty acids	AC	Continuous	450 - 550 °C	N/A	63.64	Mainly HCs compound	Chiaramonti et al. (2016)
WCO	AC	Batch	400 – 550 °C	0.5 h	73	High Aliphatic HCs Low oxygenated	Lam et al. (2016) Lam et al. (2017)

2.8.3 Response surface methodology (RSM) for experimental design

The utilization of Response Surface Methodology (RSM) in design optimization focuses on diminishing the expenses associated with costly analysis techniques. Many researchers have applied RSM techniques to their studies.

Abnisa et al. (2011) studied the optimization of bio-oil production from palm shells using RSM. Particle size, process temperature, reaction time, and nitrogen gas flow rate were used as parameters to find the optimum condition. Results showed that 500 ^{o}C with palm shell particle size 2 mm under nitrogen gas flow rate 2 L min^{-1} and reaction time 60 min gave maximum yield of bio-oil at 46.4%. Kılıç et al. (2014) optimized fast pyrolysis conditions to produce bio-oil from Euphorbia rigida using RSM. Optimum conditions to maximum bio-oil yield at 35.3 wt.% were 600 ^{o}C with heating rate 200 ^{o}C/min and nitrogen gas flow rate at 100 ml/min.

Laougé et al. (2020) studied the optimization of bio-oil from pearl millet and Sida cordifolia pyrolysis by RSM using the same process parameters as Abnisa et al. (2014)'s work for optimization. Maximum yield of bio-oil was 48.27 wt.% and 48.00 wt.% for pearl millet and Sida, respectively at optimum parameters of 400 ^{o}C with particle size 1.5 mm under nitrogen gas flow rate 200 ml min^{-1} for both biomasses. Kadlimatti et al. (2019) also used RSM to study the optimization of bio-oil from microwave-assisted pyrolysis of food waste. Maximum bio-oil yield of 30.24 wt.% was obtained from optimized pyrolysis conditions of 400 ^{o}C with 30 min residence time under 50 ml min^{-1} nitrogen gas flow rate and microwave power 450 watts.

Optimization and prediction of liquid oil yield from glycerol, polyethylene waste and waste tire pyrolysis using RSM was studied by Pinto et al. (2020), with RSM a good option to predict liquid oil product yields with minor experimental conduction. Highest conversion and liquid yields were obtained from the waste tire pyrolysis at 80% and 62 wt.%, respectively at process temperature of 450 ^{o}C with 60 min run time. Neha and Remya (2021) studied microwave co-pyrolysis of food waste and low-density polyethylene (LDPE) using RSM to optimize the operating parameters of bio-oil yield using 17 experimental runs. Maximum bio-oil yield with

minimum total acid number was performed at 42 wt.% under optimum conditions of 550 °C with residence time of 7 s along with 13 wt.% LDPE in the feed.

Recently, Gupta et al. (2022) studied the prediction of biofuel production from pine needle pyrolysis using an RSM model. The optimized condition was 552.06 °C with 50 °C /min heating rate and 164.40 ml/min inert gas flow rate, yielding maximum bio-oil at 51.11 wt.%.

CHAPTER 3
RESEARCH METHODOLOGY

As stated in the objective of this research, this chapter is organized into three major sections: the catalytic conventional pyrolysis of waste cooking oil, the optimization of waste cooking oil catalytic pyrolysis using RSM, and the catalytic supercritical ethanol liquefaction of *Saccharina Japonica Seaweed*. In the first and second section, materials, experimental setup, design of experiments (DOE) and characterization techniques for the catalytic pyrolysis of waste cooking oil are described. For the third section, it closely resembles the first section, but focusing on the catalytic supercritical ethanol liquefaction of *Saccharina Japonica Seaweed*.

3.1 The catalytic conventional pyrolysis of waste cooking oil

In this section, we present the materials and the method of our experiments together with the characterization techniques of WCO and liquid bio-oil obtained from the pyrolysis process.

3.1.1 Materials

Waste cooking oil (WCO) is collected from Thanachok Vegetable oil Ltd. Part., Thailand as shown in Figure 3.1a. The collected dark yellowish WCO sample is retained in aluminium containers at room temperature and then used for pyrolysis experiments without pre-treatment. Activated carbon (Biocat activated carbon CS1100; AC) with particle size 0.5-1.0 mm was used as a catalyst as shown in Figure 3.1b.

Figure 3.1

Materials in this study: (a) WCO as a feedstock and (b) AC as a catalyst

(a) (b)

3.1.2 Catalytic pyrolysis setup

Catalytic pyrolysis experiments were conducted as a laboratory-scale batch operation, as shown in Figure 3.2. In each batch operation, 100 g of WCO was mixed with AC at mass ratios no AC, 1:40, 1:30 on 1:20 and placed in a 1L two-necked quartz reactor. Before use, the AC was heated at 110°C for 12 h to remove moisture.

The pyrolysis system was validated with no leakages, and nitrogen was purged through the system with a flow rate of 40 mL/min to remove oxygen from the system and ensure pyrolysis under oxygen-free conditions. The system was purged with nitrogen for at least 10 min before heating. A stainless-steel thermocouple probe was immersed inside the reactor in direct contact with the WCO sample. The reaction temperature was monitored throughout the pyrolysis experiments while stirring at 40 rpm and heating by an electric magnetic stirrer heating mantle until reaching the targeted pyrolysis temperatures ranging between 350 °C and 450 °C, with monitoring for 30 min. The experimental condition is summarized in Table 3.1.

Table 3.1

Summary of pyrolysis experiment conditions

Experimental conditions	
Process temperature	350, 375, 400, 425, and 450 °C
AC:WCO ratio	1:40, 1:30, 1:20
N_2 gas flow rate	40 ml/mim

Figure 3.2

Schematic diagram of the catalytic WCO pyrolysis experiment

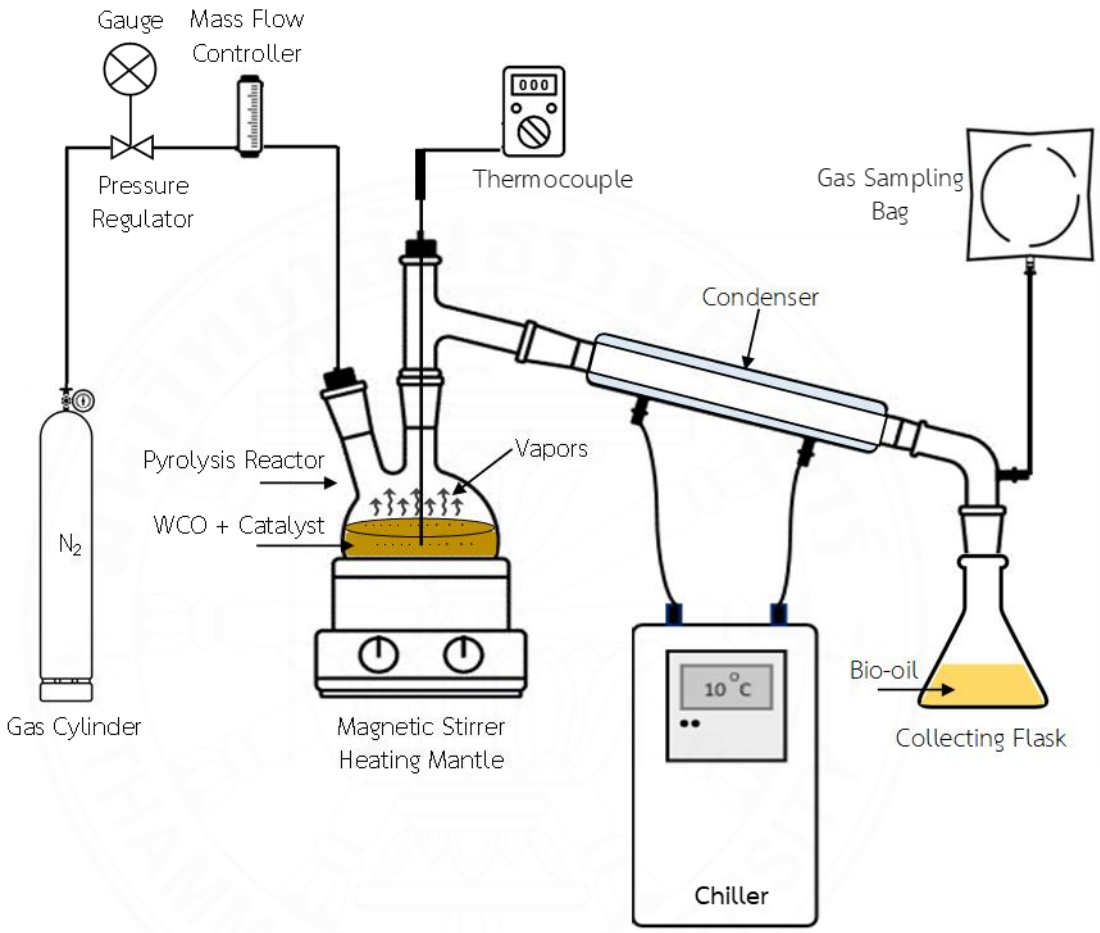

In the experiment, the gaseous product generated during the pyrolysis process passed to the condenser operated at 10 °C with circulating chilled water. The liquid product (bio-oil) was condensed and collected in a flask, while the non-condensable gases were collected in a gas sampling bag for further studies. The non-pyrolyzed residues were collected from the bottom of the reactor after cooling at room temperature. The pyrolysis experiments were conducted twice under the same reaction conditions and the mean value of product yields was calculated. Yields of liquid and residue products were measured by weight, and by mass balance for

gaseous products. Moreover, the energy recovery of the liquid bio-oil obtained from the WCO pyrolysis was calculated by the formula as shown in Equation 3.1.

$$\text{Energy recovery (\%)} = \frac{\text{(Weight of bio-oil) x (bio-oil's calorific value)}}{\text{(Weight of WCO) x (WCO's calorific value)}} \times 100 \qquad (3.1)$$

3.1.3 AC and WCO characterization and product analysis

AC was characterized by scanning electron microscope (SEM) with surface area and porosity analyzer. WCO and liquid bio-oil are characterized by using elemental analyzer, bomb calorimeter, TGA, FTIR, GC-MS and GC-SIMDIS as the summary of using analytical equipment is shown in Table 3.2.

Table 3.2

Analytical techniques for AC, WCO and liquid bio-oil characterization

Description	Characterization
WCO	Elemental analyzer, heating value, TGA, FTIR, GC-MS
AC	SEM, BET
Liquid bio-oil	Elemental analyzer, heating value, TGA, FTIR, GC-MS, GC-SIMDIS, density, viscosity, water content, acid value

3.1.3.1 Elemental analyzer

An elemental analyzer (CHN628/O628, LECO Instruments, Thailand) as shown in Figure 3.3 was used to determine the amount of carbon, hydrogen and nitrogen in the WCO and liquid bio-oil products.

Figure 3.3

Elemental analyzer (CHN628/O628, LECO Instruments, Thailand)

3.1.3.2 Gas chromatography-mass spectrometry (GC-MS)

The fatty acid compositions of WCO and the chemical compositions of bio-oil products were analyzed using a 7890B/5977AMSD-GC-MS HP (Agilent, Santa Clara, CA, USA) equipped with a mass spectrometer detector as shown in Figure 3.5. An HP-5MS capillary column (length 30 m, 0.25 mm, ID, 0.25 μm df.) was used to separate the constituents. The bio-oil products were diluted in acetone to reduce the viscosity and concentration, then a 0.2 μL sample solution was injected into the column at 250 °C with a split ratio of 10:1. Helium was applied as the carrier gas with a flow rate of 1 mL/min. The oven temperature was programmed from 100 °C to 300 °C at a heating rate of 10 °C /min, held at the initial temperature for 2 min and the final temperature for 20 min. The detector and ion source temperatures were 300 °C and 230 °C, respectively. The peaks were observed, and the compounds were identified from the W10N14 library.

Figure 3.4

Gas Chromatography-Mass Spectrometer (GC-MS)

3.1.3.3 Scanning electron microscope (SEM)

Scanning electron microscope (SEM) was carried out on a JEOL JSM-IT300, Oxford X-Max 20 (Boston, MA, USA) to study the morphology of AC. An elemental analyzer (CHN628/O628, LECO Instruments, was used to determine the amount of carbon, hydrogen, and nitrogen in the WCO and AC samples.

3.1.3.4 Fourier transform-infrared (FT–IR) spectroscopy

Fourier transform-infrared (FT–IR) spectroscopy together with a Nicolet iS50, (Thermo Scientific, Waltham, MA, USA) was used to determine the functional groups of WCO and bio-oil products, with spectra conducted at wavelengths between 4000 and 400 cm^{-1}.

3.1.3.5 Thermogravimetric analysis (TGA)

Thermal analyses of the samples were determined by thermogravimetric analysis (TGA2, Mettler Toledo, Greifensee, Switzerland) as shown in Figure 3.6 by heating from 30 ^{o}C to a final temperature of 650 ^{o}C at a heating rate of 10 ^{o}C /min in a flow of nitrogen. This was to characterize the boiling point distribution of the hydrocarbon mixtures of WCO and the peak temperature that WCO is pyrolyzed

up to a boiling point of 1013 °F (545 °C) in compliance with ASTM D2887 or up to 963 °C (517 °C) according to ASTM D86.

Figure 3.5

Thermogravimetric analysis (TGA, Mettler Toledo, Greifensee, Switzerland)

Different boiling temperatures related to the number of carbon atoms found in bio-oil were analyzed by a gas chromatograph, equipped with simulated distillation (Hewlett-Packard, HP6890 Agilent, Santa Clara, CA, USA). The boiling point of the hydrocarbon C4-C10 (gasoline) is below 180 °C, C11–C14 (kerosene) compounds have a range of 180–250 °C, C15–C20 (diesel) compounds have a range of 250 °C to 350 °C and carbon atoms above C20 (fuel oil) are distilled at temperatures above 350 °C (Heil, 2008).

To determine the fuel properties, the bio-oil samples were tested following the ASTM method. Density was measured on a K86200 automatic digital densitometer with ASTM-D1250 standard. To determine the kinematic viscosity of bio-oil at 40°C, the ASTM-D445 method was applied on a Tanaka KV-5S viscometer. The calorific values of the bio-oil samples were determined based on ASTM D240 using an IKA C600 Global Standard Bomb Calorimeter as shown in Figure 3.6. The acid value of the bio-oils was measured by the titration method following the ASTM-D664, while a hydrometer was used to determine the density at 15 °C, and water content was determined using a Mettler Toledo Coulometric Karl Fischer Titrator.

Figure 3.6

Bomb calorimeter (IKA C600 Global Standard Bomb Calorimeter)

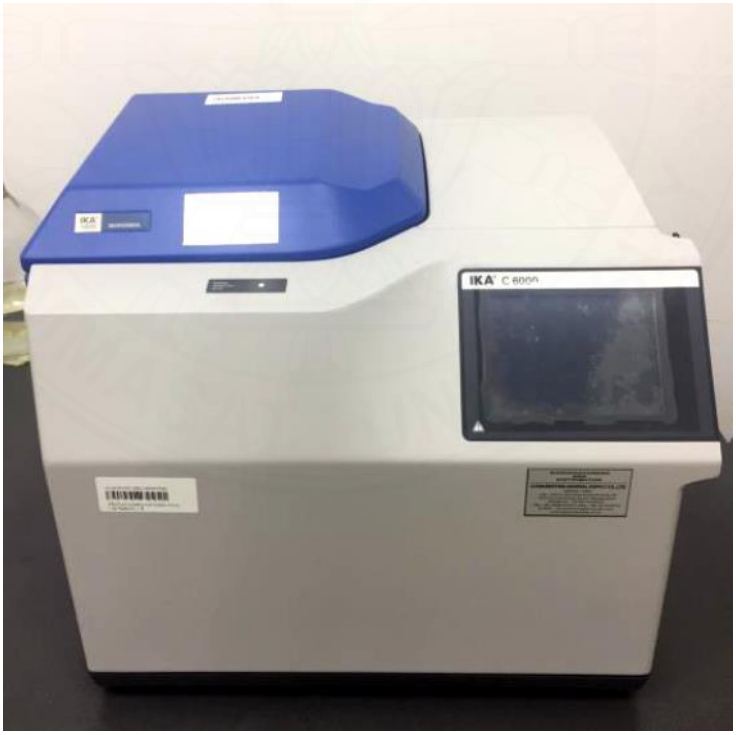

3.2 The optimization of waste cooking oil catalytic pyrolysis using RSM.

In this section, the materials, methodology, and experimental design (DOE) are provided, accompanied by a description of the characterization techniques applied to both the Waste Cooking Oil (WCO) and the liquid bio-oil from the pyrolysis process.

3.2.1 Materials

Waste cooking oil (WCO) utilized in this section was similar to the WCO mentioned in section 3.1, serving as the feedstock for the pyrolysis experimental processes.

Activated carbon (AC) with different BET surface area obtained from Biocat CS1100 (Approx. 750 m^2/g), and apricot stone activated carbon (Approx. 500 and 1000 m^2/g), synthesized from apricot stone by sealed and carbonized at 400 °C with 10 °C/min of heating rate for 1 hour and mixed with KOH at 80 °C for 2 hours then calcinated at 850 °C for 1 hour, were used as catalysts. AC was grinded and sieved to a particle size of 0.5-1.0 mm. Prior to use, AC was dried at 110 °C in an oven for 12 h.

3.2.2 Design of Experiment (DOE)

For more understanding on the parameters that affect the catalytic WCO pyrolysis besides AC dosage and process temperature, BET surface area of AC was also investigated.

The examination of the optimization of the catalytic pyrolysis process conditions for WCO is necessary to maximize bio-oil yield and energy conversion value. Investigating multifactor optimizations of the operating conditions at the laboratory scale will assist in designing a pilot-scale plant to enhance industrial-scale development of a pyrolysis reactor.

Optimum operating parameters were investigated by RSM for maximum energy recovery values based on their heating value of liquid bio-oils (calculated from Equation 3.1). Process temperature, AC dosage (AC:WCO ratio), and BET surface area were chosen as the independent parameters, with yield of liquid bio-oil and heating values as the dependent parameters. The RSM technique was used to design the number of experiments by utilizing a central composite design (CCD). The significance of each factor was evaluated through a batch experiment. The CCD was

operated by determining the specific ranges and levels of the three independent parameters, as listed in Table 3.3 and the coefficient values of three variables as listed in Table 3.4.

Design of Experiment (DOE) using the central composite design (CCD) method from Minitab software 17 was conducted to evaluate the liquid bio-oil yield (%Yield) in terms of energy conversion (calculated from heating value). A mathematical model was developed based on three variables: temperature, AC:WCO ratio, and BET surface area and analyzing the relationships between variables affecting %Yield of liquid bio-oil. A mathematical model was created to perform Analysis of Variance (ANOVA) on the variables influencing %Yield together with the energy conversion value of liquid bio-oil. Additionally, scatter plots depicting the relationships between energy conversion value and all three variables were generated in the form of contour plots and 3-D surface plots by MATLAB R2020a software.

CCD method offers the advantage of reducing the number of experiments, leading to cost and time savings. In practical, the Design of Experiments (DOE) as recommended by MiniTab software proposed a total of 15 experimental runs. However, in order to enhance the precision of the outcomes, an additional experimental run is appended, which is repeated at the central experimental conditions. Therefore, in this study, 16 experiments were designed, and CCD was operated by determining the specific ranges and levels of the three independent parameters, as listed in Table 3.3 and the coefficient values of three variables as listed in Table 3.4.

RSM was used to investigate the maximum energy conversion from the yield of liquid bio-oil together with the optimum operating condition. The impact of each independent factor and their interaction on the response was evaluated using regression analysis and analysis of variance (ANOVA). A second-order polynomial equation used to represent the model is given as Equation (3.2):

$$Y = b_0 + \sum_{i=1}^{k} b_i X_i + \sum_{i=1}^{k} b_{ii} {X_i}^2 + \sum_{i=1}^{k} \sum_{j=i+1}^{k} b_{ij} X_i X_j + \varepsilon \quad (3.2)$$

Where Y represents the predicted response used as a dependent variable; k is the number of variables studied in the experiments; b0 is the intercept (grand mean); bi is the linear coefficient; bii is the quadratic coefficient; bij is the interaction coefficient; Xi and Xj are the independent variables and **ε** is the error of the model.

Table 3.3

Variable parameter in WCO pyrolysis experiment

Variable parameters	**Range and Level**		
	-1	0	1
Temperature (°C), X_1	375	400	425
AC:WCO ratio (g/g), X_2	1:40	1:30	1:20
BET surface area (m^2/g), X_3	500	750	1000

Table 3.4

The coefficient values of the three variables used in Minitab 17 software for the experiment 16 runs.

DOE	Temperature, X_1	AC:WCO, X_2	BET, X_3
1	-1	-1	-1
2	1	-1	-1
3	-1	1	-1
4	1	1	-1
5	-1	-1	1
6	1	-1	1
7	-1	1	1
8	1	1	1
9	-1	0	0
10	1	0	0
11	0	-1	0
12	0	1	0
13	0	0	-1
14	0	0	1
15	0	0	0
16	0	0	0

3.2.3 Pyrolysis experiment setup and characterization techniques

The catalytic waste cooking oil (WCO) pyrolysis experiments conducted in this section were similar to the experiment setup according the previous described in section 3.1.2 by conducting in accordance with 16 runs of experiment proposed by Minitab software as listed in Table 3.3.

For the characterization techniques of both WCO and liquid bio-oil by following the description that was mentioned in section 3.1.3.

3.3 The catalytic supercritical ethanol liquefaction of Saccharina Japonica seaweed.

In this section, the materials, methodology, and experimental design (DOE) for the catalytic supercritical ethanol liquefaction of Saccharina Japonica are provided.

3.3.1 Materials

The feedstock used for this study is Saccharina Japonica seaweed (brown algae). The seaweed was washed in plenty of water to remove the sea salt before drying at 105 °C for 24 hours as shown in Figure 3.7, grinding, sieving, prior used for liquefaction. And ethanol, ($C_2H_5O_6$) concentration 99.9%, RCI Labscan was used in this study.

Figure 3.7

Saccharina Japonica Seaweed as a feedstock

3.3.2 Catalyst

Activated carbon activated by KOH and modified by aluminum oxide (Al_2O_3) was used as catalyst in this study. The AC was synthesized from apricot stones by carbonization in furnace at 400 °C for 1 hour with heating rate of 10 °C/min under the absence of oxygen condition. Then the apricot-char was chemical activated by using potassium hydroxide (KOH) under the controlled temperature of 80 °C for 2 hours. The slurry was filtered by using vacuum pump and dried for 12 hours at 120 °C. After that, the dried sample was placed in horizontal tubular furnace and pyrolyzed

under continuous N_2 flow from room temperature to 750 ^{o}C (heating rate 10 ^{o}C/min). After reaching carbonized temperature, the heating material was held for 1 hour.

After the activation process, the activated carbon was modified by the impregnation method with solution of aluminum nitrate (Al $(NO_3)_3.9H_2O$) for 24 hours using deionized water as a solvent. Then dried and heated at 210 ^{o}C for 1 hour under oxygen condition.

3.3.3 Catalytic liquefaction in supercritical ethanol experiment

Catalytic liquefaction experiments were carried out using stainless steel autoclave reactors with a length of 150 mm, and an inner diameter of 70 mm as shown in Figure 3.8. Seaweed, ethanol, and KOH catalyst according to the designed conditions were mixed and loaded into the reactor and sealed. The reactor was purged with nitrogen gas (99.99%) for 5 minutes to ensure that the reactor was operated under the absence of oxygen during the experiment. Then, the sealed reactor was placed into the heater for HTL process by setting the heating rate at 10 ^{o}C /min until reached the targeted process temperature and monitored for 1 hour. The pressure inside the reactor finally approached a supercritical ethanol pressure (> 6.5 MPa). After a given reaction time, the reactor was taken out from the heater and left until the temperature dropped to the room temperature. The reactor was then opened, and the product was collected under conditions of filtration and washed with ethanol several times to separate two parts of liquid product (soluble in ethanol) and solid residues (solid product and catalyst). For further analysis of the product, the ethanol solvent in liquid oil was evaporated at 40 ^{o}C using a rotary evaporator. The remaining liquid products, called liquid bio-oil, were recovered, and weighed to determine the extent of seaweed conversion. Due to practical limitation and considerations, the gaseous products were not collected in this study, but calculated by mass balancing.

Figure 3.8

Catalytic liquefaction in supercritical ethanol experiment setup.

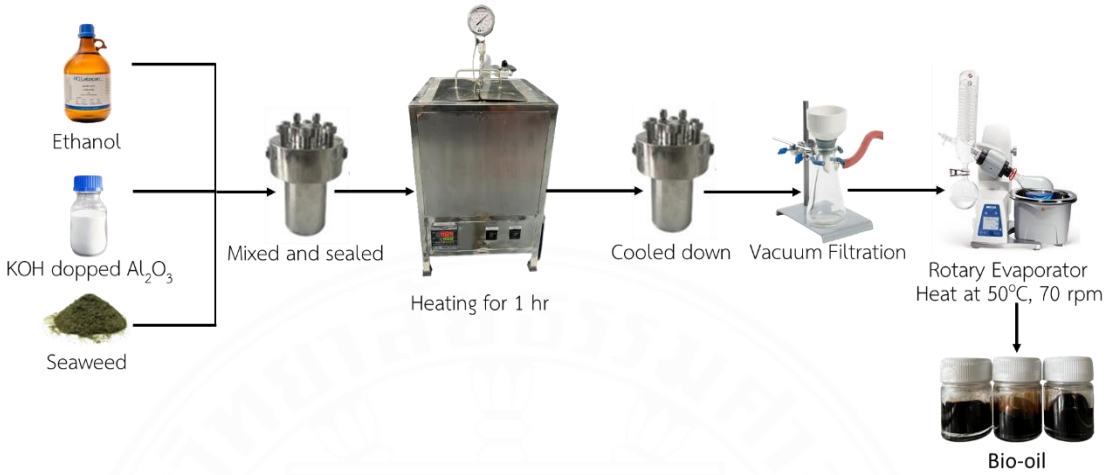

3.3.4 Design of experiment (DOE)

Optimum operating parameters were investigated by RSM for maximum liquid bio-oil yield. Process temperature, %catalyst to feedstock and, EtOH: feedstock ratio was chosen as the independent parameters, with yield of liquid bio-oil as the dependent parameters. The RSM technique was used to design the number of experiments by utilizing a Box-Behnken Design (BBD) via Minitab 17 software. The significance of each factor was evaluated through a batch experiment. The BBD was operated by determining the specific ranges and levels of the three independent parameters, as listed in Table 3.4 and Table 3.5.

Table 3.4

Experimental range and levels of independent variables

Independent Parameters	Unit	Symbol	Range and Level		
			-1	0	1
Temperature	°C	X_1	300	375	450
Catalyst per feedstock	%	X_2	15	20	25
EtOH: feedstock	g/g	X_3	0.25	0.3	0.35

Table 3.5

The coefficient values of the three variables used in Minitab 17 software for the experiment 15 runs.

DOE	Temperature, X_1	%cat:feed, X_2	EtOH:feed, X_3
1	1	1	-1
2	1	-1	-1
3	1	0	1
4	1	1	-1
5	0	1	1
6	0	-1	0
7	0	-1	1
8	0	1	0
9	-1	1	-1
10	-1	-1	-1
11	-1	0	1
12	-1	0	0
13	0	0	-1
14	0	0	-1
15	0	0	-1

3.3.5 Heating value of bio-oil analysis

The calorific values of the bio-oil samples were determined based on ASTM D240 using a Parr 6400 Calorimeter.

Figure 3.9

Bomb Calorimeter (Parr 6400 Calorimeter)

CHAPTER 4
CONVERSION OF WASTE COOKING OIL INTO BIO-FUEL VIA PYROLYSIS USING ACTIVATED CARBON AS A CATALYST

4.1 Introduction

Effective management of large amounts of waste cooking oil (WCO) is a crucial environmental issue. Selecting suitable technologies to handle the complexities of various WCOs is of paramount importance. Recently, WCO was used as a feedstock in bio-diesel production through transesterification; however, the low cetane number and calorific value of biodiesel are burdens for such utilization, while extraction costs in the glycerol recovery process during transesterification are high.

New technologies to improve WCO recycling and treatment processes now focus on the recovery of WCO energy and chemical values. The pyrolysis technique is regarded as an effective, economical, and environmentally friendly treatment process for many kinds of waste. Applying the pyrolysis technique in the thermochemical processing of WCO offers high potential to recover the energy and render valuable products (oil and gas), which can be used as feedstock in petroleum refineries and petrochemical industries.

WCO mainly consists of a mixture of triglycerides and fatty acids. Pyrolysis under the complete absence of oxygen yields more valuable products including oil, gases, and char. The yield and quality of these pyrolytic products depend on the characteristics of the feedstocks, temperature, heating rate, type of reactor, residence time, types of catalyst and catalyst dosage as the basic parameters contributing to the efficiency of the WCO pyrolysis process.

Catalysts are essential to improve the pyrolysis process for both bio-oil quality and quantity; Zeolites are popular catalysts for pyrolysis. Alumina and aluminosilicate-based catalysts have also been studied in triglyceride-based material pyrolysis. Most types of alumina catalysts generally encompass mesoporous materials such as MCM-41.

Carbonaceous material such as activated carbon (AC) has been extensively studied as a catalyst in triglyceride pyrolysis. Because AC has a large surface area and high porosity which is the most important property of solid catalysts. These properties of AC affect reactivity in decomposition process, including pyrolysis by allowing the efficient contact time between the pyrolytic feedstock and the active sites. Therefore, AC as a catalyst with a high surface area and high porosity helps the thermal cracking of pyrolytic feedstock into lighter molecules and vaporized to higher formation of gaseous prod. Not only the surface area and porosity properties but also functional groups and acidic sites of AC greatly affect the AC reactivity in the pyrolysis process.

The utilization of activated carbon (AC) as a catalyst for a lab-scale pyrolysis process to convert waste cooking oil (WCO) into more valuable hydrocarbon fuels is described. The pyrolysis process was performed with WCO and AC in an oxygen-free batch reactor at room pressure. The effects of process temperature and activated carbon dosage (AC to WCO ratio) on the yield and composition are discussed systematically.

4.2 Experimental setup

As described in chapter 3, pyrolysis experiments were conducted as a laboratory-scale batch operation. In each batch operation, 100 g of WCO was mixed with AC at mass ratios 1:40, 1:30 on 1:20 and placed in a 1L two-necked quartz reactor. The pyrolysis system was validated with no leakages, and nitrogen was purged through the system to remove oxygen from the system and ensure pyrolysis under oxygen-free conditions. The reaction temperature was monitored throughout the pyrolysis experiments while stirring at 40 rpm and heating by an electric magnetic stirrer heating mantle until reaching the targeted pyrolysis temperatures ranging between 350 °C and 450 °C, with monitoring for 30 min.

In the experiment, the gaseous product generated during the pyrolysis process passed to the condenser operated at 10 °C with a circulating chilled water. The liquid product (bio-oil) was condensed and collected in a flask, while the non-condensable gases were collected in a gas sampling bag for further studies. The non-pyrolyzed residues were collected from the bottom of the reactor after cooling at room temperature. Yields of liquid and residue products were measured by weight, and by mass balance for gaseous products.

4.3 Results and discussion

4.3.1 Characterization of WCO as pyrolysis feedstock

The characteristics of WCO were examined and are shown in Table 4.1. Carbon, oxygen, and hydrogen were the major components of WCO at 78.69, 8.20 and 12.22 wt.%, respectively. The high calorific value of 39.1 MJ/kg suggested that WCO could be a suitable feedstock in the pyrolysis process with the potential to recover the energy value from waste to bio-fuel. Moreover, the very small amounts of nitrogen and no sulfur detected in WCO were considered to generate reduced pollutant emissions as NO_x, SO_x and NH_3 during thermal cracking in the pyrolysis process. WCO primarily contained palmitic acid at 56 wt.%, oleic acid 33.72 wt.% and linoleic acid 7.53 wt.%. Thus, WCO predominantly consisted of saturated fatty acids. Results in Table 4.2 show that almost all the compounds (93.19 wt.%) in WCO were vaporized above 350 ^{o}C, relating to the boiling points of palmitic acid, oleic acid, and linoleic acid (Aslam et al., 2015). Therefore, the minimum pyrolysis temperature of WCO was determined as 350 ^{o}C in this study.

Table 4.1

Characteristics of WCO.

Elemental Composition (wt.%)	
C	78.69
H	12.22
N	0.89
S	0.00
[a]O	8.20
Fatty Acid Composition (wt.%)	
Palmitic Acid ($C_{16}H_{32}O_2$)	56.00
Oleic Acid ($C_{18}H_{34}O_2$)	33.72
Linoleic Acid ($C_{18}H_{32}O_2$)	7.53
Others	2.75
Calorific Value (MJ/kg)	39.10
Acid Value (mg KOH/g)	5.40
[b]**Distribution of Compounds (wt.%)**	
<180 °C	0.13
180-250 °C	0.80
250-350 °C	5.66
>350 °C	93.19

[a] by a mass balance; [b] by thermogravimetric analysis.

The chemical structure of WCO examined by the FT-IR spectrum was also supportive, with results shown in Figure 4.1 and Table 4.2. A characteristic of WCO is its aliphatic hydrocarbons. A significant indicator of the aliphatic groups is the high intensity of the peak bands between 2921.91 cm^{-1} and 2852.83 cm^{-1} representing aliphatic C-H bonds such as alkanes and carboxylic acid O-H stretching. Weak intensity of the bands in the range 1464.30 cm^{-1} to 1412.34 cm^{-1} and peak bands at 935.95 and 721.89 cm^{-1} also represent aliphatic group characteristics of WCO. Oxygenated

compounds were also detected at the peak band of 1708.93 cm^{-1} as C=O stretching and at 1283.64-1112.96 cm^{-1} as C-O stretching compounds.

Figure 4.1

FT-IR profile of WCO used in this study.

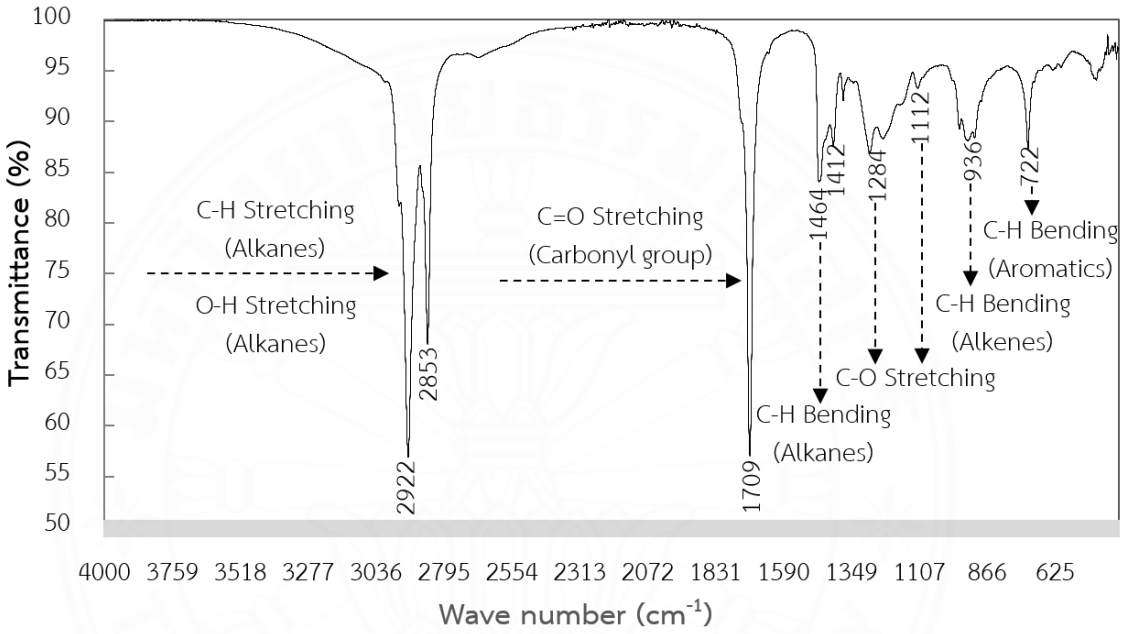

Table 4.2

FT-IR Functional group of WCO.

Wave Number (cm^{-1})	Functional Group
2921.91-2852.83	C-H stretching (alkanes) Carboxylic acid O-H stretching
1798.93	C=O stretching (carbonyl group such as aldehydes, ketones, esters, anhydrides, carboxylic acids)
1464.30-1412.34	C-H bending (Alkanes)
1283.64-1112.96	C-O stretching (ester, ethers, alcohols, carboxylic acids
935.95	C-H bending (alkene)
721.89	C-H bending (aromatics)

4.3.2 Characterization of AC as a catalyst

The physical and chemical properties of AC were characterized and shown in Table 4.3. The ultimate analysis data confirms that carbon is the dominant element of 72.33 wt.%. A BET surface area of 720 m^2/g and average pore size of 0.95 nm were obtained from the adsorption/desorption of N_2. The SEM images of AC morphology are shown in Figure 4.2. The morphology of AC is a granular shape with a high porous structure.

Moreover, the characteristics of AC used in this study were acid surfaces observed from the functional groups on surface area by FT-IR analysis. As seen in Figure 4.3, the peaks were recorded at 2352 cm^{-1} and 1017 cm^{-1} corresponding with the presence of C-O and carboxylic acids.

Table 4.3

Characteristics of activated carbon.

Physical properties	**Value**
Ultimate analysis (wt.%)	
C	72.33
H	1.97
N	1.04
*O	24.66
BET surface area (m^2/g)	720.0
Total pore volume (cm^3/g)	0.41
Average pore size (nm)	0.95

* by a mass balance.

Figure 4.2

SEM analysis of activated carbon used in this study.

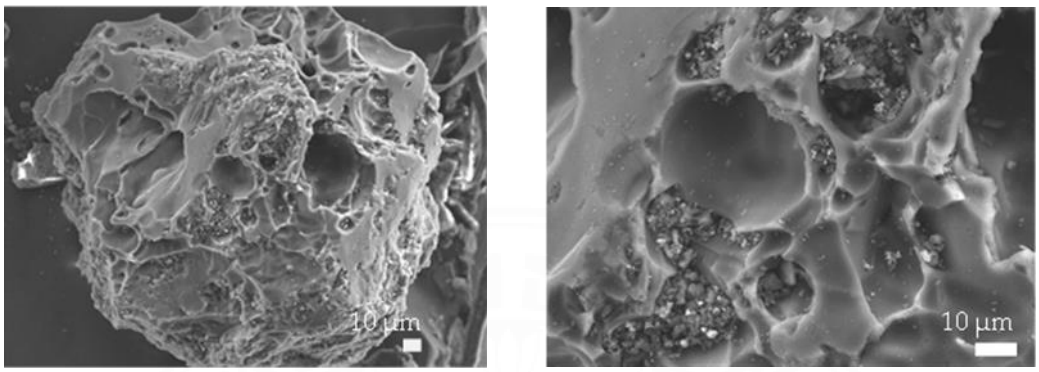

Figure 4.3

FT-IR analysis of activated carbon used in this study.

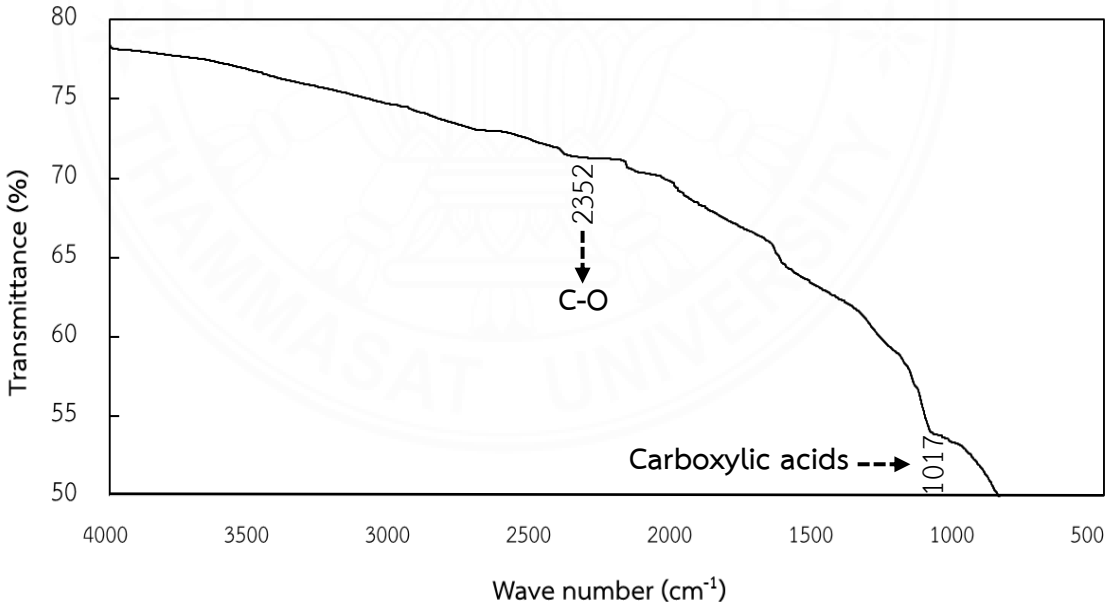

4.3.3 Pyrolysis of WCO in the absence of AC

By the first stage of the studies, the influence of process temperature on WCO pyrolysis yields of liquid, residue and gaseous products was investigated by varying different process temperature. The products distribution from the pyrolysis process including oil, gas, and residue were experimentally observed and is displayed in Figure 4.4.

Figure 4.4

Influence of temperature on product yields of pyrolysis reaction. (Operating conditions: Flow rate of N_2 of 40 mL/L without catalyst and pyrolyzed temperature range of 350–450 °C).

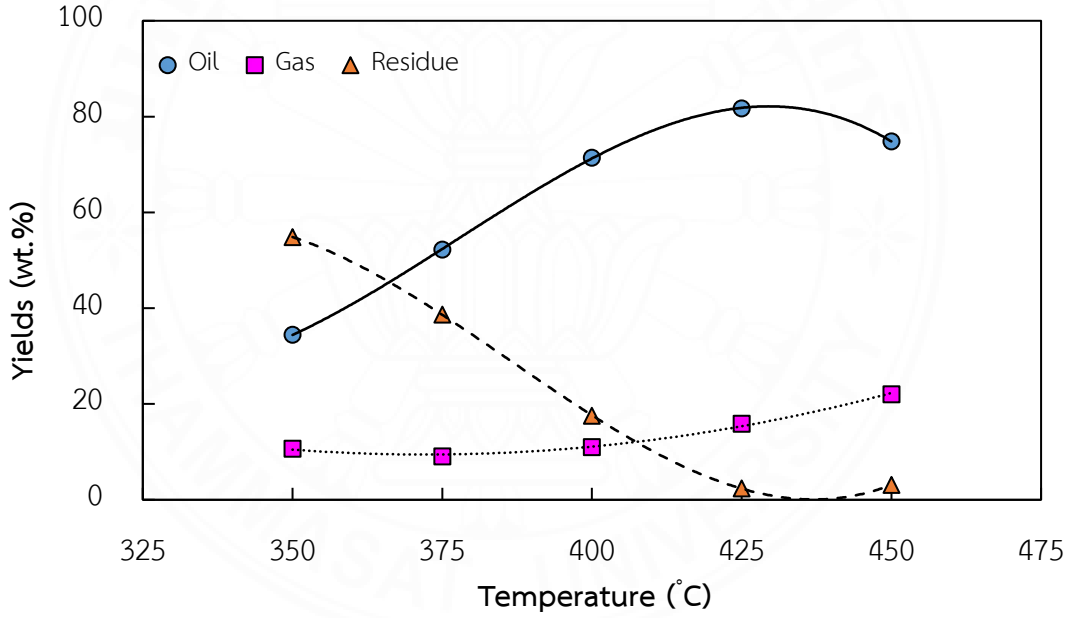

Figure 4.4 illustrates the influence of process temperature from 350 °C to 450 °C without catalyst on WCO pyrolysis yields of liquid, residue and gaseous products when using the same quantity of feedstock to ensure maximum productivity of each yield under the same conditions. Results showed that WCO samples were thermally cracked to pyrolysis products in different proportions at each process temperature. Initially, pyrolysis performed at 350 °C demonstrated incomplete cracking, with half of the WCO remaining unpyrolyzed, and only 35% bio-oil yield and

10% gaseous yield obtained. It was found that the WCO needs to be heated to a higher temperature to increase the thermal cracking in the pyrolysis process. When the temperature was increased to 425 °C, production of bio-oil increased from 35.00% to 81.70% in the first region of process temperature of 350-425 °C. The results can be implied that the optimum pyrolysis temperature was at 425 °C. The maximum bio-oil yield was achieved in this experiment by 81.70%, with minimum non-pyrolyzed (residue) yield of 2.30% and 16% gaseous product yield. This is because WCO pyrolysis is an endothermic process which can be described by the concentration of primary decomposition or depolymerization reactions to produce volatiles in bio-oil and gaseous forms (Trabelsi et al., 2018). At 450°C, bio-oil yield dropped to 75%. There was a reduction of liquid bio-oil yield when the temperature was beyond 425 °C. This is because pyrolysis bio-oil products were secondary decomposed by excess heat into gaseous products, as observed by the increased yield of pyrolysis gaseous products from 16% to 22%. Sampath (2009) had also investigated the effect of temperature on the pyrolysis product yield of camelina seed oil at 300 to 600 °C; his results showed that liquid yield ranged from 45% to 75% of total mass feed.

These results were supported by Thermogravimetric Analysis (TGA). From the TGA and DTG profile of WCO pyrolysis in Figure 4.5, it was found that the WCO was thermally cracked in pyrolysis process in the range of 300 °C-450 °C. The DTG profile showed only one sharp peak, and the maximum weight loss rate was 0.03 mg/min at around 425 °C. This indicates that almost of WCO was pyrolyzed at this temperature supported by the result from the experiment.

Figure 4.5

TGA and DTG curve of WCO pyrolysis

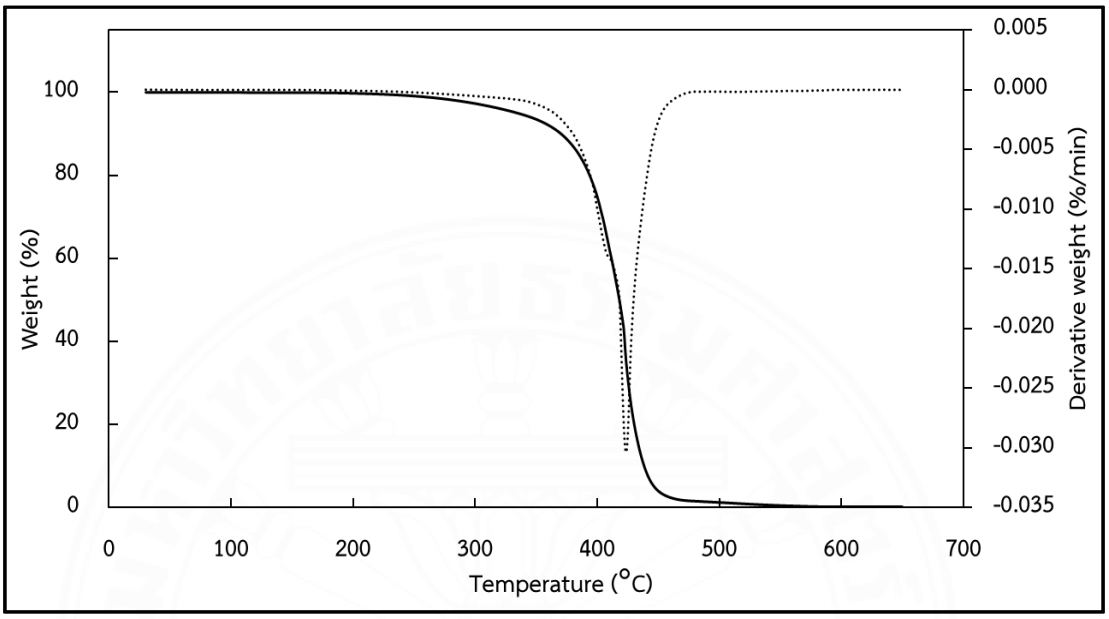

The distribution of bio-oil separated at different temperature ranges by GC-SIMDIS is presented in Figure 4.6a. At 425 °C, the optimum pyrolysis temperature, the major components in the bio-oil were fuel oil-like compounds at 43% with boiling points higher than 350 °C. Then, the diesel-like compounds with boiling temperature range of 250–350 °C (C15–C20) at 36.00% and kerosene-like compounds with boiling range of 180-250 °C (C11-C14) at 15.00%. Moreover, it can be observed that the boiling temperature distribution in the bio-oil obtained from 350 °C showed almost the same distribution in each boiling temperature range. But when the temperature increased, the distribution of diesel-like compounds and fuel oil-like compounds increased up to 39.00% and 43.00%, respectively. It also proved that direct pyrolysis was the major decomposition stage of fatty acid in WCO and when the temperature increased, the production of hydrocarbons also increased which promoted the pyrolysis of macromolecules (Wang et al., 2019). To select the optimum condition for upgrading to more valuable alternative energy, product yield as shown in Figure 4.6b and other properties must be considered. A comparative analysis of the economic aspects of these outcomes should also be conducted.

Figure 4.6

Boiling temperature distribution of liquid bio-oil obtained from pyrolysis. (a) Product distribution by percentage; (b) Production distribution by amount. (Operating conditions: Flow rate of N_2 of 40 mL/L without catalyst and pyrolyzed temperature range of 350-450 °C.).

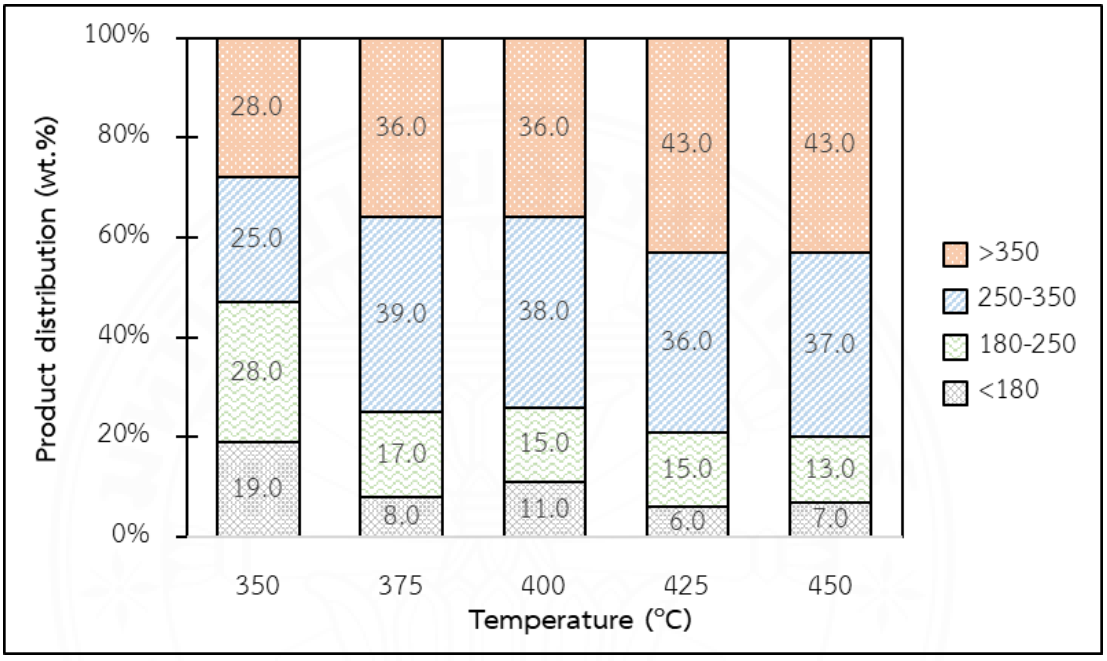

(a)

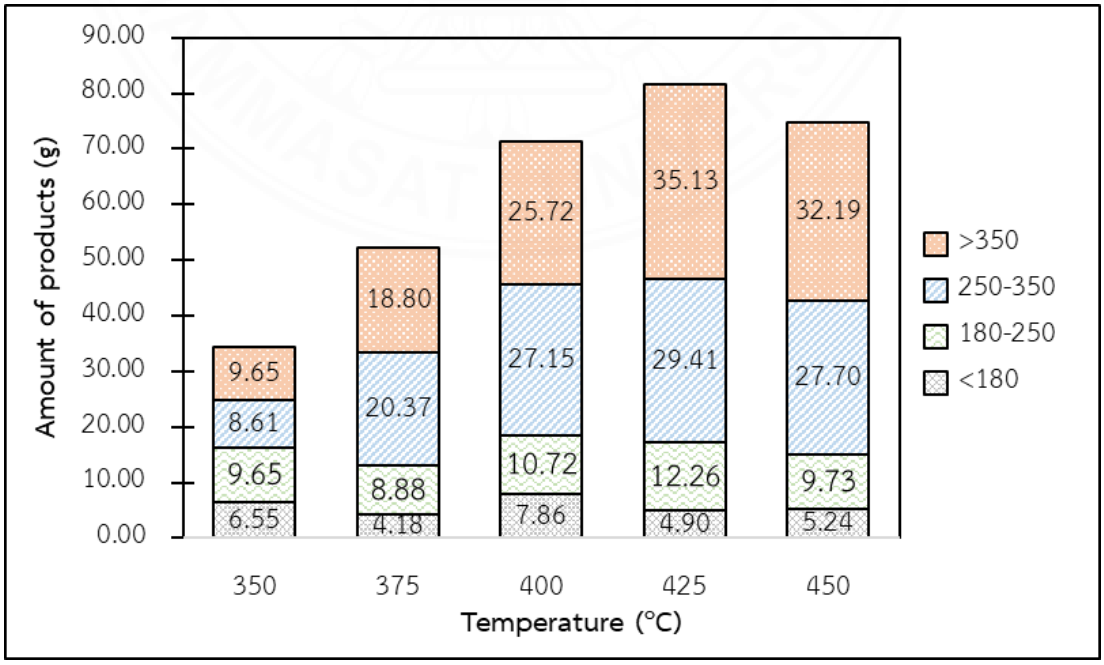

(b)

4.3.4 Pyrolysis of WCO in the presence of AC

4.3.4.1 Effect of reaction temperature and AC

The influence of reaction temperature on product yield was assessed at 350, 375, 400, 425 and 450 °C by fixing the ratio of AC to WCO at 1:40 to investigate the optimum temperature in terms of maximum bio-oil yield. As shown in Figure 4.7, bio-oil yield increased with temperature of 350 to 400 °C, with maximum yield at 400 °C of 85.35%, and then declined at higher temperatures. This phenomenon was described in the previous section. Higher reaction temperatures increased thermal cracking reactions in the pyrolysis process by breaking the carbon chain compounds and contributing volatilization of WCO, called primary decomposition (Tabelsi et al., 2018). Secondary decomposition occurred when temperature was increased to 425 °C or higher, causing reduced production of bio-oil at 83.85%, with 82.81% at 450 °C.

Figure 4.7

Influence of reaction temperature on products yields. (Operating conditions: Flow rate of N_2 of 40 mL/L; AC:WCO mass ratio of 1:40 and pyrolyzed temperature range of 350-450 °C).

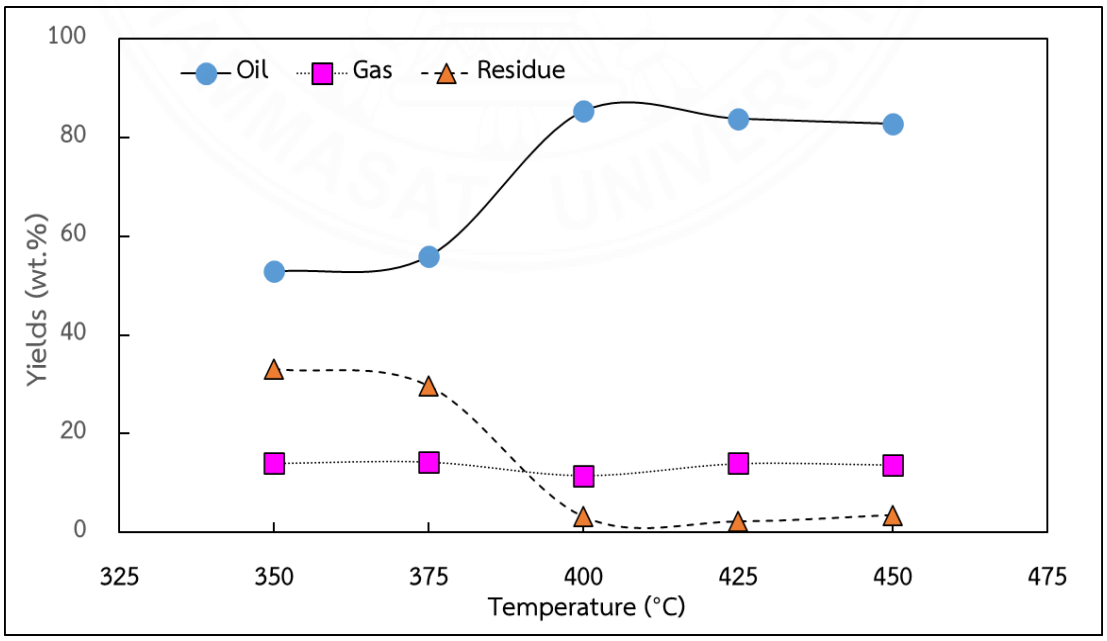

These results followed the same trend as product yield of WCO pyrolysis without AC in the previous section but differed in some interesting aspects. Bio-oil yield at all reaction temperatures in the presence of AC pyrolysis increased, especially at 350 °C from 34.45% to 52.85%, together with reduction of residue yield from 54.85% to 33.13%. Moreover, optimum endothermic reaction temperature in terms of maximum bio-oil production shifted from 425 °C to 400 °C, with a similar increase in bio-oil yield from 81.70% to 85.35%. The AC acted as catalyst as a heat transfer agent (Lam et al., 2016; Lam et al., 2017) promoted the reaction temperature in the pyrolysis process beyond 425 °C due to the electrostatic forces (Suprianto et al., 2021). Besides, the catalytic effect on WCO occurred on the entire AC surface with a high surface area and in the pores that helped the thermal decomposition of triglyceride in WCO into lighter molecules and produced large vapor products (Yang et al., 2020), while the secondary decomposition reduced. Interestingly, reducing the optimum pyrolysis temperature using a small amount of AC resulted in energy saving with efficiency maintained.

4.3.4.2 Effect of AC:WCO ratio

The influence of AC:WCO ratios at 1:40, 1:30 and 1:20 on the pyrolysis process under two reaction temperatures of 350 °C and 400 °C was also examined, as shown in Figure 4.8. Yield of bio-oil, residue and gaseous products altered, especially for bio-oil and residue.

At 350 °C (Figure 4.8a), the change in AC:WCO ratio did not significantly affect pyrolysis product yields, whereas at 400 °C (Figure 4.8b), change in AC:WCO ratio significantly impacted pyrolysis product yields. At AC:WCO ratio 1:40, maximum bio-oil yield was achieved at 85.35%, with minimum non-pyrolyzed (residue) yield of 3.16% and 11.49% gaseous product yield, similar to the results of direct pyrolysis (absence of AC) at 425 °C. This occurred because the AC catalyst at 1:40 AC:WCO ratio enhanced the process temperature from 400 °C to the final temperature at almost 425 °C. With a small increase of AC catalyst, yield of bio-oil gradually decreased from 85.35% to 78.83% and 79.09%. However, yield of residue did not significantly change at 3.16%, 5.91% and 5.65%, respectively. Bio-oil yield significantly reduced when the AC amount increased (1:30 and 1:20) because the higher the

amount of AC used, the higher the amount of the surface contacting area in the WCO pyrolysis process. This reactivity of AC enhanced the process temperature beyond 425 °C as the optimum pyrolysis temperature. The AC also caused thermal cracking secondary decomposition of WCO, resulting in a higher conversion of some WCO to pyrolysis gases (Xie et al., 2015). This further decomposed the pyrolysis bio-oil product into gaseous products, as described in the previous section.

Figure 4.8

Product yields distribution obtained from pyrolysis at various AC:WCO mass ratio at the process temperature (a) at 350 °C; (b) 400 °C.

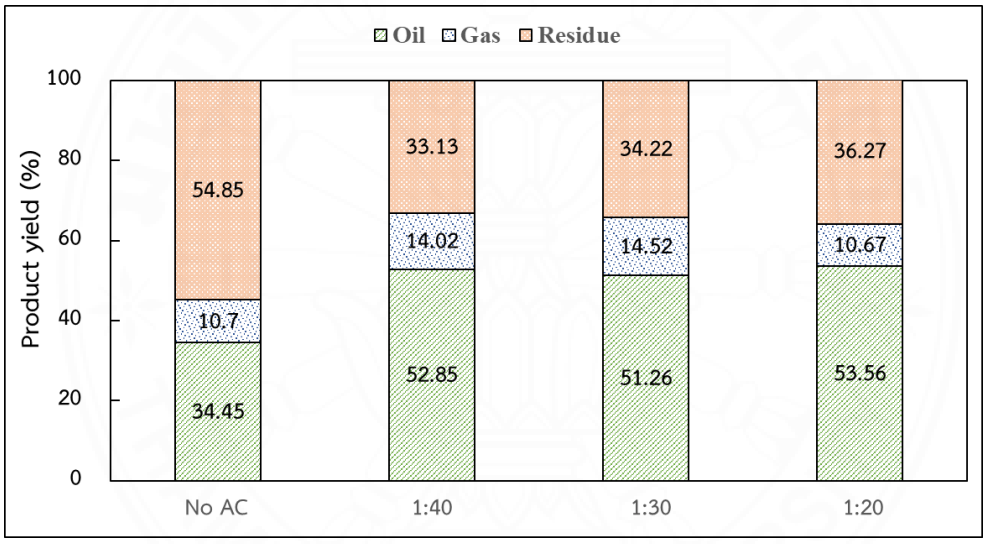

(a)

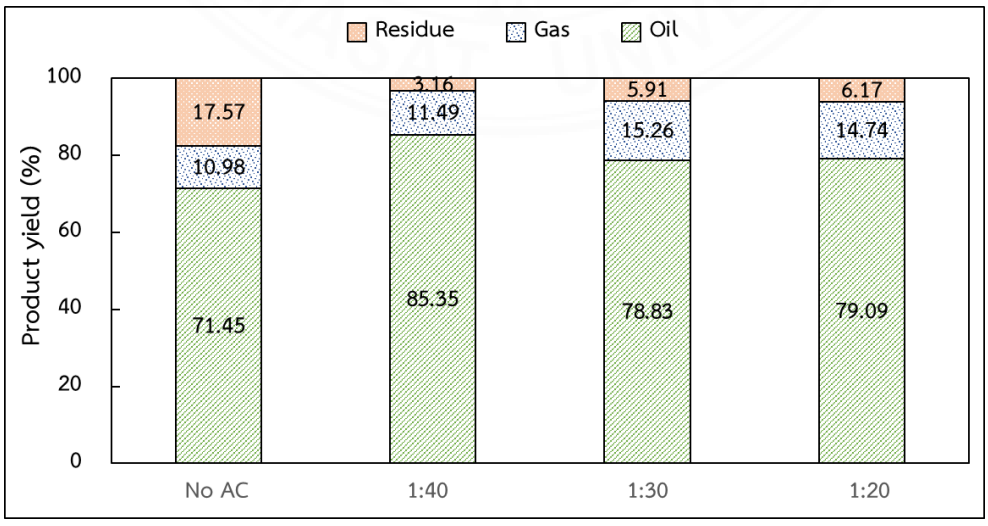

(b)

As shown in Figure 4.9 and 4.10, the boiling temperature distribution analyzed by GC-SIMDIS obviously changed when the AC was used as a catalyst especially for the bio-oil obtained from the process temperature at 350 °C (Figure 4.9a). The amount of bio-oil in the boiling range of fuel oil-like (>350 °C; C>20) did not greatly alter with AC usage. Conversely, significant changes occurred in the amount in the boiling point range of gasoline-like fuel, kerosene-like fuel, and diesel-like fuel. The proportion of diesel-like fuel significantly increased compared to those of non-AC usage from 25 wt.% to 45 wt.% (8.61 g to 23.78 g in Figure 4.9b) for bio-oil obtained from the process temperature at 350 °C with AC dosage at 1:40 and from 38 wt.% to 48 wt.% for the bio-oil obtained from the process temperature at 400 °C with AC dosage 1:30 (Figure 4.10a), respectively. Interestingly, the amount in each boiling point range did not significantly change when the AC dosage increased at low reaction temperature. At the optimum condition for maximum bio-oil yield, AC:WCO ratio of 1:40 at 400 °C, 45 wt.% or 23.78 g of bio-oil was in the boiling point range of diesel-like fuel (250-350 °C), 35 wt.% fuel oil-like fuel (>350 °C), 13 wt.% kerosene-like fuel (180-250 °C) and 7 wt.% gasoline-like fuel (<180 °C). It was revealed that AC as a catalyst enhanced the WCO pyrolysis to produce more valuable products such as diesel-like compounds in the liquid bio-oil. As mentioned before, the AC acted as a heat transfer agent that enhanced the reaction temperature in the pyrolysis process, promoting thermal cracking from long carbon-chain compounds to form low carbon-chain compounds in the bio-oil. Therefore, when selecting the optimum condition to upgrade to a more valuable alternative energy, product yield and other properties must also be considered to secure the most suitable economic value.

Figure 4.9

Boiling temperature distribution of liquid bio-oil obtained from pyrolysis of WCO at various AC:WCO mass ratio. (Operating conditions: Flow rate of N_2 of 40 mL/L; pyrolyzed temperature at 350 °C

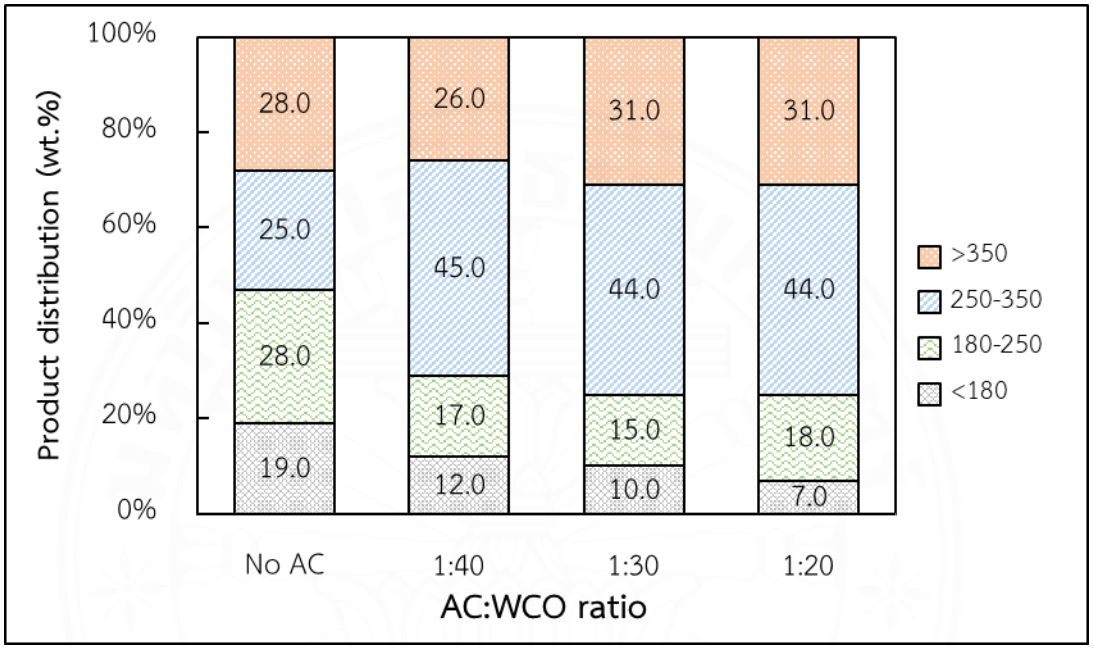

(a)

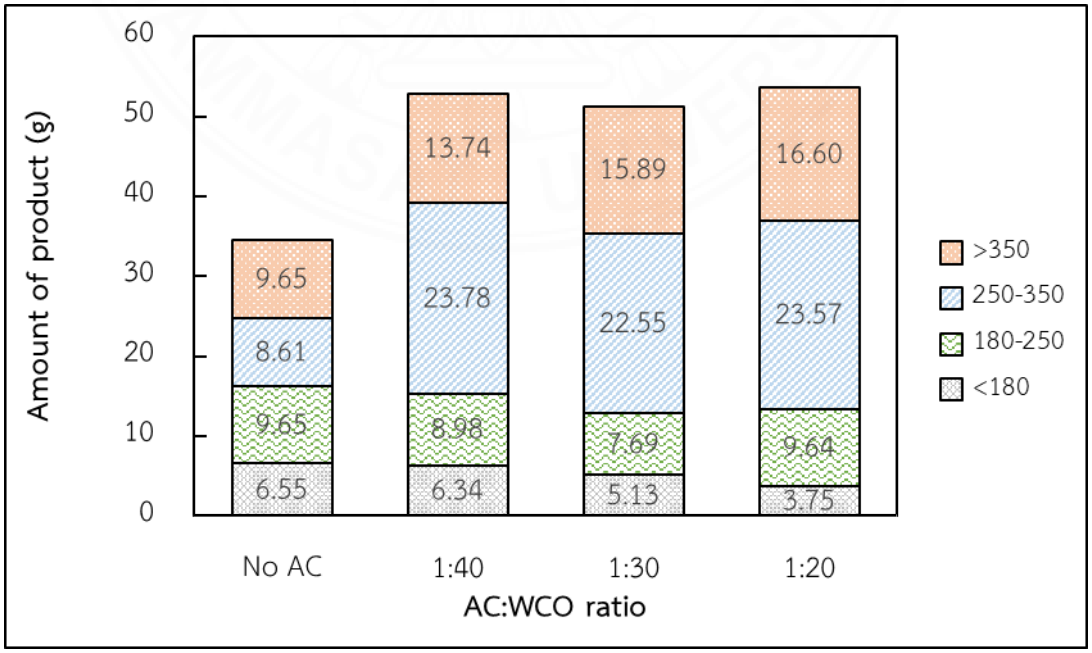

(b)

Figure 4.10

Boiling temperature distribution of liquid bio-oil obtained from pyrolysis of WCO at various AC:WCO mass ratio. (Operating conditions: Flow rate of N_2 of 40 mL/L; pyrolyzed temperature at 400 ^{o}C)

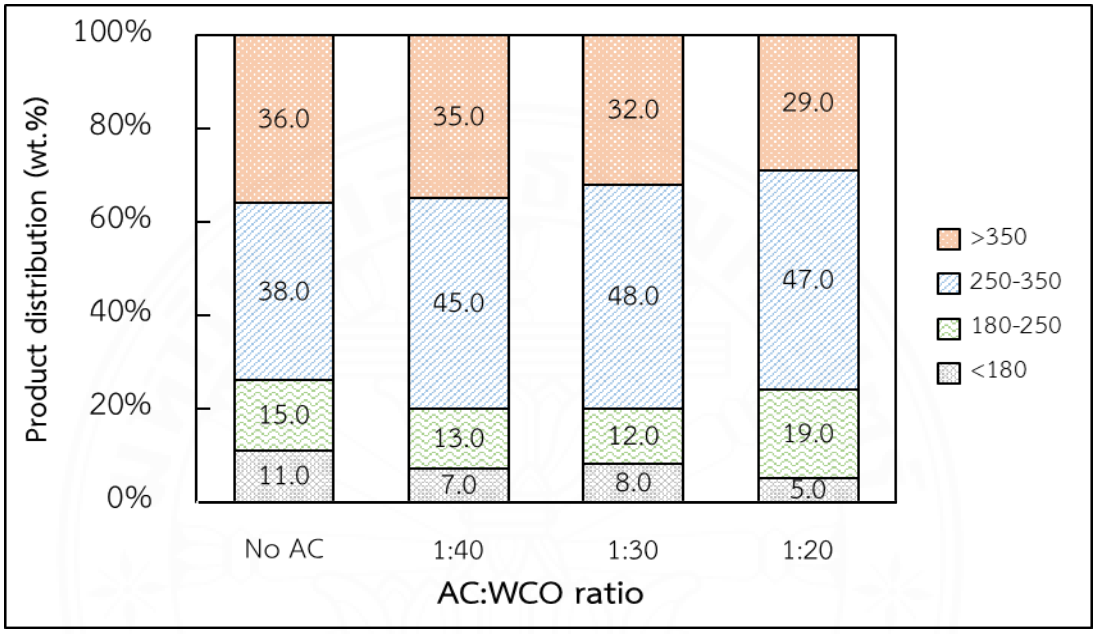

(a)

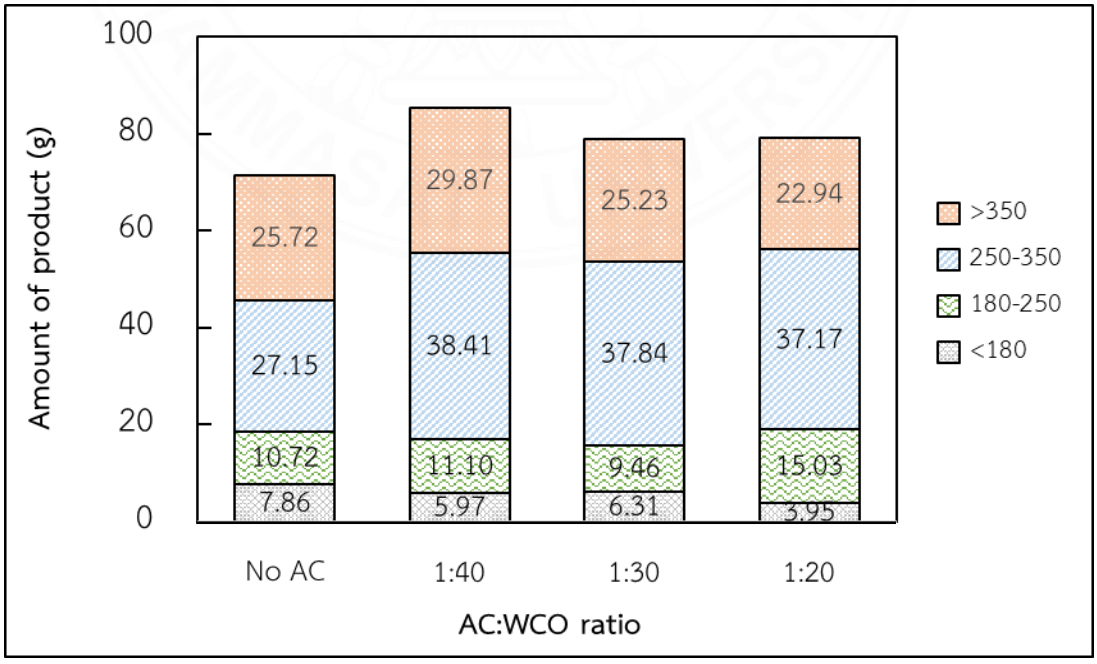

(b)

4.3.5 The Bio-oil characteristics

4.3.5.1 GC-MS analysis

Bio-oil produced from WCO catalytic pyrolysis with an AC:WCO ratio of 1:40 at 400 ^{o}C was analyzed based on chemical compositions determined by GC-MS. In this study, pyrolysis gases and char residue were excluded from the analysis due to the low yields obtained. The detected qualitative organic compounds were listed according to increased retention times and their areas were determined and summarized in Table 4.4.

Table 4.4

Group of organic compounds investigated by GC-MS analysis of bio-oil.

Compounds	**wt.%**
Without oxygen atoms	
- Alkanes	17.48
- Alkenes	6.53
- Alkynes	3.02
With oxygen atoms	
- Carboxylic acids	52.33
- Alcohols	11.12
- Esters	2.30
- Ketones	3.67
- Aldehydes	2.86
- Others	0.69

From Table 4.4, the bio-oil consisted of a complex mixture of 27.03 wt.% hydrocarbon compounds and 72.97 wt.% oxygenated compounds, as shown in Table 4.4. Compounds containing carbon atoms ranged from C10 to C27 with trace amounts of C36. The oxygenated compounds in bio-oil were 52.33 wt.% carboxylic acids, 11.12 wt.% alcohols, 3.67 wt.% ketones, 2.86 wt.% aldehydes and 2.30 wt.% esters. The hydrocarbons found in bio-oil were 17.48 wt.% alkanes, 6.53

wt.% alkenes and 3.02 wt.% alkynes. Many studies reported on the similarities of GC-MS compositions of bio-oils produced from the pyrolysis of various triglyceride materials. Trabelsi et al., (2018) investigated the GC-MS chemical compositions of a pyrolytic oil produced from waste cooking oil in a pyrolysis process using a fixed-bed reactor. Results showed that the bio-oil contained organic compounds with carbon atoms ranging from C6 to C27 as the major components, explaining the predominant presence of 89.61 wt.% carboxylic acid, 2.31 wt.% linear saturated hydrocarbons, 3.64 wt.% linear unsaturated hydrocarbons, 0.17 wt.% cyclic hydrocarbons, 1.86 wt.% alcohols, 0.25 wt.% ketones and 0.25 wt.% aldehydes (by calculation from the GC-MS result reported of Trabelsi et al. (2018)). Similarly, Kraiem et al. (2017) reported that GC-MS compositions of bio-oil obtained from the pyrolysis of waste frying oil consisted of oxygenated compounds such as 53.11 wt.% carboxylic acids, 1.71 wt.% aldehydes, 1.21 wt.% ketones, and 0.93 wt.% alcohols 4.03 wt.% linear saturated, 28.65 wt.% unsaturated and 9.54 wt.% cyclic hydrocarbons (by calculation from the GC-MS result reported of Kraiem et al. (2017)). These studies demonstrated the significant hydrocarbon compositions of bio-oils as carboxylic acids related to high fatty acid compositions in WCO.

Since the pyrolysis process in WCO involves many highly complex organic reactions, there is no definite solution to the resulting reactions that will be obtained in each execution. Figure 4.11 presents the proposed reaction scheme for triglycerides pyrolysis over an activated carbon (Wigger et al., 2017; Suprianto et al., 2021; Aswie et al., 2021). Triglyceride is decomposed to long-chain heavy oxygenated hydrocarbons. The thermal-cracking reaction continues, together with deoxygenation reactions, forming lighter oxygenated hydrocarbons (carboxylic acids, alcohols, ketones, aldehydes, esters, etc.), chain hydrocarbons such as alkanes, alkenes and dienes and gaseous products (CO_2, CO, H_2 and light hydrocarbons). Then, many reactions, for example isomerization, polymerization, aromatization and cyclization, occur to form various kinds of products, such as saturated and unsaturated hydrocarbons, aromatics, cyclic hydrocarbons, light oxygenated hydrocarbons, etc.

Figure 4.11

The proposed reaction scheme for the pyrolysis of triglycerides over activated carbon.

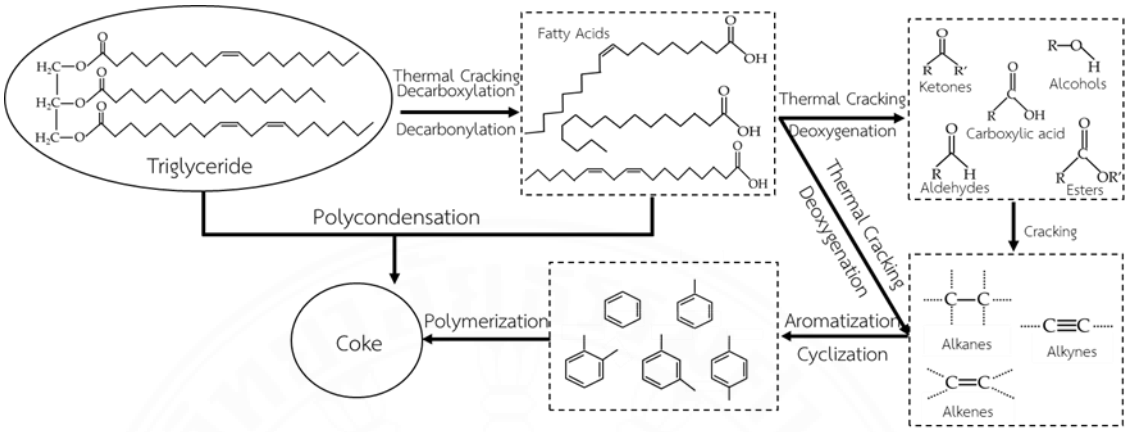

Note. Adapted from "Pyrolysis of Microalgae Chlorella sp. Using Activated Carbon as Catalyst for Biofuel Production," by V. Aswie, L. Qadariyah, and M. Mahfud, 2021, *Bulletin of Chemical Reaction Engineering & Catalysis*, 16(1), 205-213.

4.3.5.2 FT-IR analysis

Figure 4.12 presents the FT-IR spectra of liquid bio-oil obtained at the optimum operating condition. The intense peaks between 2921.81 and 2852.74 cm^{-1} represent carboxylic acids (O-H stretching) together with alkanes (C-H stretching). The high intensity of these bands highlights the dominance of saturated aliphatic hydrocarbons in bio-oil. The presence of other aliphatic groups (C-H bending) was shown by bands between 1464.30 and 1377.59 cm^{-1}, confirming the aliphatic character of bio-oil. The presence of oxygen in bio-oil was represented by the signal of C=O stretching at 1709.26 cm^{-1}, indicating carbonyl groups such as aldehydes, ketones, esters, and carboxylic acids. The C-O stretching vibration was affirmed by bands in the range 1284.02 to 1115.14 cm^{-1} representing esters, ethers, alcohols, and carboxylic acids. The weak bands between 909.66 and 721.75 were probably due to C-H bending such as alkenes and aromatic hydrocarbons in the bio-oil. The bio-oil obtained from this study was influenced by carboxylic acids, aliphatic hydrocarbons and small

amounts of aromatics, aldehydes, and ketones, related to the group of organic compounds investigated by GC-MS analysis described in Table 4.4.

Figure 4.12

FT-IR spectra of liquid bio-oil obtained at the optimum operating condition (Operating conditions: N_2 of 40 mL/L; pyrolyzed temperature at 400 °C; AC:WCO 1:40.

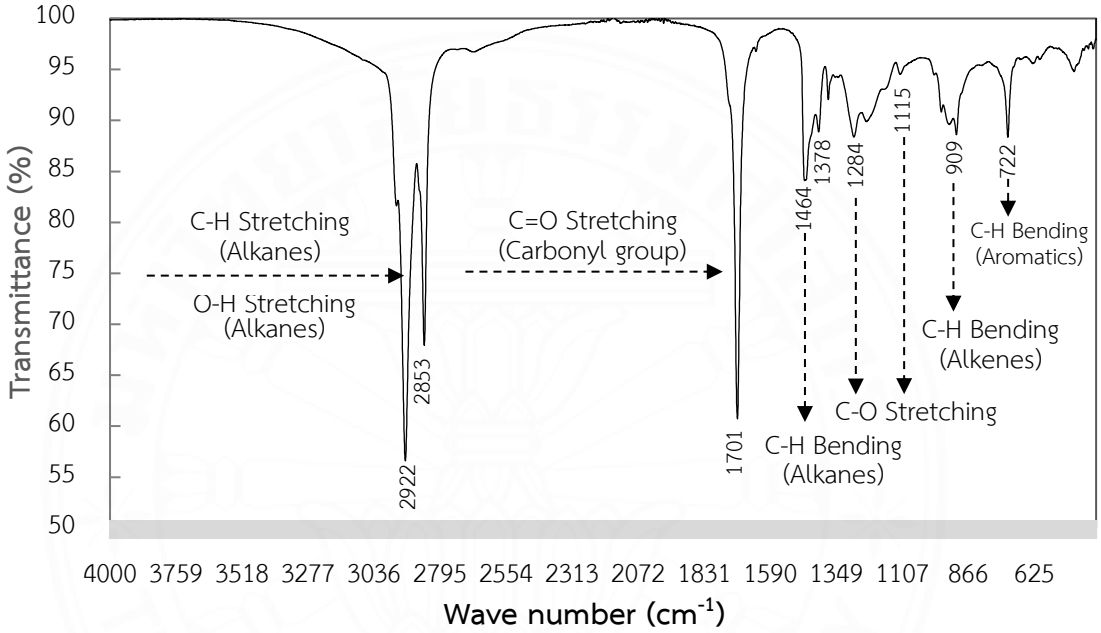

In comparison to the study of FT-IR spectra of diesel fuel and biodiesel produced from the mixture of transesterified waste canola and waste transformer oils by Qasim et al. (2017), it was found that the FT-IR spectra of liquid bio-oil was similar to diesel and biodiesel fuel in terms of high intensity of aliphatic compounds. However, there was a significant difference in the way that liquid bio-oil had intensity peaks of oxygenated compounds. These could indicate that the WCO catalytic co-pyrolysis in this study could produce a value-added liquid fuel that could potentially be upgraded to commercial diesel fuel.

4.3.6 Fuel Properties of Liquid Bio-oil

To complement the chemical compositions and functional groups of bio-oil, physical properties including density, kinematic viscosity, water content, calorific value and acid value of bio-oil obtained from catalytic pyrolysis at AC:WCO ratio of 1:40 and 400 ^{o}C were also analyzed and compared with diesel and biodiesel obtained from the transesterification process, as shown in Table 4.5.

Table 4.5 shows the calorific value of bio-oil at 40.20 kJ/g, lower than diesel petroleum fuel standard (>45 kJ/g) and biodiesel (>42 kJ/g) but higher than the original WCO before pyrolysis (39.07 kJ/g) and non-catalytic liquid bio-oil (39.73 kJ/g). This occurred because of the similar high carbon and hydrogen bio-oil contents and the low oxygen content. In previous calorific value studies of bio-oils obtained from triglyceride materials, Lam et al. (2012) reported calorific value at 40-46 kJ/g for bio-oils obtained from microwave pyrolysis of frying oil, while Ben Trabelsi et al. (2018) reported heating value of bio-oil at 36.9 kJ/g, lower than diesel and bio-diesel standards. The high calorific value of bio-oil from WCO pyrolysis with AC as a catalyst showed high potential for use as an engine fuel or as chemical feedstock to produce synthetic fuels.

Table 4.5

Fuel properties of WCO, liquid bio-oil, diesel, and biodiesel.

Fuel Properties	WCO	Noncatalytic Bio-oil [a]	Catalytic Bio-oil [a]	Biodiesel [b]	Diesel [c]
Elemental analysis, wet basis					
- Carbon (C)	78.69	77.19	79.64	76.66-79.50	85.72-86.60
- Hydrogen (H)	12.22	12.18	12.59	10.30	13.2-13.4
- Nitrogen (N)	0.89	0.47	0.37	1.30	<0.2
- Oxygen (O) [d]	0.20	10.16	7.40	8.90-11.15	-
- Sulfur (S)	-	-	-	-	<0.3
H/C ratio	1.85	1.88	1.90	1.86-1.88	1.77-1.95
Density at 15 °C (kg/m^3)	910.10	877	899	820-900	810-870
Viscosity at 40 °C (cSt)	42.50	8.03	11.16	1.8-4.5	1.8-4.1
Water content (%)	0.465	0.23	0.23	<0.5	<0.5
Calorific value (kJ/g)	39.07	39.73	40.20	>42.00	>45.00
Acid value (mgKOH/g)	5.4	128.61	126.78	0.2	5.0

The water content of bio-oil was 0.23%, conforming to the standards for diesel and biodiesel of less than 0.5%. The amount of water in the bio-oil is important because even fine droplets of water can cause damage in engine combusting cylinders and block filters. Moreover, high water content also reduces the calorific value of bio-oil.

The experimental catalytic bio-oil had a density at 15 ^{o}C of 899 kg/m^{3}, higher than the density range of diesel petroleum fuel standards (820-845 kg/m^{3}) but within the range of bio-diesel density at 820 to 900 kg/m^{3}. This result concurred with previous works (Fernandez et al., 2011; Kalargaris et al., 2017; Trabelsi et al., 2018) that recorded density of pyrolytic bio-oil produced from waste cooking oil at 899 kg/m3, indicating that bio-oil can be used directly as engine fuel. Wan Mahari et al. (2018) reported low density of liquid fuel obtained from used cooking oil by microwave co-pyrolysis, ranging from 764 to 790 kg/m^{3}.

The kinematic viscosity value of that bio-oil at 40 ^{o}C was 11.11 cSt and higher than for biodiesel (1.8-4.5 cSt) and 1.8-4.1 cSt for diesel fuel but in the same range as previous studies (Srivastava and Prasad, 2000) of pyrolytic bio-oils from triglyceride materials.

The acid values of non-catalytic bio-oil and catalytic bio-oil in this study were 118.61 and 126.78 mgKOH/g., respectively which are similar to 126.8 mgKOH/g (Trabelsi et al., 2018), 124.34 mgKOH/g (Trabelsi et al., 2014) and 124.56 mgKOH/g (Kraiem et al., 2017) in another research. This strong acidity indicated the presence of high contents of free fatty acids, especially carboxylic acid and related to the results of FT-IR and GC-MS analyses. The thermo-cracking process produces acids from triglycerides in WCO (Chiaramonti et al., 2016). The acidic components in bio-oil must be reduced for use as engine fuel because high acid components cause corrosion in fuel storage and also in other components of the engine system. One technique to reduce acidity and also enhance the properties of bio-oil is catalytic esterification (Li et al., 2020). As seen from previous work, the acid value of biodiesel obtained from the transesterification of waste cooking oil was 0.4 mgKOH/g (Santikunaporn et al., 2020)

The hydrogen to carbon ratio (H/C) is a basic characterization indicator of the presence of hydrocarbon fuels and pyrolysis oils. Alterations in H/C molar ratio indicate changes in C-C bond saturation (Yue et al., 2015). The higher the H/C ratio, the higher the energy performance of the fuels. In this study, an increase in atomic H/C ratio from 1.85 to 1.88 was observed for catalytic bio-oils compared to WCO, within the ranges of biodiesel and diesel specifications. Dehydrogenation and aromatization occurred in the WCO pyrolysis process, leading to the formation of C=C bonds, such as alkenes and aromatic compounds that were recorded in GC-MS and FT-IR analyses. Hydrogenation is one of the techniques that should be conducted to increase the H/C ratio of catalytic liquid biofuel.

The elemental composition of catalytic liquid bio-oil compared to WCO, non-catalytic bio-oil, biodiesel and diesel is shown in Table 4.5. From the analysis it can be observed that the carbon and hydrogen contents of catalytic bio-oil are 79.64 wt.% and 12.59 wt.%, respectively, which are slightly higher than those of WCO, non-catalytic bio-oil and biodiesel but lower than those of diesel. It can be said that catalytic bio-oil has superior contents of carbon and hydrogen that possibly deliver more power to the engine than biodiesel but, of course, less than diesel fuel as shown by the calorific values in Table 4.5. An important element difference between catalytic bio-oil and diesel fuel is the relatively high content of oxygen (7.4%) in catalytic bio-oil but it is less than that of biodiesel (8.90-11.15%). The oxygen composition in bio-oil is from the oxygenated compounds including carboxylic acids, alcohols, ketones, aldehydes, and ester as described in the previous section. Moreover, it could be said that AC as a catalyst in WCO pyrolysis could reduce the oxygen content compared to the oxygen content of non-catalytic bio-oil. Interestingly, the pyrolytic bio-oil has a low amount of nitrogen (0.37-0.47 wt.%) and no sulfur detected which results in lower emission of NO_x, SO_x and NH_3 to the atmosphere.

4.3.7 Energy recovery

The energy recovery of the liquid bio-oil obtained from the WCO pyrolysis at various temperatures and AC dosages calculated by Equation (1) to find the optimum condition based on the calorific value of WCO and liquid bio-oil together with the yield of liquid bio-oil is shown in Figure 4.13.

From Figure 4.13, it was found that the liquid bio-oil from the process temperature of 400°C at the AC dosage of 1:40 showed the highest energy recovery by 87.8% followed by bio-oil from the process temperature of 425 °C and 450 °C at the same AC dosage, respectively. It could be concluded that the WCO pyrolysis at 400 °C using AC as a catalyst at dosage 1:40 was the optimum condition in this batch operation study.

4.4 Conclusions

The thermo-cracking technique or pyrolysis process can be used to convert waste cooking oil into useful energy. Results revealed that temperature was the significant parameter that affects the quantity of bio-oil yield. Activated carbon in a small dosage (1:40 AC to WCO ratio) showed good catalytic performance and enhanced the pyrolysis process by reducing the optimum batch process temperature, with maximum bio-oil obtained (85.35%) at a lower temperature (400°C) compared to direct pyrolysis (425 °C) with no activated carbon as a catalyst (81.7%). Under the optimum conditions, the bio-oil had a high proportion of high calorific value diesel-like fuel with low oxygen content and no sulfur. The bio-oil also met the density value standard of biodiesel. However, the high acid value (126.78 mgKOH/g) and high viscosity of bio-oil (11.16 St) are major problems that require further study.

Figure 4.13

Energy recovery of liquid bio-oil obtained from WCO pyrolysi

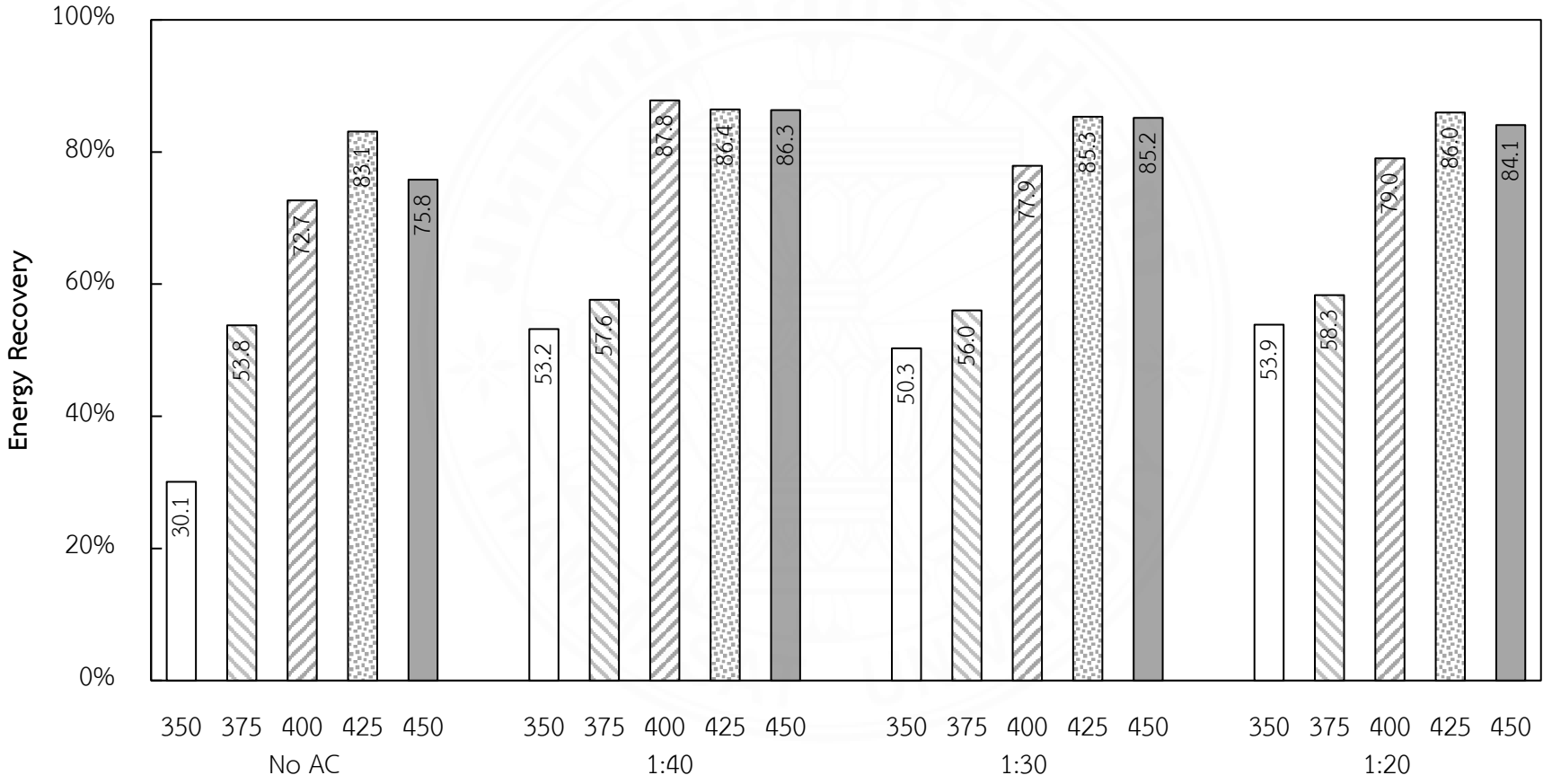

CHAPTER 5
OPTIMIZATION AND CHARACTERIZATION OF BIO-OIL PRODUCTION FROM CATALYTIC PYROLYSIS OF WASTE COOKING OIL OVER LOW-COST CARBONACEOUS CATALYST USING RESPONSE SURFACE METHODOLOGY

5.1 Introduction

The escalating demand for fossil fuels, driven by industrialization, global economic expansion, and population growth, has spurred a quest for alternative energy sources. Biofuels have emerged as a promising option due to their potential to replace or blend with fossil fuels (Zhang et al., 2014). Initial studies focused on first-generation biofuels using agricultural residues and industrial byproducts (Lu et al., 2009), while subsequent research explored second-generation biofuels, examining various biomasses and conversion methods like pyrolysis, a thermochemical technique. Pyrolysis, involving heating biomass without oxygen, produces diverse products but faces challenges such as relatively low yield and inferior properties compared to fossil fuels, mainly due to high oxygen content (Kim and Kim, 2000). Recent interest has also turned to waste cooking oil (WCO) as a feedstock for pyrolysis-based biofuel production, given its abundance and economic feasibility (Wang et al., 2012; Zhou et al., 2017). However, managing WCO remains suboptimal, lacking proper disposal guidelines, leading to socio-environmental issues. Despite economic considerations, valorizing WCO offers a potential solution to address environmental challenges associated with its disposal (Xu et al., 2016).

The direct use of waste cooking oil (WCO) as fuel in diesel engines poses combustion and air pollution challenges due to particulate matter deposition (Graboski and Cormick, 1998). Various methods have been proposed to enhance WCO properties to resemble diesel, including transesterification and thermochemical conversion via pyrolysis, the latter leveraging the organic molecules present in WCO (Demirbas, 2008). Pyrolysis parameters such as temperature, catalysts, and their dosage significantly

impact product yield and properties, particularly for liquid bio-oil (Chiaramonti et al., 2016. While activated carbon (AC) has been extensively studied as a catalyst in biomass pyrolysis, its use in WCO pyrolysis remains limited, with some studies focusing on its role as an absorber in microwave-assisted pyrolysis (Lam et al., 2016; Lam et al., 2017). AC's porosity enhances reactivity during conventional WCO pyrolysis, offering potential as a catalyst, a facet relatively unexplored compared to studies utilizing zeolites or aluminosilicates in WCO catalytic pyrolysis (Li et al., 2016; Ngo et al., 2010; Chiaramonti et al., 2016), or employing AC solely as a heat-transferring agent in microwave-assisted pyrolysis.

In addition to the activated carbon dosage in waste cooking oil pyrolysis, we also place significant emphasis on the porosity characteristics or the BET surface area of the activated carbon, which is the crucial function in the performance of AC, on the WCO pyrolysis process. In this chapter, we illustrates the effect and optimization of reaction conditions including reaction temperature, AC dosage (AC:WCO), and BET surface area on liquid bio-oil not only in terms of the bio-oil yield but also the percentage of energy conversion based on the heating value. Lam et al. (2017) also observed the effect of AC dosage not only on liquid bio-oil yield but also the energy recovery based on the heating value of liquid bio-oil from used frying oil microwave pyrolysis in order to compare the economic feasibility of liquid bio-oil production.

Various optimization techniques such as Design Expert, Super Pro Designer, and Response Surface Methodology (RSM) have been utilized to investigate the impact of process parameters on maximizing bio-oil yield in pyrolysis across different feedstock materials (Abnisa et al., 2011; Abnisa et al., 2014; Mabrouki et al., 2015; Zhuang et al., 2022). RSM particularly stands out as a simplified yet powerful approach, employing mathematical and statistical methods to analyze interactions among various process parameters and predict different pyrolytic product yields. This method allows for the selection of optimal conditions for achieving the highest liquid yields with a reduced number of experiments, while employing Analysis of Variance (ANOVA) to assess the significance and suitability of the RSM-suggested model (Nayak and Vyas, 2019; Nayak and Vyas,2022).

However, to the best of our knowledge, the optimization of carbonaceous catalytic pyrolysis parameters during the production of bio-oil from WCO using RSM has not been previously reported. Optimization of the catalytic pyrolysis process conditions for WCO is necessary to maximize not only the bio-oil yield but also the energy conversion value. Because the energy conversion value presents the energy that can be recovered in the WCO pyrolysis process instead of focusing only the quantity of liquid bio-oil. The energy conversion was calculated based on the heating value and yield of liquid bio-oil comparing to the heating value and weight of WCO as a feedstock (Lam et al., 2017). Investigating multifactor optimizations of the operating conditions at the laboratory scale will assist in designing a pilot-scale plant to enhance industrial-scale development of a pyrolysis reactor.

Therefore, the relationship between the reacting temperature, AC dosage, and various BET surface areas of AC (500, 750, 1000 m^2/g) were statistical estimate and experimental designed via a central composite design (CCD) with Response Surface Methodology (RSM) by three variables factors and three levels.

5.2 Experimental setup

Chapter 3 detailed laboratory-scale batch pyrolysis experiments conducted using waste cooking oil (WCO) mixed with activated carbon (AC) at mass ratios of 1:40, 1:30, and 1:20 together with various BET surface areas of AC (500, 750, 1000 m^2/g). Pyrolysis temperatures ranged from 375°C, 400°C, and 425°C, monitored and maintained for 30 minutes, with continuous stirring at 40 rpm using an electric magnetic stirrer heating mantle. And using the central composite design (CCD) method from Minitab software 17 to design the experiment as described in Chapter 3.

5.3 Results and discussion

5.3.1 Changes in percentage compound distribution of liquid bio-oil and WCO

Figure 5.1 illustrates the changes in the percentage compounds distribution of liquid bio-oil at various process temperatures in comparison to those found in WCO, as analyzed by the GC-SIMDIS technique. The analysis revealed that almost all compounds (>90 wt.%) in WCO were distilled at temperatures exceeding 350 ^{o}C, indicating the presence of heavy compounds with a carbon atom greater than 20 (C>20), relating to the boiling points of palmitic acid, oleic acid and linoleic acid (Aslam et al., 2015).

In contrast, an examination of the compound distribution in catalytic liquid bio-oil derived from WCO pyrolysis revealed a shift towards lower distillation temperatures, ranging from 350 ^{o}C down to 100 ^{o}C, especially for at the process temperature at 400 ^{o}C and 425 ^{o}C as shown in Figure 5.1a and 5.1b, respectively. This shift indicated the prevalence of lighter compounds within the liquid bio-oil. It was evident that catalytic WCO pyrolysis facilitated the conversion of heavy, long carbon-chain compounds into more valuable products characterized by lower carbon-chain compounds present in the liquid bio-oil.

Consequently, in the selection of optimizing conditions for generating more valuable alternative energy, enhancing product yield, and improving energy conversion in terms of heating value, it becomes essential to consider securing the most suitable economic feasibility.

Figure 5.1

Compounds distribution of liquid bio-oil obtained from catalytic WCO pyrolysis at various temperatures: (a) at 375 °C, (b) at 400 °C and (c) at 425 °C.

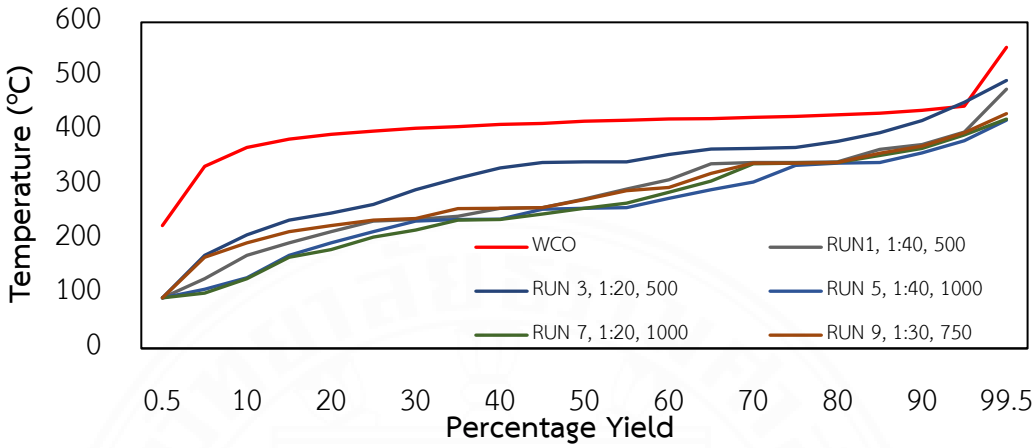

(a) At 375 °C

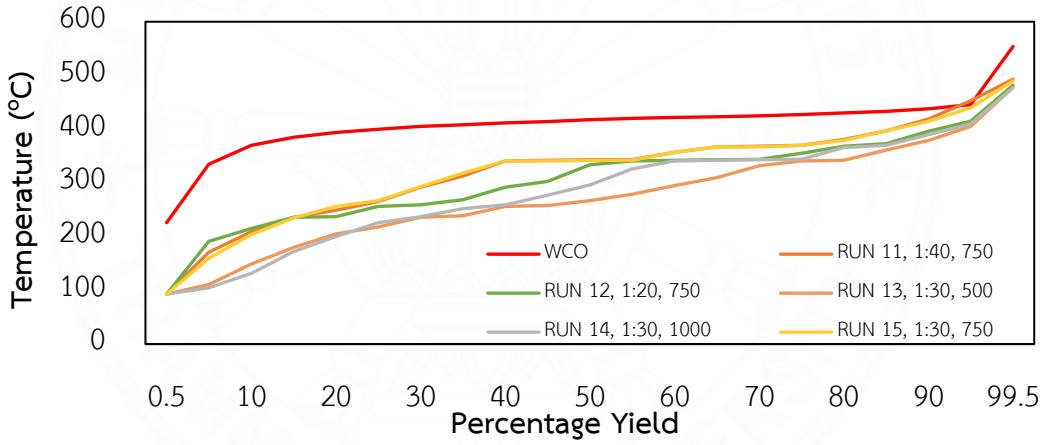

(b) At 400 °C

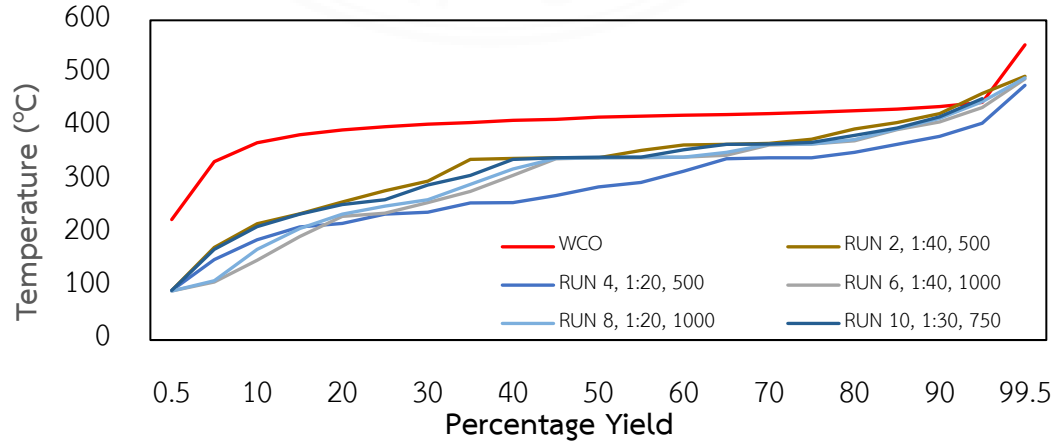

(c) At 425 °C

5.3.2 Experimental design and optimum condition based on RSM

For more understanding on the parameters that affect the catalytic WCO pyrolysis besides AC dosage and process temperature, BET surface area of AC was also investigated.

The examination of the optimization of the catalytic pyrolysis process conditions for WCO is necessary to maximize bio-oil yield and energy recovery value. Investigating multifactor optimizations of the operating conditions at the laboratory scale will assist in designing a pilot-scale plant to enhance industrial-scale development of a pyrolysis reactor.

Optimum operating parameters were investigated by RSM for maximum energy recovery values based on their heating value of liquid bio-oils (calculated from Equation 3.1). Process temperature, AC dosage (AC:WCO ratio), and BET surface area were chosen as the independent parameters, with yield of liquid bio-oil and heating values as the dependent parameters. The RSM technique was used to design the number of experiments by utilizing a central composite design (CCD). The significance of each factor was evaluated through a batch experiment. The CCD was operated by determining the specific ranges and levels of the three independent parameters, as listed in Table 3.2 and the coefficient values of three variables as listed in Table 3.3.

5.3.3 Experimental design and optimum condition for energy conversion of bio-oil

Liquid bio-oil was produced from WCO pyrolysis in a batch reactor at 30 min over temperature range 375 to 425 °C by varying the AC to WCO ratio at 1:40, 1:30 and 1:20 together with BET variation from 500-1,000 m^2/g. The heating value of liquid bio-oils was investigated. The calculated energy recovery from the production yield of liquid bio-oil in each experiment was calculated from Equation 3.1. Responses obtained from 16 experimental runs according to the CCD are shown in Table 5.1. The optimum condition was achieved in run number 6 with AC:WCO ratio of 1:40 under process temperature 425 °C and BET surface area 1,000 m^2/g. Maximum energy conversion values from the optimum condition determined from the experiment and predicted from the model were 88.135% and 89.359%, respectively. After the

optimization, the maximum value of energy conversion was analyzed from Minitab Software version 17 found to be 93.41% with the condition of process temperature 425 °C, AC:WCO ratio of 1:40 and BET surface area 757.58 m^2/g. Consequently, the optimum condition for liquid bio-oil production with highest energy conversion was achieved by an experimental design using RSM.

Table 5.1

Experimental design and results of the energy conversion of liquid bio-oil yields from WCO pyrolysis

Run	Parameter			Bio-oil yield (wt.%)	Heating value (kJ/g)	Energy Conversion (%)	
	X_1 (°C)	X_2 (AC:WCO)	X_3 (m^2/g)	Experimental	Experimental	Experimental	Predicted
1	375	1:40	500	62.11	40.033	63.638	60.672
2	425	1:40	500	85.33	40.092	87.558	87.708
3	375	1:20	500	66.58	38.762	66.052	65.841
4	425	1:20	500	85.31	40.268	87.921	85.369
5	375	1:40	1000	53.75	38.195	52.544	55.849
6	425	1:40	1000	87.82	39.212	88.135	89.356
7	375	1:20	1000	59.60	38.090	58.102	57.127
8	425	1:20	1000	83.02	38.236	81.244	83.126
9	375	1:30	750	57.43	38.112	56.019	56.864
10	425	1:30	750	85.18	39.143	85.335	84.633
11	400	1:40	750	85.35	40.197	87.807	86.095
12	400	1:20	750	79.09	41.354	83.709	85.565
13	400	1:30	500	69.34	38.333	68.029	73.607
14	400	1:30	1000	77.93	38.181	76.158	70.772
15	400	1:30	750	78.83	38.614	77.906	77.806
16	400	1:30	750	78.67	38.735	77.991	77.806

5.3.4 Regression model, statistical analysis, and response surface contour plots of energy conversion from liquid bio-oil production

From experimental and predicted results were shown in Table 5.2, regression analysis was used to derive the relationship between an energy conversion of liquid bio-oil yields and 3 dependent parameters in the form of a polynomial equation obtained in Equation 5.1.

$$Y = -1925.87306+9.594996X_1-1766.00991X_2+0.03645X_3-0.01128X_1X_1+58409.73504X_2X_2-0.00009X_3X_3-6.00624X_1X_2+0.00026X_1X_3-0.31126X_2X_3 \quad (5.1)$$

Table 5.2

Estimated the regression coefficients for regression model.

Source	Coefficients	Standard Error	t Stat	P-value	Remark
Intercept	-1925.87306	637.894	-3.016	0.02352	Significant
X_1	9.594996	3.237	2.962	0.02523	Significant
X_2	-1769.00991	2332.890	-0.759	0.47676	
X_3	0.03645	0.112	0.324	0.75709	
X_1X_1	-0.01128	0.004	-2.796	0.03132	Significant
X_2X_2	58409.73504	18416.776	3.174	0.01921	Significant
X_3X_3	-0.00009	0.00004	-2.235	0.06685	
X_1X_2	-6.00624	4.581	-1.311	0.23774	
X_1X_3	0.00026	0.0002	1.118	0.30638	
X_2X_3	-0.31126	0.458	-0.679	0.52217	
Regression Statistics					
Multiple R	0.97798				
R^2	0.95645				
Adjusted R^2	0.89112				
Standard Error	4.0942	Observations		16	

From Table 5.2, The coefficient of determination illustrated R^2 of 0.95645 and the adjusted R^2 of 0.89112 demonstrate a high level of precision and reliability in the 16 different experimental runs, as depicted in Figure 5.2. Moreover, P-values below 0.05 indicate that the corresponding model variables have a noteworthy impact on the response. The analysis indicates that the linear term, process temperature (X_1), was a significant factor in the model. Additionally, X_1X_1 and X_2X_2 are also significant factors, with P-values lower than 0.05. Although certain parameters may not exhibit statistical significance, they are retained in the equation to ensure precise predictions. Every component of the equation plays a role in achieving accurate results.

Figure 5.2

Comparison between actual and predicted energy conversion from bio-oils

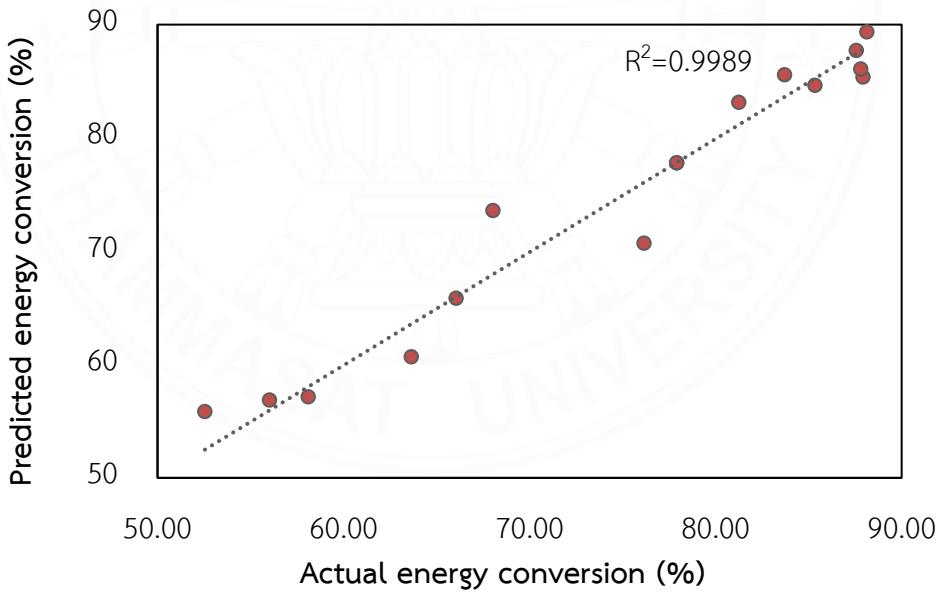

ANOVA was used to validate the statistical significance of the regression model. The ANOVA results for the RSM are presented in Table 5.3. The F-significance value of the model was found as 0.00197, which is less than the significance level of 0.05. Therefore, the model is deemed significant at a confidence level of 95%.

Table 5.3

ANOVA for the response surface model.

Source	Degree of freedom	Sum of square	Mean square	F-value	Significance F
Regression	9	2208.182	245.354	14.6401	0.00197
Residual	6	100.549	16.758		
Total	15	2308.732			

5.3.5 Effect of process parameters on energy conversion

Numerical optimization was utilized to optimize the energy conversion of liquid bio-oil in the pyrolysis process of WCO. This was accomplished by employing RSM to generate a three-dimensional (3-D) plot for visualization. The 3-D plot effectively demonstrated the relationship between the process response and two selected parameters while keeping the other parameters constant. In Figure 5.3, the 3-D and 2-D response surface plots depict the impact of temperature and AC:WCO ratio, temperature, and BET, and BET surface area and AC:WCO ratio, as the key factors influencing energy conversion of liquid bio-oil in the WCO pyrolysis process.

5.3.5.1 Effect of temperature on energy conversion of bio-oil yield

The response surface plots in Figures 5.3a and 5.3b illustrate the interaction between temperature and AC:WCO ratio (X_1X_2) and between temperature and BET surface area (X_1X_3), respectively. Temperature (X_1) with P-value of 0.02523 was the most significant term of the model for production of liquid bio-oil from WCO pyrolysis, while interaction of X_1X_1 was also a significant term with P-value 0.03132. These terms significantly influenced the yield of liquid bio-oil with optimum temperature determined as 425 ^{o}C. The higher the temperature, the lower the liquid bio-oil yield. The liquid bio-oil yield increased with increasing temperature up to the optimum temperature and then decreased due to secondary decomposition leading to increasing gas yield (Xie et al., 2015).

5.3.5.2 Effect of AC:WCO ratio on energy conversion of bio-oil yield

In this study, the AC:WCO ratio (X_2) with a high P-value of 0.47676 was a non-significant model term for the conversion of energy in liquid bio-oil from WCO pyrolysis. This was the same for interactions between temperature and AC:WCO ratio (X_1X_2) (Figure 5.3a) and between AC:WCO ratio and BET (X_2X_3) (Figure 5.3c). However, the interactions X_2X_2 had a P-value of 0.01921 which was lower than 0.05 and considered significant. Therefore, there was no need to add AC as an activating agent at more than 1:20 ratio.

5.3.5.3 Effect of BET surface area on energy conversion of bio-oil yield

BET (X_3) with P-value 0.75709 was also described as a non-significant term of WCO pyrolysis. At constant temperature and AC:WCO ratio, Figure 5.3c showed small changes of liquid bio-oil increase with increasing BET surface area but at a non-significant level. The interaction of X_3X_3 had a high P-value of 0.06685, which was higher than 0.05 but showed some changes in energy conversion and was considered less significant, even though having a positive effect, as observed from Equation 5.1. Thus, a high BET surface area of AC as a catalyst was not necessary for the WCO pyrolysis process. A high BET surface area of AC is necessary for the adsorption-desorption process, while pyrolysis is a thermo-cracking process. Therefore, AC enhanced the pyrolysis process as a catalyst by acting as a heat-transfer agent (Lam et al., 2016; Lam et al., 2016; Lam et al., 2017) that enhanced the reaction temperature and assisted the thermal cracking of long carbon-chain compounds into light carbon-chain compounds in the form of condensable gases, resulting in a higher yield of liquid bio-oil.

Figure 5.3

3-D and 2-D surface response plots showing the effect of (a) temperature and AC:WCO ratio, (b) temperature and BET, and (c) BET and AC:WCO ratio on liquid bio-yield produced from WCO pyrolysis.

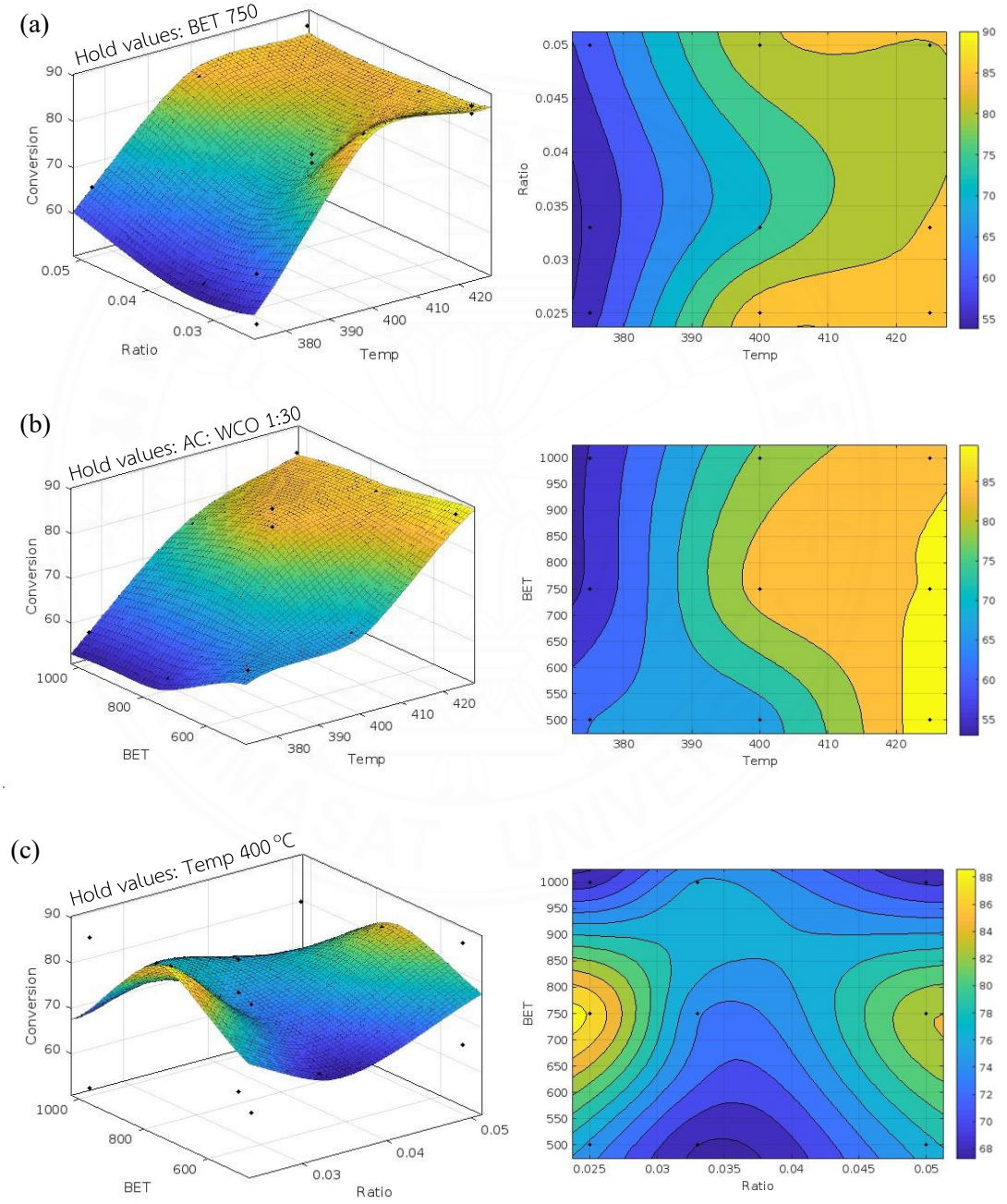

5.5 Liquid bio-oil characterization

The characterization and fuel properties of liquid bio-oil were investigated using the liquid bio-oil obtained from the optimum condition by the proportion AC:WCO ratio of 1:40 under process temperature 425 ^{o}C and BET surface area 1,000 m^2/g of WCO pyrolysis.

5.5.1 GC-MS Analysis

Chemical compositions present in liquid bio-oil obtained from the optimum condition were investigated by GC-MS analysis. Major organic compositions identified by their wt.% in liquid bio-oil are shown in Figure 5.4. The liquid bio-oil produced from WCO pyrolysis consisted of 31.96 wt.% of hydrocarbon compounds and 68.04 wt.% of oxygenated compounds. The hydrocarbon compounds in liquid bio-oil were 21.38 wt.% alkanes, 10.47 wt.% alkenes, and a small amount of 0.11 wt.% alkynes, while the oxygenated compounds were 44.82 wt.% carboxylic acids, 12.85 wt.% alcohol, 3.86 wt.% esters, 3.47 wt.% ketones and 1.62 wt.% aldehydes. Similar compounds found in bio-oils were reported by many previous studies of various types of triglyceride feedstock pyrolysis. Trabelsi et al. (2014) reported that the major compounds in bio-oil produced from WCO pyrolysis were 89.61wt.% carboxylic acid, 2.31 wt.% linear saturated hydrocarbons, 3.64 wt.% linear unsaturated hydrocarbons, 0.17 wt.% cyclic-hydrocarbons,1.86 wt.% alcohols, 0.25 wt.% ketones and 0.25 wt.% aldehydes. Similarly, Kraiem et al. (2017) observed that the composition of bio-oil obtained from pyrolysis analyzed by GC-MS included various oxygenated compounds including 53.11% carboxylic acids, 1.71% aldehydes, 1.21% ketones and 0.93% alcohols. The bio-oil also contained 4.03% linear-saturated-hydrocarbons, 28.65% unsaturated hydrocarbons and 9.54% cyclic-hydrocarbons. These findings highlighted the significant presence of hydrocarbon components, particularly carboxylic acids, which were associated with the high concentration of fatty acids in waste frying oil. Ngo et al. (2010) investigated the GC-MS chemical compositions of bio-oil products obtained from soybean oil pyrolysis with various catalysts using a fixed-bed reactor.

Results showed that the major components in bio-oil were organic compounds with carbon atoms ranging from C5 to C11 at 21.7% and C12 to C18 at 17.8%.

5.5.2 FT-IR Analysis

The FTIR spectrum indicating functional groups of organic compounds present in liquid bio-oil obtained from the optimum operating condition is shown in Figure 5.5. Intense peaks observed within the wave number range 2916 and 2848 cm−1 corresponded to carboxylic acids and alkanes. The high intensity of these peaks indicated the prevalence of saturated aliphatic hydrocarbons in the bio-oil. The existence of other aliphatic groups was evident from wave numbers ranging between 1464 and 1430 cm−1, confirming the aliphatic character of the bio-oil. The presence of oxygen in the bio-oil was indicated by wave number of 1702 cm−1 which represented the signal of C=O stretching, signifying the presence of carbonyl groups such as aldehydes, ketones, esters, and carboxylic acids. The C-O stretching vibration was confirmed by bands observed within the range 1292 to 1188 cm−1 representing esters, ethers, alcohols, and carboxylic acids. Weaker bands ranging from 938 to 686 cm−1 were attributed to C-H bending, indicating the presence of alkenes and aromatic hydrocarbons in the bio-oil. The bio-oil derived from this study was influenced by carboxylic acids, aliphatic hydrocarbons, and small quantities of aromatics, aldehydes, and ketones. These results were consistent with the organic compound groups analyzed using GC-MS.

The FTIR spectrum of liquid bio-oil in this study was compared to the FTIR spectra of diesel fuel and biodiesel produced from a mixture of transesterified waste canola and waste transformer oils in a study conducted by Qasim et al. (2017). The comparison revealed that the liquid bio-oil shared similarities with diesel and biodiesel fuels in terms of the presence of aliphatic compounds which exhibited high intensity. However, there was a noticeable difference in the intensity peaks of oxygenated compounds observed in the liquid bio-oil.

Figure 5.4

Major group of organic compositions in liquid bio-oil obtained from the optimum condition of WCO pyrolysis.

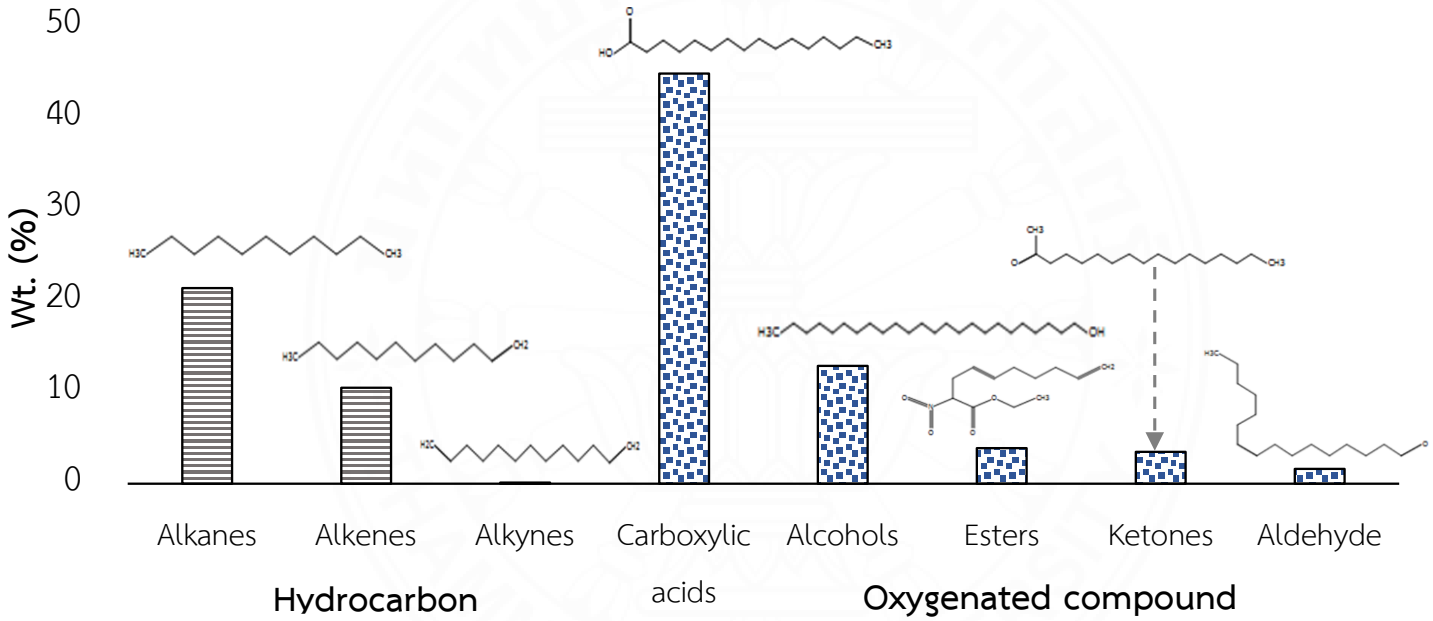

Figure 5.5

FT-IR spectra of liquid bio-oil obtained at the optimum operating condition.

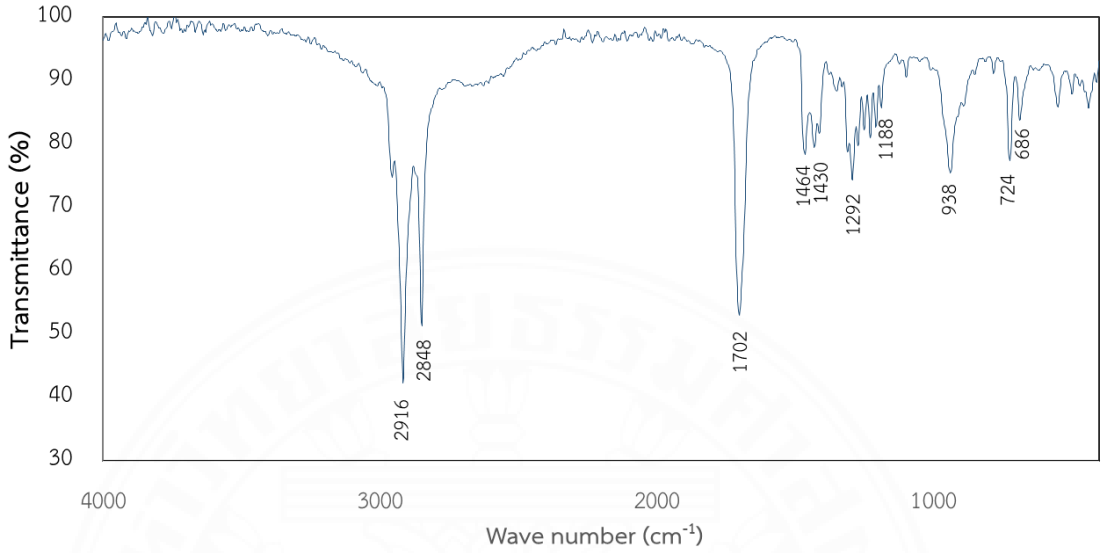

5.5.3 Fuel properties of liquid bio-oil

The physical characteristics of liquid bio-oil obtained from the optimum condition such as density, kinematic viscosity, water content, calorific value, and acid value were examined and compared to the diesel and biodiesel standards through ASTM and EN, as shown in Table 5.4.

Table 5.4

The fuel properties of liquid bio-oil obtained at the optimum condition compared to ASTM and EN biodiesel standards.

Fuel Properties	Bio-oil [a]	ASTM Standard [b]	EN Standard [b]	Diesel [c]
Density at 15 °C (kg/m^3)	890	860-900	860-900	810-870
Viscosity at 40 °C (cSt.)	11.62	1.9-6.0	3.5-5.0	1.8-4.1
Calorific value (kJ/g)	39.21	-	-	>45.0
Water content (%)	0.31	<0.5	<0.5	<0.5
Acid value (mgKOH/g)	126.67	<0.5	<0.5	<0.5

[a] Bio-oil from this work; [b] Biodiesel standard (Montero and Stoytcheva, 2011)

[c] Specification of diesel (Mahari et al., 2017; Tutunea et al., 2018; Ilkilic and Oner, 2017; Hansdah et al., 2013; Mamat et al., 2015).

Liquid bio-oil had a density at 15 ^{o}C of 890 kg/m^{3}, which was within the range of ASTM and EN standards but slightly higher than the diesel fuel standard (810-870 kg/m^{3}). This result concurred with previous studies (Trabelsri et al., 2018; Banchapattanasakda et al., 2023; Mahari et al., 2018) that reported density ranging 880-899 kg/m^{3} for pyrolytic bio-oil derived from waste cooking oil pyrolysis. Results suggested that liquid bio-oil could be utilized as a fuel for engines without requiring any additional processing in terms of density character.

Kinematic viscosity at 40 ^{o}C was 11.62 cSt which was greater than the biodiesel standards (ranging 1.9-6.0 cSt for ASTM and 3.5-5.0 cSt for EN) and for diesel fuel (ranging 1.8-4.1 cSt). Kinematic viscosity was within the ranges observed in previous research (Kalargaris et al., 2017) on pyrolytic bio-oils derived from triglyceride pyrolysis.

The liquid bio-oil had a calorific value of 39.21 kJ/g which was lower than the diesel fuel standard. This result followed the same trend as a previous study where pyrolytic bio-oil produced from waste cooking oil pyrolysis was reported with a low heating value of 36.9 kJ/g (Trabelsi et al., 2018). Results indicated that liquid bio-oil in this study had significant potential for use in synthetic fuel production as a feedstock.

The water content of the liquid bio-oil was 0.31%, which met the standard criteria for biodiesel and diesel fuel (<0.5%).

The major weakness of catalytic liquid bio-oil in this study was the acid value at 126.67 mgKOH/g, and higher than ASTM, EN and the diesel fuel standards but comparable to values found in previous studies as 126.8, 124.3, 126.78, and 124.56mgKOH/g, respectively (Trabelsi et al., 2014; Trabelsi et al., 2018; Banchapattanasakda et al., 2023; Qasim et al., 2017). The presence of acidic elements must be minimized for bio-oil to be suitable as engine fuel as these can lead to corrosion and plugging problems in engine systems. Compared to the biodiesel and diesel fuel standards, the catalytic co-pyrolysis of waste cooking oil in this study showed potential to produce a valuable liquid fuel that could be further improved for commercial diesel fuel applications.

5.5.4 GC-SIMDIS Analysis

In this study, the characterization of bio-oil obtained under optimal conditions (425 °C, 1:40, 1000) was performed using GC-SIMDIS analysis. Additionally, an examination was conducted on four additional samples of bio-oil, selected based on their maximum energy conversion values as obtained from section 5.3 including (425 °C, 1:20, 500), (400 °C, 1:40, 750), (425 °C, 1:40, 500), and (425 °C, 1:30, 750), respectively. It is noteworthy that the selection of the optimal condition in the catalytic WCO pyrolysis process is not only dependent on the yield of bio-oil and the percentage of energy conversion, but also on the presence of desirable compounds within the bio-oil as a second screening criteria for selecting the optimum condition for catalytic WCO pyrolysis over activated carbon as catalysts.

In particular, the presence of the diesel-like fraction in the bio-oil was identified as the most desirable compound in this context. Therefore, it is imperative to consider the abundance of such valuable compounds alongside the quantitative criteria when determining the optimum condition for the catalytic WCO pyrolysis process.

The distribution of each bio-oil separated at different temperature ranges by GC-SIMDIS is presented in Figure 5.6. The liquid bio-oil were fractionated into the fuel-like compounds with boiling temperature higher than 350 °C (>C20), the diesel-like compounds with boiling temperature range of 250–350 °C (C15–C20), the kerosene-like compounds with boiling range of 180-250 °C (C11-C14) and the gasoline-like compounds with boiling temperature lower than 180 °C (<C11). At the optimum condition, the major components in the bio-oil were the diesel-like compounds by 40%. Then, the fuel oil-like compounds by 34.00%, the kerosene-like compounds by 14.00% and the gasoline-like compounds by 12% as can be seen in Figure 5.6a. Compared to the liquid bio-oil obtained from the same condition but absence of AC, it can be observed that when the AC was used, the distribution of diesel-like compounds and gasoline-like compounds increased from 39% to 40%, and from 6% to 12%, respectively. But when compared to another conditions, the maximum of

diesel-like fraction was 45% from the reacting condition of 1:40 AC:WCO ratio with BET 750 m^2/g under the reaction temperature of 400 ^{o}C.

Moreover, the liquid bio-oil yield as shown in Figure 5.6b must also be considered. When the AC was used, the production of liquid bio-oil increased from 81.70 g to 85.35 g which results in the diesel-like compound as the maximum yield by 38.41 g of liquid bio-oil obtained from the reacting condition of 1:40 AC:WCO ratio with BET 750 m^2/g under the reaction temperature of 400 ^{o}C, while 35.13 g from the optimum reaction condition. From these results, it can be said that direct pyrolysis was the major decomposition mechanism of triglycerides in WCO. And when the AC was used, AC acted as a heat-transfer agent (Lam et al., 2016; Lam et al., 2017; Banchapattanasakda et al., 2023) that enhanced the reaction temperature in the pyrolysis process by promoting thermal cracking from heavy carbon compounds (43%) to form lighter carbon compounds (34%) and produce more valuable products such as diesel-like compounds in the liquid bio-oil in this study (Banchapattanasakda et al. (2023).

The adoption of a multifaceted approach in the evaluation of bio-oil production contributes significantly to a thorough and comprehensive analysis. By employing such an approach, well-informed decisions can be made pertaining to the identification of optimal operating conditions, leading to improved energy conversion efficiencies and the attainment of desirable product outcomes. Additionally, the implementation of energy-saving measures in the pyrolysis process can be facilitated. In order to advance the scope of research, it is essential to incorporate the design of experiment (DOE) methodology, which enables a systematic investigation of the impacts of various reacting parameters on key product yields, such as the fraction of diesel-like fuel. This systematic investigation should further enhance the understanding and potential optimization of the bio-oil production process.

Figure 5.6

The fractionated compounds of liquid bio-oil according to the boiling temperature distribution by GC-SIMDIS analysis. (a) Product distribution by percentage; (b) yield of liquid bio-oil and product distribution by amount.

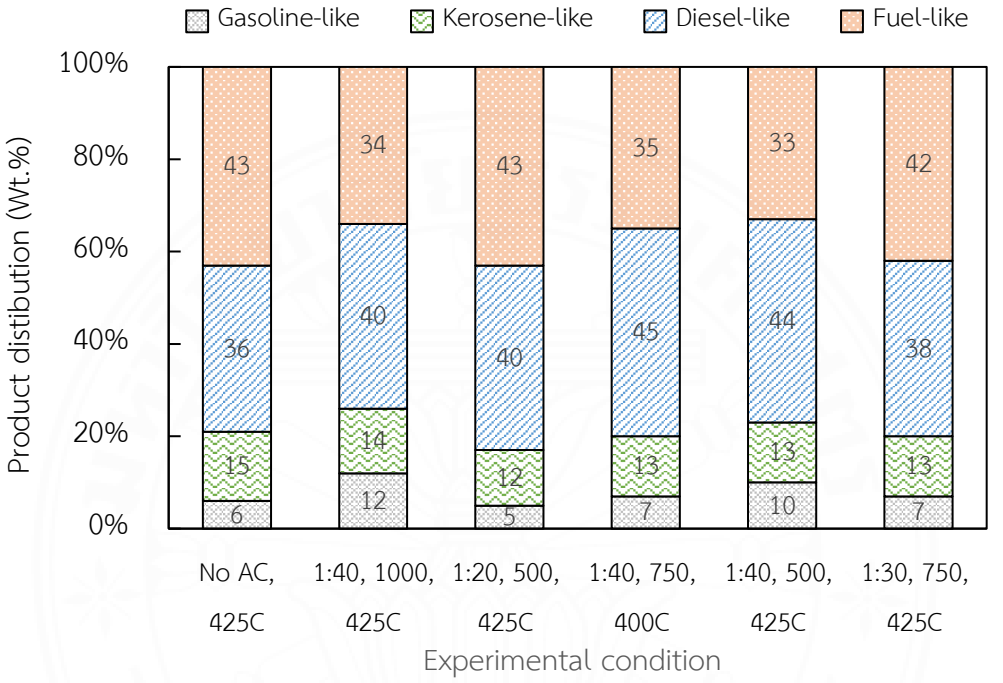

(a)

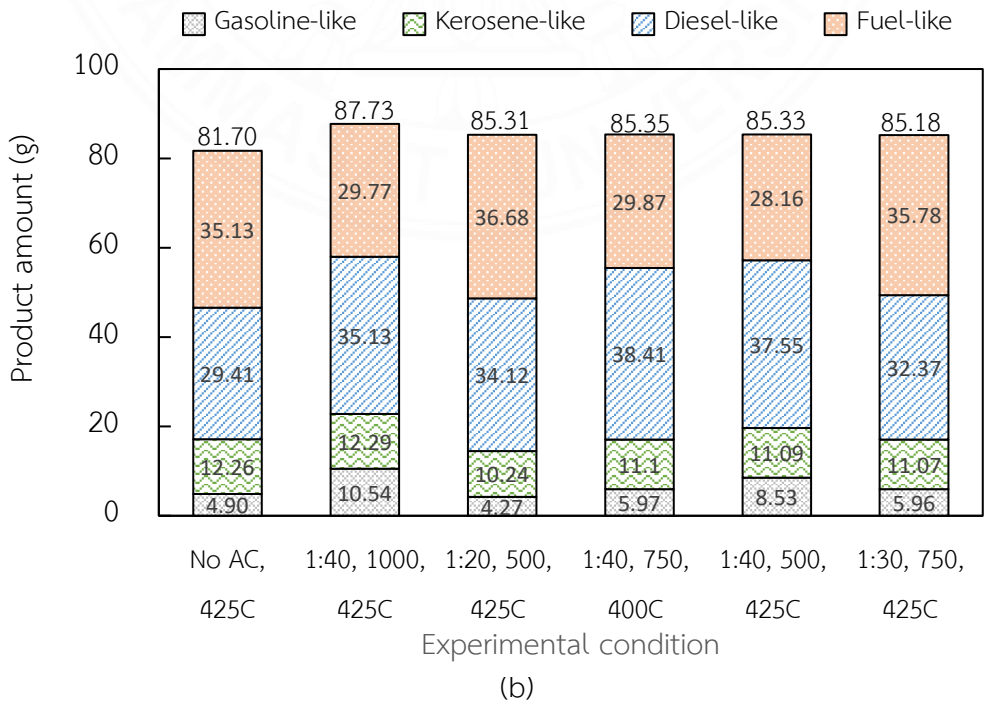

(b)

CHAPTER 6
BIO-OIL PRODUCTION VIA CATALYTIC SUPERCRITICAL ETHANOL LIQUEFACTION OF SACCHARINA JAPONICA SEAWEED

6.1 Introduction

Rising energy demands and a scarcity of petroleum-based resources have spurred extensive exploration into renewable and alternative raw materials for generating transportation fuel and electricity. This issue has gained momentum due to the environmental impact of fossil fuels, notably their contribution to global warming through greenhouse gas emissions, potentially causing acid rain and ozone layer depletion (Kunkes et al., 2008, Thøgersen et al., 2021). Hence, to mitigate the potential challenges associated with fossil fuels, seeking renewable and environmentally friendly energy alternatives becomes imperative (addressing concerns about global warming and resource depletion). In this regard, biofuels present a promising alternative compared to the traditional fuels (Faucheux et al., 2016).

Exploration into renewable energy sources and their advancement is underway due to their potential in generating enduring, low-carbon fuels. Initial investigations concentrated on first-generation biofuels, utilizing agricultural residues and industrial byproducts (Lu et al., 2009). Subsequent studies delved into second-generation biofuels, examining a wide type of biomasses. Nevertheless, a significant challenge in converting biomass into energy lies in the presence of lignin within its structure. These lignocellulosic biomass materials have undergone diverse chemical reactions, encompassing both acidic homogeneous and heterogeneous reactions at elevated temperatures and pressures.

Hence, the third-generation biofuels have been investigating new alternative energy sources to produce low-carbon and long-term fuels. This generation is the utilization of microalgae and macroalgae for biofuel production. Microalgae represent a type of photosynthetic single-celled organism that utilizes CO_2 fixation to convert solar energy into chemical energy (Razzak et al., 2022). Research by

Razzak et al., 2019 and Valdovinos-García, 2020 indicates that their efficiency in CO_2 fixation surpasses that of any other terrestrial plant by 10 to 50 times. During photosynthesis, microalgae use CO_2 from the atmosphere as a carbon source to foster cell growth and reproduction. Carbon constitutes roughly half of the weight of microalgal cells.

Utilizing algae as a source for generating energy is a well-explored area, with numerous research teams globally investigating its potential as a valuable marine resource. Algae possess distinct carbohydrates compared to terrestrial biomass (Anastasakis et al., 2011), and these carbohydrates exhibit diverse behaviors during different conversion processes. Various investigated methodologies fall under either biochemical conversion such as fermentation and anaerobic digestion (Adams et al., 2011) or thermochemical techniques such as combustion (Wang et al., 2009), pyrolysis (Ross et al., 2008), hydrothermal liquefaction (Anastasakis et al., 2011) and gasification, focusing on converting this biomass into energy carriers. Among thermochemical techniques, hydrothermal liquefaction or hydrothermal gasification (Onwudili et al., 2013) are favored due to their compatibility with wet feedstock, matching the moisture content typically present in macroalgae. Furthermore, these methods offer advantages by addressing the higher alkali content inherent in macroalgae, which might otherwise lead to complications like slagging and fouling during combustion and potentially in pyrolysis processes (Ross et al., 2009, Adam et al., 2011).

Liquefaction involves a catalyzed decomposition reaction utilizing alkaline catalysts like potassium hydroxide and sodium carbonate. To boost liquefaction efficiency, some studies have conducted the process using alcoholic solvents such as methanol, ethyl acetate, and acetone under supercritical conditions. Solvents under these conditions exhibit properties of both gas and liquid, showcasing low viscosity akin to gases but possessing high density like liquids (Mei et al., 2019). Moreover, the supercritical medium offers increased diffusivities, thus enhancing chemical reactions.

However, to the best of our knowledge, there hasn't been any prior report on the optimization of catalytic liquefaction parameters while producing bio-oil from Saccharina Japonica Seaweed. Therefore, this chapter provides the preliminary

investigated and discussed of the effect of reaction conditions including temperature, percentage of catalysts to feedstock, and EtOH per feedstock ratio on liquid bio-yields from catalytic supercritical ethanol liquefaction of Saccharina Japonica Seaweed. The relationship and the optimization of these three parameters on the liquid bio-oil yield using Box-Behnken Design (BBD) with RSM to design the experiment and analyzed the effect of these parameters.

6.2 Experimental setup

Chapter 3 detailed laboratory-scale batch catalytic liquefaction in supercritical ethanol experiment conducted using Saccharina Japonica Seaweed mixed in-situ with ethanol and KOH catalyst according to the designed conditions placed in stainless steel autoclave reactors and sealed. Then, the sealed reactor was placed into the heater for HTL process by setting the heating rate at 10 ^{o}C /min until reached the targeted process temperature and monitored for 1 hour. The experimental conditions were designed using Box Behnken Design (BBD) method from Minitab software 17 to design the experiment and created the analysis of variance (ANOVA).

6.3 Results and discussion

The data obtained from the experiments were input into the Minitab software and analyzed using the Box-Behnken method. Subsequently, a polynomial equation was generated based on the coefficients derived from the software. Furthermore, the model's validity was confirmed by comparing it with those of the experimental data obtained under specific operating conditions.

6.3.1 Polynomial equation of liquefaction

Liquid bio-oil yield from 15 experimental runs of supercritical ethanol liquefaction of Saccharina Japonica Seaweed in the presence of KOH catalyst according to the Box-Behnken is shown in Table 6.1. The predicted bio-oil yields were

calculated using the polynomial equation from equation 6.1 with coefficients obtained from the regression model through Minitab software.

$$Y = -315.2+1.139*X_1+7.71*X_2+368*X_3-0.001386*X_1^2-0.1685*X_2^2 -403*X_3^2+0.00356*X_1*X_2-0.05*X_1*X_3-8.66*X_2*X_3 \quad (6.1)$$

Where, Y represents bio-oil yield, X_1 represents process temperature, X_2 represents %catalyst: feedstock, X_3 represents EtOH: feedstock ratio, (X_1X_2, X_1X_3, X_2X_3) represents interaction coefficients, and (X_1^2, X_2^2, X_3^2) represents squared coefficients.

Table 6.1

Experimental design and results of liquid bio-oil yields

Run	Parameter			Bio-oil yield (wt.%)	
	X_1 (°C)	X_2 (%cat: feed)	X_3 (EtOH: feed)	Experimental	Predicted
1	450	25	0.25	49.551	51.235
2	450	15	0.25	47.219	47.165
3	450	20	0.35	45.314	46.463
4	450	25	0.3	49.180	46.603
5	375	25	0.35	34.568	34.926
6	375	15	0.3	43.777	44.316
7	375	15	0.35	42.727	42.186
8	375	25	0.3	40.159	41.386
9	300	25	0.25	25.359	24.835
10	300	15	0.25	25.751	26.105
11	300	20	0.35	24.137	23.483
12	300	20	0.3	26.566	27.590
13	375	20	0.25	49.220	49.344
14	375	20	0.25	49.259	49.344
15	375	20	0.25	49.539	49.344

From Table 6.1, the optimum condition was achieved in run number 1 with catalyst: feedstock of 20% under process temperature 425 °C and EtOH: feedstock ratio of 0.25. Maximum yield of bio-oil from the optimum condition determined from the experiment and predicted from the model were 49.551% and 51.235%, respectively.

The Box-Behnken design technique was utilized in conjunction with response surface methodology to observe the influence of three variables on supercritical ethanol liquefaction. Consequently, a polynomial equation was formulated to illustrate the interactive relationships among the variables and the bio-oil yield. The software-generated ANOVA results are presented in Tables 6.1 and 6.2. The coefficients extracted from Table 6.2 were incorporated into the generic polynomial equation 6.1.

Table 6.2

ANOVA for the response surface model.

Source	Degree of freedom	Sum of square	Mean square	F-value	P-value
Model Regression	9	1425.00	158.333	49.93	0.000
Residual error	5	15.85	3.171		
Lack of fit error	3	15.32	5.105	18.92	0.051
Pure error	2	0.54	0.270		
Total	14	1440.86			
S = 1.78072, R^2 = 98.90%, Adjusted R^2 = 96.92%					

The R square value of the model was found as 98.90%, which is higher than the significance level of 95.00%. Therefore, the model is deemed significant at a confidence level of 95%. Furthermore, ANOVA analysis was used to determine the significance and suitability of the statistical methodology employed as shown in Table 6.3. The p-value of 2 independent parameters including the temperature (X_1), and EtOH: feedstock ratio (X_3) was 0.000, and 0.002, respectively, which is less than 0.05

represents significant parameter, whilst the %catalyst per feedstock was 0.073 considered as non-significant.

Table 6.3

Estimated regression coefficients for regression model.

Source	Coefficients	Standard Error	t Stat	P-value	Remark
Intercept	47.000	1.240	37.99	0.000	Significant
X_1	11.674	0.684	17.06	0.000	Significant
X_2	-1.444	0.637	-2.27	0.073	
X_3	-3.307	0.560	-5.90	0.002	Significant
X_1X_1	-7.794	0.935	-8.33	0.000	Significant
X_2X_2	-4.212	0.978	-4.31	0.008	Significant
X_3X_3	-1.010	1.100	-0.91	0.402	
X_1X_2	1.335	0.839	1.59	0.172	
X_1X_3	-0.189	0.762	-0.25	0.814	
X_2X_3	-2.164	0.757	-2.86	0.035	Significant

6.3.2 Effect of process parameters on bio-oil yield

The relationship between the process response and two specific parameters while keeping all other factors constant is presented in the form of a three-dimensional and contour response surface plots by RSM as shown in Figure 6.1. The 3-D and 2-D graphical representations illustrate how temperature and %catalyst dosage per feedstock, as well as temperature and EtOH: feedstock, and %catalyst dosage and EtOH: feedstock ratio, act as crucial parameters influencing the production of liquid bio-oil during the catalytic liquefaction process. The liquid bio-oil yield increased with increasing temperature up to the optimum temperature and then decreased due to secondary decomposition leading to increasing gas yield (Xie et al., 2015).

The response surface plots in Figures 6.1a illustrate the interaction between temperature and catalyst dosage per feedstock (X_1X_2). Temperature (X_1) with P-value of 0.000 was the most significant term of the model for production of liquid

bio-oil from seaweed catalytic liquefaction, while %catalyst dosage per feedstock (X_2) and the interaction of X_1X_2 was not significant terms with P-value 0.073 and 0.172, respectively. The yield of liquid bio-oil clearly increased with the temperature raised up to approximately 430 °C the decreased the temperature higher than 430 °C. While the increasing of % catalyst dosage showed a small increase of liquid bio-oil at 20% catalyst dosage.

Figure 6.1b illustrates the interaction between temperature (X_1) and EtOH: feedstock ratio (X_3). The %EtOH: feedstock ratio (X_3) with P-value of 0.002 was the significant term of the model. While the interaction of X_1X_3 with P-value 0.814 was not significant. The yield of liquid bio-oil sharply increased with the temperature raised up to approximately 430 °C then declined but no changes for the increasing of EtOH: feedstock ratio.

The interaction between %catalyst dosage (X_2) and EtOH: feedstock ratio (X_3) is shown in Figure 6.1C. The P-value of X_2X_3 was 0.035, considered as the significant term of the model. The yield of liquid bio-oil increased when the %catalyst dosage increased up to approximately 23% then decreased when %catalyst dosage increased. Whilst the increasing of EtOH: feedstock ratio showed the opposite way by decreasing the liquid bio-oil yield.

Figure 6.1

3-D and 2-D surface response plots showing the effect of (a) how temperature and catalyst dosage per feedstock, (b) temperature and EtOH: feedstock, and (c) %catalyst dosage and EtOH: feedstock ratio on liquid bio-yield produced from WCO pyrolysis.

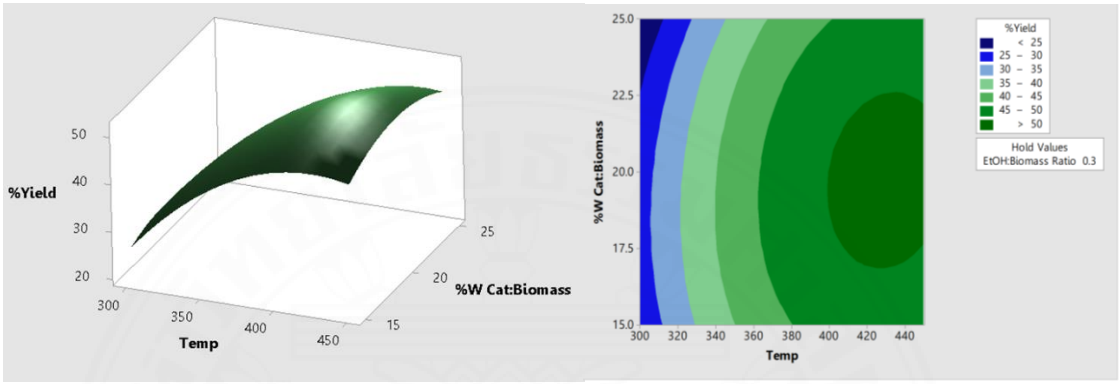

(a)

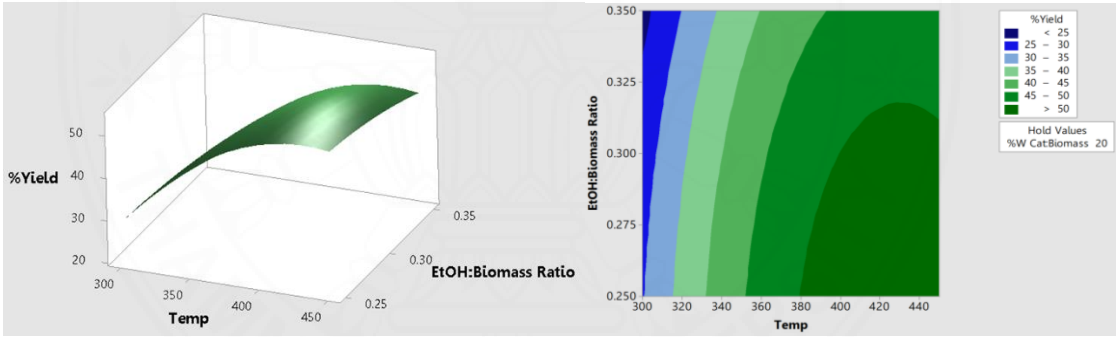

(b)

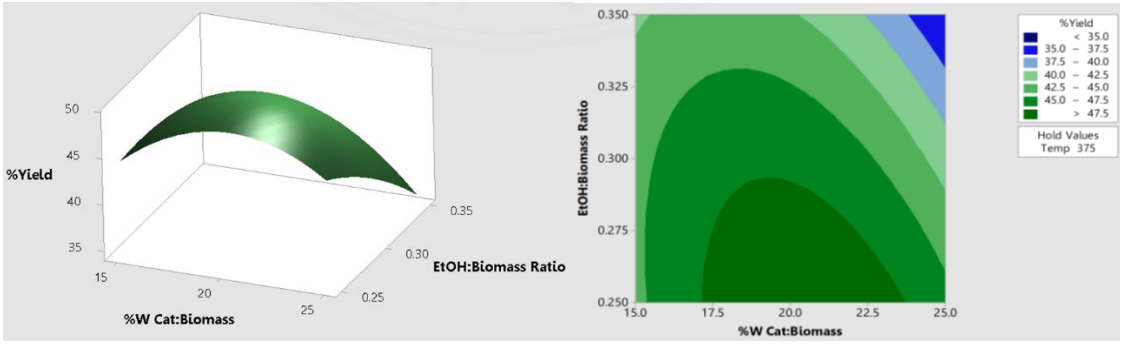

(c)

6.3.3 The optimized condition for maximized bio-oil production.

Predicting the optimal conditions for each variable in the bio-oil synthesis process to achieve the highest % yield is performed using the Response Optimizer feature in Minitab 17 software. The overall satisfaction with the response is measured using the Composite Desirability (D) function, which has a value between 0 and 1. A value of 1 for D indicates complete satisfaction with the response.

As shown in Figure 6.2, it was found that the most suitable condition for the synthesis of bio-oil with the highest % yield is at a reaction temperature of 433.33 ^{o}C, a catalyst amount per feedstock by 21.06%, and an EtOH: feedstock ratio of 0.25. Under this condition, the yield of liquid bio-oil was found to be 53.99%. The value of D was calculated to be 1. However, due to the results of ANOVA, it was found that the mathematical model is only moderately suitable for the experimental data, as evidenced by the coefficient of determination R^2 = 98.90%. Since this optimal condition was not confirmed through actual experimental verification.

Figure 6.2

The optimal condition results in the highest yield of bio-oil through the Response Optimizer function

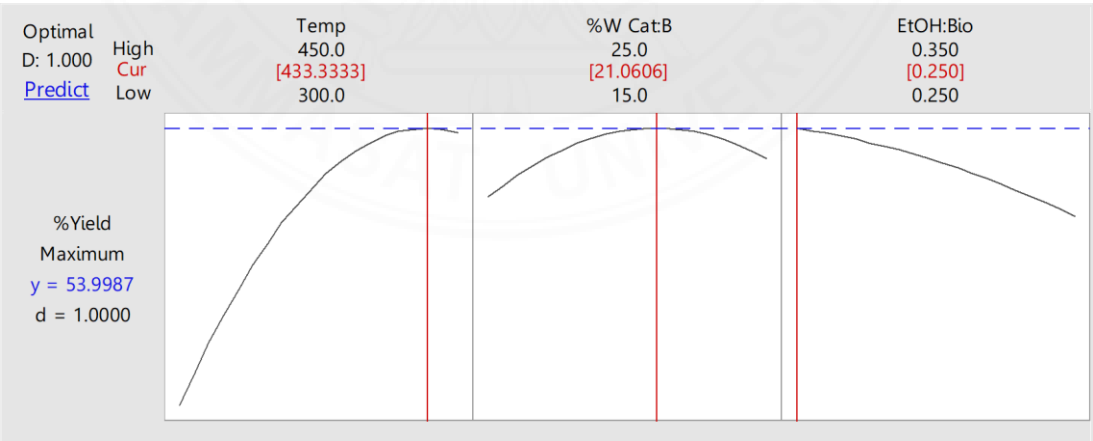

6.3.4 Heating value of liquid bio-oil

The heating value of the liquid bio-oil obtained from the catalytic liquefaction of Saccharina Japonica seaweed in supercritical ethanol at various temperatures, catalyst dosages, and %EtOH to feedstock ratio is shown in Table 6.4.

From Table 6.4, it was found that the Heating Value (HV) of liquid bio-oil was within the range of 21.18-32.55 KJ/g. It can be observed that run number 1 with catalyst: feedstock of 20% under process temperature 425 ^{o}C and EtOH: feedstock ratio of 0.25 showed the highest heating value at 32.55 (kJ/g) which is comparable to another research (Anastasakis and Ross, 2015, Jasiunas et al., 2021). When compared to the HV value of diesel fuel obtained from petroleum, which is above 45 KJ/g, it can be observed that the HV value of liquid bio-oil was lower than that of diesel fuel derived from petroleum. This could be attributed to the internal components of liquid bio-oil, such as the presence of moisture or a higher amount of oxygen content in the liquid bio-oil. Consequently, this results in a lower HV value.

Table 6.4

Heating value of liquid bio-oil.

Run	Parameter			Liquid Bio-oil	
	X_1 (°C)	X_2 (%cat: feed)	X_3 (EtOH: feed)	Yield (wt.%)	Heating value (kJ/g)
1	450	25	0.25	49.551	32.55
2	450	15	0.25	47.219	28.55
3	450	20	0.35	45.314	28.64
4	450	25	0.3	49.180	28.25
5	375	25	0.35	34.568	23.20
6	375	15	0.3	43.777	25.81
7	375	15	0.35	42.727	25.95
8	375	25	0.3	40.159	26.32
9	300	25	0.25	25.359	21.34
10	300	15	0.25	25.751	22.13
11	300	20	0.35	24.137	21.22
12	300	20	0.3	26.566	21.18
13	375	20	0.25	49.220	23.70
14	375	20	0.25	50.259	24.03
15	375	20	0.25	49.739	23.84

CHAPTER 7
CONCLUSIONS AND RECOMMENDATIONS

7.1 Conclusions

The thermo-cracking technique or pyrolysis process can be used to convert waste cooking oil into useful energy. Results revealed that temperature was the significant parameter that affects the quantity of bio-oil yield. Activated carbon in a small dosage (1:40 AC to WCO ratio) showed good catalytic performance and enhanced the pyrolysis process by reducing the optimum batch process temperature, with maximum bio-oil obtained (85.35%) at a lower temperature (400 ^{o}C) compared to direct pyrolysis (425 ^{o}C) with no activated carbon as a catalyst (81.7%). Under the optimum conditions, the bio-oil had a high proportion of high calorific value diesel-like fuel with low oxygen content and no sulfur. The bio-oil also met the density value standard of biodiesel. However, the high acid value (126.78 mgKOH/g) and high viscosity of bio-oil (11.16 cSt) are major problems that require further study.

RSM is an effective approach to predict the energy conversion of liquid bio-oil yield generated from the pyrolysis of WCO, requiring only minimal experimental runs. Optimum operating conditions resulting in the highest energy conversion (88.135%) and liquid bio-oil yield (87.82%) were process temperature 425 ^{o}C, AC:WCO ratio 1:40 and BET surface area 1,000 m^2/g. Regression analysis demonstrated an excellent fit of the quadratic model equation to the experimental data, with coefficient of determination value (R^2) 0.97 and F-value 14.64. Results revealed that process temperature was the most significant parameter impacting the yield of liquid bio-oil together with energy conversion, while AC:WCO ratio and BET surface area were non-significant parameters. Fuel properties of liquid bio-oil such as density and water content met the standards set by ASTM and EN for biodiesel and exhibited high calorific value. However, liquid bio-oil presented two significant issues that require improvement as high acid value (126.67 mgKOH/g) and high viscosity (11.62 cSt).

For the liquefaction of Saccharina Japonica seaweed, the RSM technique proves to be a highly effective method for estimating the yield of liquid bio-oil produced from the catalytic liquefaction in supercritical ethanol of Saccharina Japonica seaweed. This approach demands minimal experimental runs. The best conditions for optimal performance, achieving the highest liquid bio-oil yield (50.259%) with heating value of 24.03, was found to be a process temperature of 375 ^{o}C, %catalyst dosage of 20%, and EtOH: feedstock ratio of 0.25. The findings indicated that the process temperature and EtOH: feedstock ratio had the most significant impact on the yield of liquid bio-oil, while the %catalyst dosage had negligible effects.

In summary, this research proposes a reliable and practical model for catalytic waste cooking oil pyrolysis. We designed and conducted the experiment to investigate the optimum condition to produce liquid bio-oil with high value of energy conversion using technique called Response Surface Methodology. Our proposed optimizes the parameter conditions and derived the equation that could be used to predict the energy conversion value from activated carbon catalytic waste cooking oil pyrolysis accurately. Moreover, our design of experiments demonstrated that our proposed model improves the quality of liquid bio-oil in terms of the increasing of diesel-like fuel fraction.

7.2 Recommendations

Due to the experimental nature of this study, it is important to acknowledge that the results obtained at the laboratory scale may not possess the same level of accuracy as those obtained at a larger industrial scale. To address this concern, it is recommended that pyrolysis be conducted on a pilot scale, utilizing a larger reactor, and allowing for more adjustments in conditions such as temperature, pressure, and gas flowrate. This approach would enable the investigation of a greater number of variables related to pyrolysis behavior. By employing a larger reactor volume, increasing the amount of feedstock, extending the temperature range, and providing longer retention times commonly found in industrial pyrolysis processes, it

is anticipated that a higher yield of bio-oil can be achieved due to an enhanced rate of decomposition of the source material. With an increased quantity of bio-oil, it would be possible to perform more comprehensive analyses in order to obtain a precise characterization of the product's properties.

Further exploration of the distinctive features of all products is necessary to obtain more precise product properties for determining their respective applications. Gas products should be analyzed; Therefore, it is crucial to conduct an analysis of non-hydrocarbon components (such as CO_2, CO, N_2, H_2, O_2) in the gas product to assess the environmental impact arising from the quantities of CO_2 and CO present in the gas product.

The practical utilization of liquid bio-oil products in a combustion engine, such as a burner, can serve as confirmation for the belief that the obtained liquid bio-oil can be valuable sources of energy. If the actual outcomes align with this assumption, the catalytic pyrolysis of WCO would be advantageous and significant in advancing knowledge within the relevant field of study.

REFERENCES

Books

Basu, P. (2010), *Biomass Gasification and Pyrolysis*, Handbook. https://doi.org/ http://dx.doi.org/10.1016/B978-0-12-374988-8.00001-5.

Boyle, G., Everett, B., Peake, S., & Ramage, J. (2012). Energy Systems and Sustainability: Power for a Sustainable Future, 2nd Ed. Oxford, UK: Oxford University Press.

Fernandez, Y.; Arenillas, A.; & Angel Menendez, J. (2011). *Microwave heating applied to pyrolysis* (pp. 723-752). In S. Grundas (Eds). In Advances in Induction and Microwave Heating of Mineral and Organic Material. Intech Open. https://doi.org/10.5772/13548

Kraushaar, J., & Ristinen, R. (2006). *Energy and the Environment,* 2nd ed. Hoboken, NJ, U.S.A.: John Wiley & Sons, Inc.

Montgomery, D.C., & Runger, G.C. (2003). *Applied Statistics and Probability for Engineers. Design and Analysis of Experiments.* John Wiley and Sons Inc.

Montero, G. & Stoytcheva, M. (2011). *Biodiesel quality, standards and properties. Biodiesel Quality* (pp. 3-28), In Quality, Emissions and By-Product, InTech Open. https://doi.org/10.5772/25370

Myers, R.H., & Montgomery, D.C. (2002). *Response Surface Methodology*. In Bloomfield, P., Cressie, N.A.C., Fisher, N.I., Johnstone, I.M., Kadane, J.B., Ryan, L.M., et al. (Eds.). John Wiley & Sons Inc.

Speight, J.G., & Singh, K. (2014). *Environmental Management of Energy from biofuels and biofeedstocks*. Haboken: John Wiley & Sons, Inc. https://doi.org/ 10.1002/9781118915141.

Wiggers, V.R., Beims, R.F., Ender, L., Simionatto, E.L., & Meier, H.F. (2017). *Renewable Hydrocarbons from Triglyceride's Thermal Cracking*. In Jacob-Lopes, E. & Zepka, L.Q. (Eds.), Frontiers in Bioenergy and Biofuels (pp. 407-424). Intech Open. https://doi.org/10.5772/65498

Articles

Abnisa, F., Wan Daud, W.M.A., & Sahu, J.N. (2011). Optimization and characterization studies on bio-oil production from palm shell by pyrolysis using response surface methodology. *Biomass Bioenergy*, 35(8), 3604–3616.

Abnisa, F., Wan Daud, & W.M.A., (2014). A review on co-pyrolysis of biomass: An optional technique to obtain a high-grade pyrolysis oil. *Energy Conversion Management*, 87, 71–85.

Adams, J.M.M., Ross, A.B., Anastasakis, K., Hodgson, E.M., Gallagher, J.A., Jones, J.M., & Donnison, I.S. (2011). Seasonal variation in the chemical composition of the bioenergy feedstock Lamninaria digitata for thermochemical conversion. *Bioresource Technology*, 102, 226-234.

Ahmad, A.A., Zawawi, N.A., Kasim, F.H., Inayat, A. & Khasri, A. (2016). Assessing the gasification performance of biomass: a review on biomass gasification process conditions, optimization and economic evaluation. *Renewable and Sustainable Energy Reviews*, 53, 1333-1347.

Al-Kharusi, G., Dunne, N.J., Little, S., & Levingstone, T.J. (2022). The role of machine learning and design of experiment in the advancement of biomaterial and tissue engineering research. *Bioengineering*, 9(10), 561.

Ale, M.T., Mikkelsen, J.D., & Meyer, A.S. Important determinants for fucoidan bioactivity: A critical review of structure-function relations and extraction methods for fucose-containing sulfated polysaccharides from brown sea-weeds. *Marine Drugs*, 2011, 9, 2106–2130.

Anastasakis, K., & Ross, A.B. (2011). Hydrothermal liquefaction of the brown macro-algae Laminaria Saccharina: Effect of reaction conditions on product distribution and composition. *Bioresource Technology*, 102, 4876-4883.

Anastasakis, K., Ross, A.B., & Jones, J.M. (2011). Pyrolysis behaviour of the main carbohydrates of brown macro-algae. *Fuel*, 90, 598-607.

Anastasakis, K., & Ross, A.B. (2015). Hydrothermal liquefaction of four brown macro-algae commonly found on the UK coasts: An energetic analysis of the process and comparison with bio-chemical conversion methods. *Fuel*, 139. 546-553.

Aresta, M., Dibenedetto, A. & Barberio, G. (2005). Utilization of macro-algae for enhanced CO_2 fixation and biofuels production: Development of a computing software for an LCA study. *Fuel Processing Technology*, 86, 1679-1693.

Ashraf, A. (2012). Distillation process of crude oil. Bachelor Thesis, Qatar University.

Aslam, M., Kothiyal, N.C., & Sarma, A.K. (2015). True boiling point distillation and product quality assessment of biocrude obtained from Mesua ferrea L. seed oil via hydroprocessing. *Clean Technologies and Environmental Policy*, 17, 175-185.

Aswie, V., Qadariyah, L., & Mahfud, M. (2021). Pyrolysis of Microalge Chlorella sp. Using Activated Carbon as Catalyst for Biofuel Production. *Bulletin of Chemical Reaction Engineering & Catalysis*, 16(1), 205-213.

Banchapattanasakda, W., Asavatesanupap, C., & Santikunaporn, M. (2023). Conversion of waste cooking oil into Bio-fuel via pyrolysis using activated carbon as a catalyst. *Molecules*, 28, 3590.

Ben Hassen Trabelsi, A., Kraiem, T., Naoui, S., & Belayouni, H. (2014). Pyrolysis of waste animal fats in a fixed-bed reactor: Production and characterization of bio-oil and bio-char. *Waste Management*. 34, 210-218.

Ben Hassen Trabelsi, A., Zaafouri, K., Baghdadi, W., Naoui, S., & Ouerghi, A. (2018). Second generation biofuels production from waste cooking oil via pyrolysis process. *Renewable Energy*, 126, 888-896.

Bridgwater, A.V. (1999). Principles and practice of biomass and fast pyrolysis process for liquids. *Journal of Analytical and Applied Pyrolysis*, 51, 3-22.

Bridgwater, A.V. & Peacocke, G.V.C. (2000). Fast pyrolysis processes for biomass. *Renewable and Sustainable Energy Reviews*, 4(1), 1-73.

Bok, J., Choi, H., Choi, Y., Park, H., & Kim, S. (2012). Fast pyrolysis of coffee grounds: Characteristics of product yields and biocrude oil quality. *Energy*, 47(1):17-24.

Buzetzki, E., Sidorova, K., Cvengrosova, Z., Kaszonyi, A., & Cvengros, J. (2011). The influence of zeolite catalysts on the products of rapeseed oil cracking. *Fuel Process Technology*, 92, 1623-1631.

Cai, D., Li, P., Luo, Z., Qin, P., Chen, C., Wang, Y., Wang, Z., & Tan, T. (2016). Effect of dilute alkaline pretreatment on the conversion of different parts of corn stalk to fermentable sugars and its application in acetone-butanol-ethanol fermentation. *Bioresource Technology*, 211, 117-124.

Cantrell, K.B., Ducey, T., Ro, K.S., & Hunt, P.G. (2008). Livestock waste-to-bioenergy generation opportunities. *Bioresource Technology*, 99, 7941-7953.

Carlson, T.R., Cheng, T.T. Jae, J., & Huber G.W. (2011). Production of green aromatics and olefins by catalytic fast pyrolysis of wood sawdust. *Energy and Environmental Science*, 4, 145-161.

Cerveró, J.M., Skovgaard, P.A., Felby, C., Sørensen, H.R., & Jørgensen, H. (2010). Enzymatic hydrolysis and fermentation of palm kernel press cake for production of bioethanol. *Enzyme and Microbial Technology*, 46, 177–184.

Chandel, A.K., Silva, S.S., Carvalho, W., & Singh, O.V. (2012). Sugarcane bagasse and leaves: foreseeable biomass of biofuel and bio-products. *Journal of Chemical Technology & Biotechnology*, 87, 11-20.

Chang, C.C., Wan, & S.W. (1947). China's motor fuels from tung oil. *Industrial & Engineering Chemistry Research*, 39, 1543-1548.

Chen, H., Zhou, D., Luo, G., Zhang, S., & Chen, J. (2015). Macroalgae for biofuels production: Progress and perspectives. *Renewable and Sustainable Energy Reviews*, 47, 427–437.

Chen, G., Liu, C., Ma, W., Zhang, X., Li, Y., Yan, B., & Zhou, W. (2015). Co-pyrolysis of corn-cob and waste cooking oil in a fixed bed. *Bioresource Technology*, 166, 500-507.

Chen, W., Li, K., Xia, M., Yang, H., Chen, Y., Chen, X., Che, Q., & Chen, H. (2018). Catalytic deoxygenation co-pyrolysis of bamboo wastes and microalgae with biochar catalyst. *Energy*, 157, 472–482.

Chew, T.L., & Bhatia, S. (2009). Effect of catalyst additives on the production of biofuels from palm oil cracking in a transport riser reactor. *Bioresource Technology*, 100, 2540-2545.

Chiaramonti, D., Buffi, M., Rizzo, A.M., Lotti, G., & Prussi, M. (2016). Bio-hydrocarbons through catalytic pyrolysis of used cooking oils and fatty acids for sustainable jet and road fuel production. *Biomass and Bioenergy*, 95, 424-435.

Conesa, J.A., Marcilla, A., Moral, R., Moreno-Caselles, J., & Perez-Espionsa, A. (1998). Evolution of the gases in the primary pyrolysis of different sewage sludges. *Thermochimica Acta*, 313(1), 63-67.

Dandik, L., Aksoy, & H.A. (1998). Pyrolysis of used sunflower oil in the presence of sodium carbonate by using fractionating pyrolysis reactor. *Fuel Process Technology*, 57, 81-92.

Demirbas, A. (2002). Partly chemical analysis of liquid fraction of flash pyrolysis products from biomass in the presence of sodium carbonate. *Energy Conversion and Management*, 8, 1801-1809

Demirbas, A. (2008). Relationships derived from physical properties from vegetable oil and biodiesel fuels. *Fuel*, 87, 1743-1748.

Dhyani, V., & Bhaskar, T. (2018). A comprehensive review on the pyrolysis of lignocellulosic biomass. *Renewable Energy*, 129, 695-716.

Dimitriadia, A., & Bezergianni, S. (2017). Hydrothermal liquefaction of various biomass and waste feedstocks for biocrude production: a state of the art review. *Renewable and Sustainable Energy Reviews*, 68, 113-115.

Dominguez, A. Fernandez, Y., Fidalgo, B., Pis J.J., & Menendez, J.A. (2008). Bio-syngas production with low concentrations of CO_2 and CH_4 from microwave-induced pyrolysis of wet and dried sewage sludge. *Chemosphere*, 70, 397-403.

Dominguez, A., Menendez, J.A., Fernandez, Y., Pis, J.J., Nabais, J.M.V., Carrott, P.J.M., & Carrott, M.M.L.R. (2007). Conventional and microwave induced pyrolysis of coffee hulls for the production of a hydrogen rich fuel gas. *Journal of Analytical and Applied Pyrolysis*, 79, 128-135.

Echaroj, S., Asavatesanupap, C., Chavadej, S., & Santikunaporn, M. (2021). Kinetic study on microwave-assisted oligomerization of 1-decene over a HY catalyst. *Catalysts*, 11, 1105-1123.

Faucheux, N., Heitz, M., Brzezinski, R., Rodriguez P.d.M. (2016). Enzymatic Transesterification of lipids from microalgae into biodiesel: a review, *AIMS Energy*, 4, 817–855.

Fisher, T., Hajaligol, M., Waymack, B., & Kellogg, D. (2002). Pyrolysis behavior and kinetics of biomass derived materials. *Journal of Analytical and Applied Pyrolysis*, 62, 331-349.

Fraunhofer Institute for Environmental, Safety and Energy Technology, UMSICHT, GREASOLINE (2008). Report of New Technology for the Conversion of Waste Fats to High Quality Fuels (Research Project No. 018109). https://cordis.europa.eu/project/id/18109/reporting

Geogiev, D., Bogdanov, B., Angelova, K., Markovska, I., & Hristov, Y. (2009, June 4-5). *Synthesis zeolites-structure, classification, current trends in zeolite synthesis* [Paper presentation]. International Science Conference. Stara Zagora, Prof. Dr. Assen Zlatarov University, Bulgaria.

Ghoreishi, S.M., Moein, P., 2013. Biodiesel synthesis from waste vegetable oil via transesterification reaction in supercritical methanol. Journal of Supercritical Fluids 76, 24–31.

Graboski, M.S., & McCormick, R.L. (1998). Combustion of fat and vegetable oil derived fuels in diesel engines, Progress in Energy and Combustion Science, 24(2), 125-164.

Gupta, G.K., & Mondal, M.K. (2019). Bio-energy generation from sagwan sawdust via pyrolysis: Product distributions, characterizations and optimization using response surface methodology. *Energy*, 170, 423–37. https://doi.org/10.1016/j.energy.2018.12.166.

Gupta, S., Patel, P., & Mondal, P. (2022). Biofuels production from pine needles via pyrolysis: Process parameter modeling and optimization through combined RSM and ANN based approach. *Fuel*, 310, 122230.

Han, T., Ding, S., Yang, W., & Jönsson, P. (2019). Catalytic pyrolysis of lignin using low-cost materials with different acidities and textural properties as catalysts. *Chemical Engineering Journal*, 2019, 373, 846–856.

Hansdah, D., Murugan, S., & Das, L.M. (2013). Experimental studies on a DI diesel engine fueled with bioethanol-diesel emulsions. *Alexandria Engineering Journal*, 52, 267-276.

Heil, V., Kraft, A., Menne, A., & Unger, C.A. (2013, January 15-17). *Catalytic cracking of fatty oils and fatty acids e a novel route towards bio-jet fuel* [Paper presentation]. 9th International Colloquium Fuels: Conventional and Future Energy for Automobiles, Technische Akademie Esslingen in Stuttgart, Ostfildern.

Hossain, A.B.M.F., Salleh, A., Boyce, A.N., Chowdhury, P., & Naqiuddin, M. (2008). Biodiesel fuel production from algae as renewable energy. *American Journal of Biochemistry and Biotechnology*, 4(3), 250-254.

Hossain M.A., Ganesan P., Jewaratnam, J., & Chinna, K. (2017). Optimization of process parameters for microwave pyrolysis of oil palm fiber (OPF) for hydrogen and biochar production, *Energy Conversion and Management*, 133, 349-362. https://doi.org/10.1016/j.enconman.2016.10.046.

Ilkilic, C.; & Oner, C. (2017). Biodiesel fuel obtained from sunflower oil as an alternative fuel for diesel engines. *The Online Journal of Science and Technology,* 7(3), 12-18.

Inyang, M., Gao, B., Pullammanappallil, P., Ding, W., & Zimmerman, A.R. (2010). Biochar from anaerobically digested sugarcane bagasse. *Bioresource Technology*, 101, 8868–8872.

Isahak, W.N.R.W., Hisham, M.W.M., Yarmo, M.A., & Hin, T.Y.Y. (2012). A review on bio-oil production from biomass by using pyrolysis method. *Renewable and Sustainable Energy Reviews*, 16(8), 5910-5923.

Jacobson, K., Gopinath, R., Meher, L., & Dalai, A. (2008). Solid acid catalyzed biodiesel production from waste cooking oil. *Applied Catalyst: B Environmental*, 85, 86–91.

Jaroen, D. (2017). *Functionalized metal-organic frameworks as selective metal*

adsorbents [Doctoral dissertation, Ghent University.] https://www.researchgate.net/publication/317577477

Jørgensen, H., Sanadi, A.R., Felby, C., Lange, N.E.K., Fische,r M., & Ernst, S. (2010). Production of ethanol and feed by high dry matter hydrolysis and fermentation of palm kernel press cake. *Applied Biochemistry and Biotechnology*, 161, 318–332.

Junming, X., Jianchun, J., Yanju, L., & Jie, C. (2009). Liquid hydrocarbon fuels obtained by the pyrolysis of soybean oils. *Bioresource Technology*, 100, 4867-4870.

Kader, M., Islam, M., Parveen, M., Haniu, H., & Takai K. (2013). Pyrolysis decomposition of tamarind seed for alternative fuel. *Bioresource Technology*, 149, 1-7.

Kadlimatti, H.M., Raj Mohan, B., & Saidutta, M.B. (2019). Bio-oil from microwave assisted pyrolysis of food waste-optimization using response surface methodology. *Biomass and Bioenergy*, 123, 25-33.

Kan, T., Strezov, V., & Evans, T.J. (2016). Lignocellulosic biomass pyrolysis: A review of product properties and effects of pyrolysis parameter. *Renewable and Sustainable Energy Reviews*. 57, 1126-1140.

Khan, S., Siddique, R., Sajjad, W., Nabi, G., Hayat, K.M., Duan, P., & Yao, L. (2017). Biodiesel production from algae to overcome the energy crisis. *HAYATI Journal of Biosciences*, 24(4) 163-167.

Kılıç, M., Pütün, E., & Pütün, A.E. (2014). Optimization of Euphorbia rigida fast pyrolysis conditions by using response surface methodology. *Journal of Analytical and Applied Pyrolysis*, 110, 163-171.

Kalargaris, I., Tian, G., & Gu, S. (2017). The utilization of oils produced from plastic waste at different pyrolysis temperatures in a DI diesel engine. *Energy*, 131, 179-185.

Khanday, W.A., Kabir, G., & Hameed, B.H. (2016). Catalytic pyrolysis of oil palm mesocarp fibre on a zeolite derived from low-cost oil palm ash. *Energy Conversion and Management*, 127, 265-272.

Kim, S.S., & Kim, S.H. (2000). Pyrolysis kinetics of waste automobile lubricating oil. *Fuel,* 79, 1943-1949.

Kirszensztejn, P., Przekop, R., Tolinska, A., & Mackowska, E. (2009). Pyrolytic and catalytic conversion of rape oil into aromatic and aliphatic fractions in a fixed bed reactor on Al2O3 and Al2O3/B2O3 catalysts, *Chemical Papers*. 63, 226-232.

Kraiem, T., Hassen, A.B., Belayouni, H., & Jeguirim, M. (2017). Production and characterization of bio-oil from the pyrolysis of waste frying oil. *Environmental Science and Pollution Research*, 24, 9951-9961.

Krishnan, C., Sousa, L.D.C., Jin, M., Chang, L., Dale, B.E., & Balan, V. (2010). Alkali-based AFEX pretreatment for the conversion of sugarcane bagasse and cane leaf residues to ethanol. *Biotechnology Bioengineering*, 107, 441–450.

Kumar, S., & Gupta, R.B. (2008). Hydrolysis of microcrystalline cellulose in subcritical and supercritical resources for a thriving bioeconomy. *Industrial & Engineering Chemistry Research*, 47, 9321-9329.

Kunkes, E.L., Simonetti, D.A., West, R.M., Serrano-Ruiz, J.C., Gärtner, C.A., & Dumesic, J.A. (2008). Catalytic conversion of biomass to monofunctional hydrocarbons and targeted liquid-fuel classes. *Science,* 322(5900), 417–421.

John, R.P., Anisha, G.S., Nampoothiri, K.M., & Pandey, A. (2011). Micro and macroalgal biomass: a renewable source for bioethanol. *Bioresource Technology*, 102, 186-193.

Lam, S.S., Russel, A.D., Lee, C.L., & Chase, H.A. (2012). Microwave-heated pyrolysis of waste automotive engine oil: influence of operation parameters on the yield, composition, and fuel properties of pyrolysis oil. *Fuel*, 92, 327-339.

Lam, S.S., Liew, R.K., Jusoh, a., Chong, C.T., Ani, F.N., & Chase, H.A. (2016). Progress in waste oil to sustainable energy, with emphasis on pyrolysis technique. *Renewable Sustainable Energy Reviews*, 53, 741-753.

Lam, S.S., Wan Mahari, W.A., Jusoh, A., Chong, C.T., Lee, C.L., & Chase, H.A. (2017). Pyrolysis using microwave absorbents as reaction bed: An improved approach to transform used frying oil into biofuel product with desirable properties. *Journal of Cleaner Production*, 147, 263-272.

Lappi, H., & Alén, R. (2011). Pyrolysis of vegetable oil soaps-Palm, olive, rapeseed and castor oils. Journal of Analytical and Applied Pyrolysis, 91, 154-158.

Lee, S.Y., Sankaran, R., Chew, K.W., Tan, C.H., Krishnamoorthy, R., Chu, D.T., & Show, P.L. (2019). Waste to bioenergy: a review on the recent conversion technologies. *BMC Energy*, 1, 4. https://doi.org/10.1186/s42500-019-0004-7.

Li, L., Ding, Z., Li, K., Xu, J., Liu, F., Liu, S., Yu, S., Xie, C. & Ge, X. (2016). Liquid hydrocarbon fuels from catalytic cracking of waste cooking oils using ultrastable zeolite USY as catalyst. *Journal of Analytical and Applied Pyrolysis*, 117, 268-272.

Li, L., Yan, B., Li, H., Yu, S., & Ge, X. (2020). Decreasing the acid value of pyrolysis oil via esterification using ZrO2/SBA-15 as a solid acid catalyst. *Renew Energy*, 146, 643-650.

Lima, D.G., Soares, V.C.D., Ribeiro, E.B., Carvalho, D.A., Cardoso, E.C.V., Rassi, F.C., Mundim, K.C., Rubim, J.C., & Suarez, P.A.Z. (2004). Diesel-like fuel obtained by pyrolysis of vegetable oils. *Journal of Analytical and Applied Pyrolysis*, 71, 987-996.

Lopresto, C.G., Naccarato, S., Albo, L., De Paola, M.G., Chakraborty, S., Curcio, S., & Calabro, V. (2015). Enzymatic transesterification of waste vegetable oil to produce biodiesel. *Ecotoxicology and Environmental Safety*, 121, 229-235.

Lu, Q., Li, W.Z., & Zhu, X.F. (2009). Overview of fuel properties of biomass fast pyrolysis oils. *Energy Conversion Management*, 50, 1376-1383.

Mahari, W.A., Zainuddin, N.F., Chong, C.T., Lee, C.L., Lam, W.H., Poh, S.C., & Lam, S.S. (2017). Conversion of waste shipping oil into diesel-like oil via microwave-assisted pyrolysis. *Journal of Environmental Chemical Engineering*, 5(6), 5836-5842.

Mahari, W.A. Chong, C.T. Cheng, C.K. lee, C.L. Hendrata, K., Yuh Yek, P.N., Ma, N.L., & Lam, S.S. (2018). Production of value-added liquid fuel via microwave co-pyrolysis of used frying oil and plastic waste. *Energy*, 162, 309-317.

Mabrouki, J., Abbassi, M.A., Guedri, K., Omri, A., & Jeguirim, M. (2015). Simulation of biofuel production via fast pyrolysis of palm oil residues. *Fuel*, 159, 819–27.

Malkow, T. (2004). Novel and innovative pyrolysis and gasification technologies for

energy efficient and environmentally sound MSW disposal. *Waste Management*, 24, 53-79.

Mamat, R., Hainin, M.R., Hassan, N.A., Rahman, N.A.A., Warid, M.N.M., & Idhamb, M.K. (2015). A review of performance asphalt mixtures using bio-binder as alternative binder. *Jurnal Teknologi*, 77(23), 17-20.

Mazaheri, H., Lee, K.T., Bhatia, S., & Mohamed, A.R. (2010). Sub/supercritical liquefaction of oil palm fruit press fiber for the production of bio-oil: Effect of solvents. *Bioresource Technology*, 101(19), 7641-7647.

Menéndez, J.A., Domínguez, A., Fernández, Y. & Pis, J.J. (2007). Evidence of self gasification during the microwave-induced pyrolysis of coffee hulls. *Energy & Fuels*, 21(1), 373-378.

Motasemi, F., & Muhammad Afzal, T. (2013). A review on the microwave-assisted pyrolysis technique. *Renewable and Sustainable Energy Reviews*, 28, 317-330.

Naik, S.N., Goud, W., Rout, P.K., & Dalai, A.K. (2010). Production of first and second generation biofuels: a comprehensive review. *Renewable and Sustainable Energy Reviews*, 14(2), 578-597.

Nayak, M.G, & Vyas, A.P., (2019). Optimization of microwave-assisted biodiesel production from Papaya oil using response surface methodology, *Renewable Energy*, 138, 18- 28.

Nayak, M.G., & Vyas, AP. (2022). Parametric study and optimization of microwave assisted biodiesel synthesis from Argemone Mexicana oil using response surface methodology. *Chemical Engineering Process - Process Intensification*, 170, 108665.

Neha, S., & Remya, N. (2021). Optimization of bio-oil production from microwave co-pyrolysis of food waste and low-density polyethylene with response surface methodology. *Journal of Environmental Management*, 297, 113345.

Neves, D., Thunman, H., Matos, A., Tarelho, L., & Gomez-Barea, A. (2011).

Characterization and prediction of biomass pyrolysis products. *Progress in Energy and Combustion Science*, 7, 611-630.

Neveux, N., Yuen, A., Jazrawi, C., He, Y., Magnusson, M., Haynes, B., Masters, A., Montoya, A., Paul, N., Maschmeyer, T., & Nys, R. (2014). Pre- and post-harvest treatment of macroalgae to improve the quality of feedstock for hydrothermal liquefaction. *Algal Research*. 2014, 6, 22–31.

Ngo, T.A., Kim, J., & Kim, S.S. 2010. Pyrolysis of soybean oil with H-ZSM5 (Proton-exchange of Zeolite Socony Mobil #5) and MCM41 (Mobil Composition of Matter No.41) catalysts in a fixed-bed reactor. *Energy*, 35, 2723-2728.

Nguyen, T.S., Zabeti, M. Lefferts, L., Brem, G., & Sashan, K. (2013). Catalytic upgrading of biomass pyrolysis vapours using faujasite zeolite catalysts. *Biomass Bioenergy*, 48, 100-110.

Onwudili, J.A., Insura, N., & Williams, P.T. (2009). Composition of products from the pyrolysis of polyethylene and polystyrene in a closed batch reactor: Effects of temperature and residence time. *Journal of Analytical and Applied Pyrolysis*, 86, 293-303.

Onwudili, J.A., Lea-Langton, A.R., Ross, A.B., & Williams, P.T. (2013). Catalytic hydrothermal gasification of algae for hydrogen production: Composition of reaction products and potential for nutrient recycling. Bioresource Technology. 127, 72-80.

Parihar, M.F., Kamil, M., Goyal, H.B., Gupta, A.K., & Bhatnagar, A.K. (2007). An experimental study on pyrolysis of biomass. Process Safety and Environmental Protection, 85, 458-465.

Phung, T.K., Casazza, A.A., Perego, P., Capranica, P., & Busca, G. (2015). Catalytic pyrolysis of vegetable oils to biofuels: catalyst functionalities and the role of ketonization on the oxygenate paths. *Fuel Process Technology*, 140, 119-124.

Pinto, F., Hidalgo-Herrador, J.M., Paradela, F., Costa, P., André, R., Fratczak, J., Snape, C., Anděl, L., & Kusy, J. (2020). Coal and waste direct liquefaction, using glycerol, polyethylene waste and waste tyres pyrolysis oil. Optimisation of liquids yield

by response surface methodology. *Journal of Cleaner Production*, 255, 120192 https://doi.org/10.1016/j.jclepro.2020.120192

Prado, C.M.R., & Antoniosi Filho, N.R. (2009). Production and characterization of the biofuels obtained by thermal cracking and thermal catalytic cracking of vegetable oils. *Journal of Analytical and Applied Pyrolysis*, 86, 338-347.

Qasim, M., Ansari, T.M., & Hussain, M. (2017). Combustion, Performance, and Emission Evaluation of Diesel Engine with Biodiesel Like Fuel Blends Derived from a Mixture of Pakistani Waste Canola and Waste Transformer Oils. *Energies*, 10(7), 1023.

Qi, Z., Jie, C.H., Tiejun, W., & Ying, X. (2007). Review of biomass pyrolysis oil properties and upgrading research. *Energy Conversion and Management*, 48, 87-92.

Qureshi, N., Saha, B.C., Hector, R.E. Dien, B., Hughes, S., Liu, S., Iten, L., Bowman, M.J., Sarath, G., & Cotta, M.A. (2010). Production of butanol (a biofuel) from agricultural residues: PartII – Use of corn stover and switchgrass hydrolysates. *Biomass and Bioenergy*, 34(4), 566-571.

Qureshi, S.S., Nizamuddin, S., Baloch, H.A., Siddiqui,v M.T.H., Mubarak, N.M., & Griffin, G.J. (2019). An overview of OPS from oil palm industry as feedstock for bio-oil production. *Biomass Conversion and Biorefinery*, 9, 827-841.

Rashid, U., Soltani, A., Yaw Choong, T.S., Nehdi, I.A., Ahmad, J., & Ngamcharussrivichai, C. (2019). Palm biochar-based sulphated zirconium (Zr-AC-HSO_3) catalyst for methyl ester production from palm fatty acid distillate. *Catalysts*, 9, 1029.

Raveendran, K., Ganesh, A. & Khilar, K.C. (1995). Influence of mineral matter on biomass pyrolysis characteristics. *Fuel*, 74(12), 1812-1822.

Rangel, M.d.C., Mayer, F.M., Carvalho, M.d.S., Saboia, G., & de Andrade, A.M. (2023). Selecting Catalysts for Pyrolysis of Lignocellulosic Biomass. *Biomass*, 3, 31-63.

Razzak, S.A., Lucky, R.A., Hossain, M.M., & Delasa, H. (2022). Valorization of microalgae biomass to biofuel production: A review. *Energy Nexus*, 7, 100139.

Romero, M.J., Pizzi, A., Toscano, G., Busca, G., Bosio, B., & Arato, E. (2016). Deoxygenation of waste cooking oil and non-edible oil for the production of liquid hydrocarbon biofuels. *Waste Management*, 47, 62-68,

Ross, A.B., Jones, J.M., Kubacki, M.L., & Bridgeman, T. (2008). Classification of macroalgae As fuel and its thermochemical behaviour. *Bioresource Technology*, 99, 6494-6504.

Ross, A.B., Anastasakis, K., Kubacki, M., & Jones, J.M. (2209). Investigation of the pyrolysis behaviour of brown algae before and after pre-treatment using PY-GC/MS and TGA. *Journal of Analytical and Applied Pyrolysis*, 85, 3-10

Sanahuja-Parejo, O., Veses, A., Navarro, M., López, J., Murillo, R., Callén, M., & Garcia, T. (2018). Catalytic co-pyrolysis of grape seeds and waste tyres for the production of drop-in biofuels. *Energy Conversion and Management*, 171, 1202-1212.

Sampath, A. (2009). *Chemical Characterization of Camelina Seed Oil*. (Master's degree thesis, Graduate School Nue Brnswick Rutgers, The State University of New Jersey, New Jersey.

Saraeian, A., Nolte, M.W., & Shanks, B.H. (2019). Deoxygenation of biomass pyrolysis vapors: Improving clarity on the fate of carbon. *Renewable and Sustainable Energy Reviews*, 262, 262-280.

Saxena, S.K., & Viswanadham, N. (2014). Selective production of green gasoline by catalytic conversion of Jatropha oil, *Fuel Processing Technology*, 119, 158-165.

Schaefer, W.D., (1975). Disposing of solid wastes by pyrolysis. *Environmental Science & Technology*, 9, 98-98.

Sharma, Y.C., Agrawal, S., Singh, B., & Frometa, A.E.N. (2012). Synthesis of economically viable biodiesel from waste frying oils (WFO). *The Canadian Journal of Chemical Engineering*, 90, 483-488.

Sims, R.E.H., Mabee, W., Saddler, J.N., & Taylor, M. (2010). An overview of second generation biofuel technologies. *Bioresource Technology*, 101, 1570-1580.

Sirajudin, N., Jusoff, K., Yani, S., Ifa, L., & Roesyadi, A. (2013). Biofuel production from catalytic cracking of palm oil. *World Applied Sciences Journal*, 26, 67-71.

Smit, A.J. Medicinal and pharmaceutical uses of seaweed natural products: A review. (2004). *Environmental Biology of Fishes*. 16, 245–262.

Soysa, R., Choi, S., Jeong, Y., Kim, S., & Choi, Y. (2015). Pyrolysis of Douglas fir and coffee Grounds and product biocrude-oil characteristics. *Journal of Analytical and Applied Pyrolysis*, 115, 51-56.

Srivastava, A., & Prasad, R. (2000). Triglycerides-based diesel fuel. *Renewable and Sustainable Energy Reviews*, 4(2), 111-133.

Stephanidis, S., Nitsos, C., Kalogiannis, K., Iliopoulou, E.F., Lappas, A.A., & Triantafyllidis, K.S. (2011). Catalytic upgrading of lignocellulosic biomass pyrolysis vapours: Effect of hydrothermal pro-treatment of biomass. *Catalyst Today*, 167, 37-45.

Suprianto, T., Wijayanti, W.-W., & Wardan, I. (2021). Effect of activated carbon catalyst on the cracking of biomass molecules into light hydrocarbons in biomass pyrolysis. *IOP Conference Series: Materials Science and Engineering*, 1034, 012079.

Talebian-Kiakalaieh, A., Amin, N.A.S., & Mazaheri, H. (2013). A review on novel processes of biodiesel production from waste cooking oil. *Applied Energy*, 104, 683–710.

Tani, H., Hasegawa, T., Shimouchi, M., Asami, K., & Fujimoto, K. (2011). Selective catalytic decarboxy-cracking of triglyceride to middle-distillate hydrocarbon, *Catalysis Today*, 164, 410-414.

Teo, C.L, Jamaludding, H., & Zain, N.A.M. (2014), Biodiesel production via lipase catalyzed transesterification of microalgae lipids from Tetraselmis sp. *Renewable Energy*, 68, 1-5.

Thøgersen, J., Nørnberg, P., Finster, K., & Knak Jensen, S.J. (2021). Greenhouse gas capture by triboelectric charging. *Chemical Physics Letters*, 783, 139069.

Thushari, I., & Babel, S. (2022). Comparative study of the environment impacts of used cooking oil valorization options in Thailand. *Journal of Environmental Management*, 310, 114810.

Tripathi, M., Sahu, J.N., & Ganesan, P. (2016). Effect of process parameters on production of biochar from biomass waste through pyrolysis: A review. *Renewable and Sustainable Energy Reviews*, 55, 467-81.

Tutunea, D., Dumitru, I., Racila, L., Otat, O., Matei, L., & Geonea, I. (2018). Characterization of sunflower oil biodiesel as alternative for diesel fuel. In *Proceeding of the 4th International Congress of Automotive and Transport Engineering (AMMA 2018)* (pp. 172-180), Technical University of Cluj-Napoca, Romania.

Twaiq, F.A., Zabidi, N.A.M., Mohamed, A.R., & Bhatia, S. (2003). Catalytic conversion of palm oil over mesoporous aluminosilicate MCM-41 for the production of liquid hydrocarbon fuels. *Fuel Processing Technology*, 84, 105-120.

Vainio E. (2014), *Fate of Fuel-Bound Nitrogen and Sulfur in Biomass-Fired Industrial Boilers* [Doctoral thesis, Åbo Akademi University] https://www.researchgate.net/publication/260243997

Valliyappan, T., Bakhshi, N.N., & Dalai, A.K. (2008). Pyrolysis of glycerol for the production of hydrogen or syn gas. *Bioresource Technology*, 99, 4476-4483.

Vasudevan, P.T., & Briggs, M. (2008). Biodiesel production-current state of the art and challenges. *Journal of Industrial Microbiology and Biotechnology*, 35, 421-30.

Wang, L., Lei, H., Ren, S., Bu, Q., Liang, J., Wei, Y., Liu, Y., Lee, G.S.J., Chen, S., Tang, J., Zhang, Q., & Ruan, R. (2012). Aromatics and phenols from catalytic pyrolysis of Douglas fir pellets in microwave with ZSM-5 as a catalyst. *Journal of Analytical and Applied Pyrolysis*, 98, 194-200.

Wang, S., Jiang, X. M., Han, X.X. & Liu, J.G. (2009). Combustion Characteristics of Seaweed Biomass. 1.Combustion Characteristics of Enteromorpha clathrata and Sargassum natans. *Energy & Fuels*, 23, 5173-5178.

Wang, W.C. Thapaliy, N., Campos, a., Stikeleather, L.F., & Roberts, W.L. (2012). Hydrocarbon fuels from vegetable oils via hydrolysis and thermo-catalytic decarboxylation. *Fuel*. 95, 622-629.

Wang, Y., Dai, L., Fan, L., Duan, D., Liu, Y., Ruan, R., Yu, Z., Liu, Y., & Jiang, L. (2017). Microwave-assisted catalytic fast co-pyrolysis of bamboo sawdust and waste tire for bio-oil production. *Journal of Analytical and Applied Pyrolysis*, 123, 224-228.

Wang, Y., Dai, L., Fan, L., Cao, L., Zhou, Y., Zhao, Y., Liu, Y., & Ruan, R. (2017). Catalytic

co pyrolysis of waste vegetable oil and high-density polyethylene for hydrocarbon fuel production. Waste Management, 61, 276-282.

Wang, S., Yuan, C., Esakkimuthu, S., Xu, L., Cao, B., Abomohra, A.E.F., Qian, L., Liu, L., & Hu, Y. (2019). Catalytic pyrolysis of waste clay oil to produce high quality biofuel. *Journal of Analytical and Applied Pyrolysis*, 141, 104633.

Wiggers, V.R., Meier, H.F., Wisniewski Jr., A., Chivanga Barros, A.A., & Wolf Maciel, M.R. (2009). Biofuels from continuous fast pyrolysis of soybean oil: a pilot plant study. *Bioresource Technology*. 100, 6570-6577.

Xie, Q., Addy, M., Liu, S., Zhang, B., Cheng, Y., Wan, Y., Li, Y., Lin, X., Chen, P., & Ruan, R. (2015). Fast Microwave-assisted catalytic co-pyrolysis of microalgae and scum for bio-oil production. *Fuel*, 160, 577-582.

Xu, J., Jiang, J., & Zhao, J. (2016). Thermochemical conversion of triglycerides for production of drop-in liquid fuels. *Renewable and Sustainable Energy Reviews*, 58, 331-340.

Yang, H., Chen, Z., Chen,W., Chen, Y., Wang, X., & Chen, H. (2020). Role of porous structure and active O-containing groups of activated biochar catalyst during biomass catalytic pyrolysis. *Energy*, 210, 118646

Yigezu, Z.D., & Muthukumar, K. (2014). Catalytic cracking of vegetable oil with metal oxides for biofuel production, *Energy Conversion and Management*, 84, 326-333

Yu, F., Gao, L., Wang, W., Zhang, G., & Ji, J. (2013). Bio-fuel production from the catalytic pyrolysis of soybean oil over Me-Al-MCM-41 (Me=La, Ni or Fe) mesoporous materials. *Journal of Analytical and Applied Pyrolysis*, 104, 325-329.

Yue, L., Li, G., He, G., Guo, Y., Xu, L., & Fang, W. (2015). Impacts of hydrogen to carbon ratio (H/C) on fundamental properties and supercritical cracking performance of hydrocarbon fuels. *Chemical Engineering Journal*, 283, 1216-1223.

Zadeh, Z.E., Abdulkhani, A., Aboelazayem, O., & Saha, B. (2020). Recent insights into lignocellulosic biomass pyrolysis: A critical review on pretreatment, characterization, and products upgrading. *Processes*, 8(7), 799.

Zeng, X., Ma, Y., & Ma, L. (2007). Utilization for straw in biomass energy in China.

Renewable and Sustainable Energy Reviews, 11, 976-987.

Zhang, Q., Wang, T., Xu, Y., Zhang, Q, & Ma, L. (2014). Production of liquid alkanes by controlling reactivity of sorbitol hydrogenation with a Ni/HZSM-5 catalyst in water. *Energy Conversion Management*, 77, 26-28.

Zhou, Y., Wang, Y., Fan, L., Dai, L., Duan, D., Liu, Y., Ruan, R., Zhao, Y., Yu, Z., & Hu, Y. (2017). Fast microwave-assisted catalytic co-pyrolysis of straw stalk and soapstock for bio-oil production. *Journal of Analytical and Applied Pyrolysis*. 124, 35-41.

Zhuang, X., Gan, Z., Cen, K., Ba, Y., Chen, F., & Chen, D. (2022). Upgrading biochar by co-pyrolysis of heavy bio-oil and apricot shell using response surface methodology. *Fuel*, 310, 122447.

APPENDICES

APPENDIX A

PRODUCT EXPERIMENT DATA

Table A-1

Product yield (% & gram), calorific value and energy conversion

Temp	Ratio	Product yield			Calorific value	Energy
		Oil	Gas	Residue	kJ/g	conversion
350C	Blank	34.45	10.7	54.85	34.108	30.1
	1:40	52.85	14.02	33.13	39.325	53.2
	1:30	51.26	14.52	34.22	38.327	50.3
	1:20	53.56	10.67	36.27	39.29	53.9
375C	Blank	52.23	9.08	38.69	40.216	53.8
	1:40	55.99	14.31	29.7	40.214	57.6
	1:30	57.43	13.59	28.98	38.112	56.0
	1:20	57.01	13.32	29.67	39.975	58.3
400C	Blank	71.45	10.98	17.57	39.739	72.7
	1:40	85.35	11.49	3.16	40.197	87.8
	1:30	78.83	15.26	5.91	38.614	77.9
	1:20	79.09	14.74	6.17	39.047	79.0
425C	Blank	81.7	15.91	2.39	39.739	83.1
	1:40	83.85	13.97	2.18	40.279	86.4
	1:30	85.18	9.39	5.43	39.143	85.3
	1:20	83.57	10.39	6.04	40.194	86.0
450C	Blank	74.86	22.02	3.12	39.57	75.8
	1:40	82.81	13.7	3.49	40.737	86.3
	1:30	85.35	9.7	4.95	38.996	85.2
	1:20	83.58	11.06	5.36	39.313	84.1

Figure A-1

Bio-oil product of WCO pyrolysis at 1:40 AC:WCO ratio

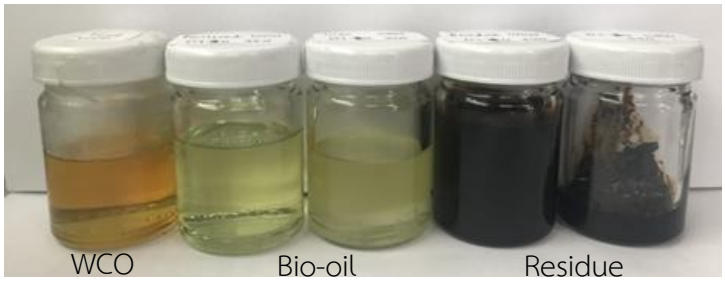

(a) 350 °C

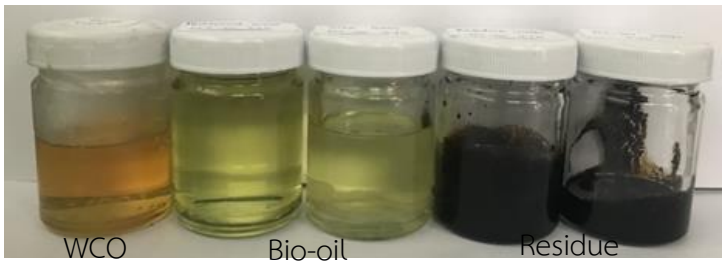

(b) 375 °C

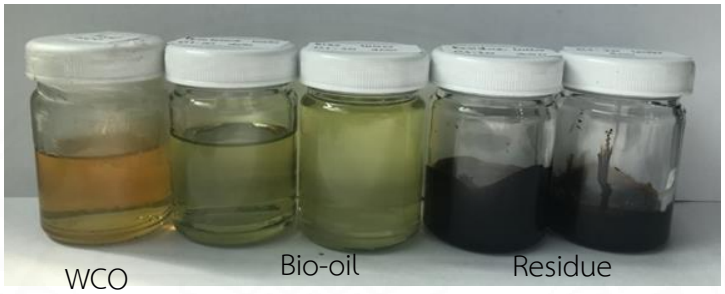

(c) 400 °C

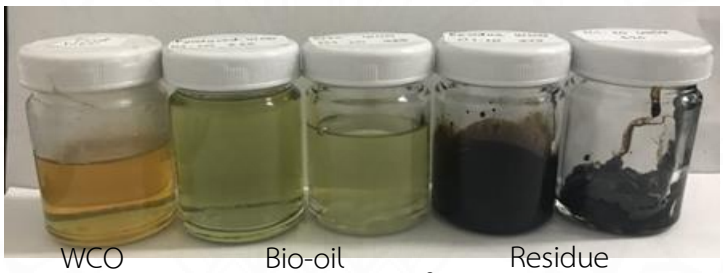

(d) 425 °C

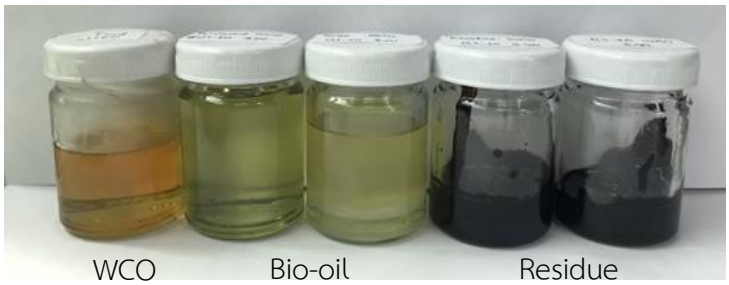

(e) 450 °C

APPENDIX B

WCO OIL AND BIO-OIL CHARACTERIZATION DATA

Table B-1

Chromatogram peak list from GC-MS analysis of WCO

No.	RT	Height	Height %	Area	Area Sum %	Name	Formula	No.	RT	Height	Height %	Area	Area Sum %	Name	Formula
1	3.684	9241738	23.38	27505118	1.23	1-Decanol, 2-methyl-	C11H24O	45	10.987	11409849	28.87	22960114	1.03	cis-9-Hexadecenal	C16H30O
2	3.856	3738272	9.46	8380585	0.37	13-OXABICYCLO[10.1.0]TRIDECANE	C12H22O	46	11.144	6931892	17.54	12553218	0.56	Z-8-Methyl-9-tetradecenoic acid	C15H28O2
3	4.2	612346	1.55	2369318	0.11	7-Oxabicyclo[4.1.0]heptane, 1-methyl-4-(2-methyloxiranyl)-	C10H16O2	47	11.241	20355977	51.5	50163856	2.24	Docosane, 11-decyl-	C32H66
4	4.313	738490	1.87	2212298	0.1	Tricyclo[5.2.1.0(1,5)]decane-8,9-diol	C10H16O2	48	11.406	5014140	12.69	10119460	0.45	9-Hexadecenoic acid	C16H30O2
5	4.432	1608627	4.07	6514034	0.29	5,7-Dodecadiyn-1,12-diol	C12H18O2	49	11.495	1319896	3.34	2819653	0.13	Hexadecadienoic acid, methyl ester	C17H30O2
6	4.597	804736	2.04	1618332	0.07	1,4-Naphthalenediol, 1,2,3,4,4a,5,8,8a-octahydro-, (1.alpha.,4.alpha.,4a.beta.,8a.beta.)-	C10H16O2	50	11.705	991380	2.51	2962157	0.13	3H-Cyclodeca[b]furan-2-one, 4,9-dihydroxy-6-methyl-3,10-dimethylene-3a,4,7,8,9,10,11,11a-	C15H20O4
7	4.836	9466202	23.95	24611226	1.1	1-Dodecene	C12H24	51	11.952	405834	1.03	2485042	0.11	Hexadecadienoic acid, methyl ester	C17H30O2
8	4.941	14277459	36.12	30945245	1.38	Dodecane	C12H26	52	12.042	5016256	12.69	11671362	0.52	7-Methyl-Z-tetradecen-1-ol acetate	C17H32O2
9	5.128	942482	2.38	3346074	0.15	17-Octadecynoic acid	C18H32O2	53	12.296	3767379	9.53	16770629	0.75	7-Methyl-Z-tetradecen-1-ol acetate	C17H32O2
10	5.398	308712	0.78	1495011	0.07	9-Octadecynoic acid	C18H32O2	54	12.483	1392595	3.52	4205660	0.19	01297107001 TETRANEURIN - A -	C15H20O5
11	5.525	963595	2.44	3440883	0.15	4,9-Decadienoic acid, 2-nitro-, ethyl ester	C12H19NO4	55	13.082	3176272	8.04	9483997	0.42	01297107001 TETRANEURIN - A - DIOL	C15H20O5
12	5.794	1397418	3.54	5070706	0.23	1,2-Epoxy-5,9-cyclododecadiene	C12H18O	56	13.388	15599279	39.47	28961411	1.29	2-Heptadecanone	C17H34O
13	5.906	1269965	3.21	4220412	0.19	2,5-Octadecadiynoic acid, methyl ester	C19H30O2	57	13.59	1339933	3.39	2644622	0.12	01297107001 TETRANEURIN - A -	C15H20O5
14	6.183	14861630	37.6	38907147	1.74	6-Tridecene, (Z)-	C13H26	58	13.777	497645	1.26	1349217	0.06	01297107001 TETRANEURIN - A -	C15H20O5
15	6.295	20284027	51.32	44888001	2.01	Tridecane	C13H28	59	13.867	1050433	2.66	2059661	0.09	01297107001 TETRANEURIN - A -	C15H20O5
16	6.475	666835	1.69	2172144	0.1	17-Octadecynoic acid	C18H32O2	60	14.496	39523778	100	629266522	28.12	Hexadecanoic acid	C16H32O2
17	6.602	511419	1.29	2211041	0.1	2,5-Octadecadiynoic acid, methyl ester	C19H30O2	61	15.139	3814220	9.65	11199569	0.5	Oleic Acid	C18H34O2
18	6.789	544525	1.38	2266695	0.1	1,2-Epoxy-5,9-cyclododecadiene	C12H18O	62	15.349	3734652	9.45	8213092	0.37	Oleic Acid	C18H34O2
19	6.901	1931790	4.89	4948083	0.22	Oxacyclotetradecan-2-one	C13H24O2	63	16.037	29562788	74.8	305035572	13.63	Oleic Acid	C18H34O2
20	6.999	1428478	3.61	3742776	0.17	1,2-Epoxy-5,9-cyclododecadiene	C12H18O	64	16.665	10169579	25.73	23629977	1.06	Oleic Acid	C18H34O2
21	7.163	1392597	3.52	3620865	0.16	2,5-Octadecadiynoic acid, methyl ester	C19H30O2	65	16.912	6460391	16.35	30643629	1.37	Oleic Acid	C18H34O2
22	7.522	25382814	64.22	68549783	3.06	1-Tetradecanol	C14H30O	66	17.032	2129535	5.39	4619672	0.21	((3aS,6S,6aR,9aS,9bR)-6a-hydroxy-6-methyl-3-methylene-2,9-	C19H26O6
23	7.627	22624218	57.24	48283610	2.16	Tetradecane	C14H30	67	17.496	1508434	3.82	5749018	0.26	((3aS,6S,6aR,9aS,9bR)-6a-hydroxy-6-methyl-3-methylene-2,9-	C19H26O6
24	7.754	5988645	15.15	15186169	0.68	Decanoic acid	C10H20O2	68	17.698	26793575	67.79	143698109	6.42	n-Tetracosanol-1	C24H50O
25	8.069	713707	1.81	2032073	0.09	2,5-Octadecadiynoic acid, methyl ester	C19H30O2	69	17.863	1885828	4.77	2261994	0.1	ISOCHIAPIN B	C19H22O6
26	8.248	4514293	11.42	8327603	0.37	Z-10-Tetradecen-1-ol acetate	C16H30O2	70	18.124	2599432	6.58	6661508	0.3	ISOCHIAPIN B	C19H22O6
27	8.33	3277728	8.29	6185293	0.28	17-Octadecynoic acid	C18H32O2	71	18.312	1661896	4.2	5996338	0.27	((3aS,6S,6aR,9aS,9bR)-6a-hydroxy-6-methyl-3-methylene-2,9-	C19H26O6
28	8.503	2950888	7.47	6409139	0.29	17-Octadecynoic acid	C18H32O2	72	18.536	7068611	17.88	23275028	1.04	((3aS,6S,6aR,9aS,9bR)-6a-hydroxy-6-methyl-3-methylene-2,9-	C19H26O6
29	8.705	2017712	5.11	5708199	0.26	Thiosulfuric acid (H2S2O3), S-(2-aminoethyl) ester	C2H7NO3S2	73	18.648	614636	1.56	1494781	0.07	ISOCHIAPIN B	C19H22O6
30	8.794	11673017	29.53	32598829	1.46	1-Pentadecene	C15H30	74	19.075	6971300	17.64	14100840	0.63	Z,E-2,13-Octadecadien-1-ol	C18H34O
31	8.944	38773294	98.1	140171264	6.26	Pentadecane	C15H32	75	19.314	10519750	26.62	34555481	1.54	17-Pentatriacontene	C35H70
32	9.071	923670	2.34	1547791	0.07	NEROLIDOL-EPOXYACETATE	C17H28O4	76	19.404	832935	2.11	1513927	0.07	((3aS,6S,6aR,9aS,9bR)-6a-hydroxy-	C19H26O6
33	9.146	1232086	3.12	3569645	0.16	ETHYL (9Z,12Z)-9,12-	C20H36O2	77	20.047	8517710	21.55	18116859	0.81	((3aS,6S,6aR,9aS,9bR)-6a-hydroxy-	C19H26O6
34	9.251	2448043	6.19	4539728	0.2	17-Octadecynoic acid	C18H32O2	78	20.638	631365	1.6	1412747	0.06	Hahnfett (stopcock grease)	
35	9.363	700236	1.77	1791998	0.08	3H-Cyclodeca[b]furan-2-one, 4,9-dihydroxy-6-methyl-3,10-dimethylene-	C15H20O4	79	20.766	2645699	6.69	6376253	0.28	Hahnfett (stopcock grease)	
36	9.543	6105475	15.45	10835002	0.48	17-Octadecynoic acid	C18H32O2	80	21.334	993570	2.51	3601488	0.16	Hahnfett (stopcock grease)	
37	9.782	9402845	23.79	44008936	1.97	17-Octadecynoic acid	C18H32O2	81	21.461	2204663	5.58	4176695	0.19	4H-1-Benzopyran-4-one, 2-(3,4-	C27H30O16
38	9.999	13977784	35.37	26830786	1.2	Cyclohexadecane	C16H32	82	22.015	5035122	12.74	20072134	0.9	Hahnfett (stopcock grease)	
39	10.089	12018797	30.41	22210580	0.99	1,1-DIDEUTERIO-HEXADECANYL	C17H34D2O3S	83	22.853	1464545	3.71	2922157	0.13	4H-1-Benzopyran-4-one, 2-(3,4-	C27H30O16
40	10.208	1122231	2.84	3158005	0.14	3H-Cyclodeca[b]furan-2-one, 4,9-dihydroxy-6-methyl-3,10-dimethylene-	C15H20O4	84	23.354	877799	2.22	3161245	0.14	Hahnfett (stopcock grease)	
41	10.388	2751871	6.96	5358209	0.24	17-Octadecynoic acid	C18H32O2	85	24.649	10717142	27.12	30939471	1.38	16-Hentriacontanone	C31H62O
42	10.463	816795	2.07	1566876	0.07	3H-Cyclodeca[b]furan-2-one, 4,9-dihydroxy-6-methyl-3,10-dimethylene-	C15H20O4	86	26.452	350207	0.89	1588528	0.07	03027205002 FLAVONE 4'-OH,5-OH,7-DI-O-GLUCOSIDE	C27H30O15
43	10.613	1275823	3.23	4069246	0.18	3H-Cyclodeca[b]furan-2-one, 4,9-dihydroxy-6-methyl-3,10-dimethylene-	C15H20O4	87	26.826	2032375	5.14	13493153	0.6	Hahnfett (stopcock grease)	
44	10.844	2438375	6.17	3210401	0.14	9-Hexadecenoic acid	C16H30O2	88	27.051	1910086	4.83	8487142	0.38	18-Pentatriacontanone	C35H70O

Figure B-1

Chromatogram profile from GC-MS analysis of WCO

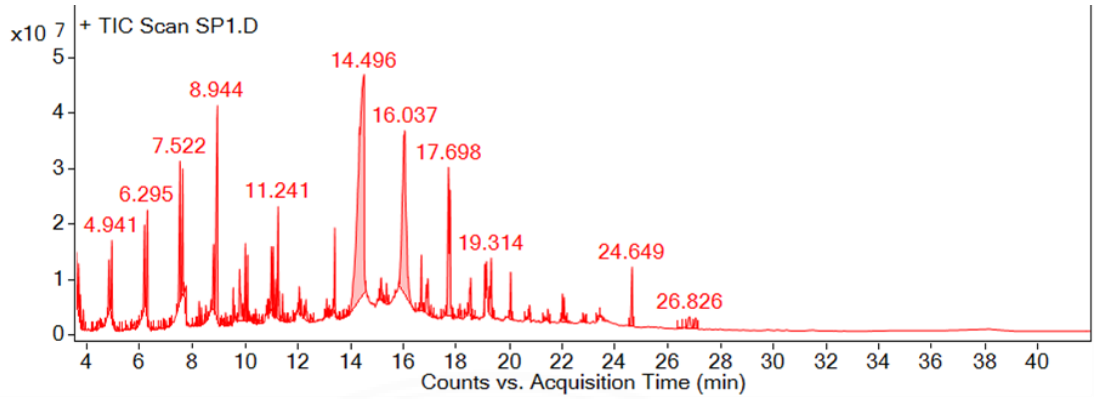

Table B-2

Chromatogram peak list from GC-MS analysis of bio-oil obtained from WCO pyrolysis at processes temperature 400 °C with 1:40 AC:WCO ratio

No	RT	Height	Height %	Area	Area Sum %	Name	Formula	No	RT	Height	Height %	Area	Area Sum %	Name	Formula
1	3.692	8771652	22.1	4E+07	1.62	1-Decanol, 2-methyl-	C11H24O	47	11.002	15204467	38.31	63008138	2.86	cis-9-Hexadecenal	C16H30O
2	3.864	4140380	10.43	9E+06	0.42	2,4-Pentadien-1-ol, 3-pentyl-, (ZZ)-	C10H18O	48	11.151	6253727	15.76	10938543	0.5	Z-8-Methyl-9-tetradecenoic acid	C15H28O2
3	4.051	551885	1.39	2E+06	0.09	1,12-Tridecadiene	C13H24	49	11.248	19315492	48.67	44279435	2.01	Tetradecane, 2,6,10-trimethyl-	C17H36
4	4.215	483167	1.22	2E+06	0.09	7-Oxabicyclo[4.1.0]heptane, 1-methyl-4-(2-methyloxiranyl)-	C10H16O2	50	11.413	5192926	13.09	10594068	0.48	9-Octadecenoic acid (Z)-	C18H34O2
5	4.32	683345	1.72	2E+06	0.09	Tricyclo[5.2.1.0(1,5)]decane-8,9-diol	C10H16O2	51	11.712	962250	2.42	3086862	0.14	3H-Cyclodeca[b]furan-2-one, 4,9-dihydroxy-6-methyl-	C15H20O4
6	4.44	1740663	4.39	8E+06	0.34	5,7-Dodecadiyn-1,12-diol	C12H18O2	52	11.989	1089498	2.75	4893046	0.22	9-Octadecenoic acid (Z)-	C18H34O2
7	4.604	834363	2.1	2E+06	0.07	1,4-Naphthalenediol, 1,2,3,4,4a,5,8,8a-octahydro-,	C10H16O2	53	12.056	5837988	14.71	10322478	0.47	7-Methyl-Z-tetradecen-1-ol acetate	C17H32O2
8	4.836	9373672	23.62	2E+07	1.11	1-Dodecene	C12H24	54	12.229	1881107	4.74	2705840	0.12	9-Octadecenoic acid (Z)-	C18H34O2
9	4.949	13601952	34.27	4E+07	1.63	Dodecane	C12H26	55	12.303	2549204	6.42	5588818	0.25	7-Methyl-Z-tetradecen-1-ol acetate	C17H32O2
10	5.128	966180	2.43	4E+06	0.17	10-Undecenoyl chloride	C11H19ClO	56	12.49	1503882	3.79	5350963	0.24	01297107001 TETRANEURIN - A - DIOL	C15H20O5
11	5.405	282603	0.71	2E+06	0.07	9-Octadecynoic acid	C18H32O2	57	13.022	1123389	2.83	1934224	0.09	9-Octadecenoic acid (Z)-	C18H34O2
12	5.525	957099	2.41	4E+06	0.16	4,9-Decadienoic acid, 2-nitro-, ethyl ester	C12H19NO4	58	13.089	2698722	6.8	3908131	0.18	7-Methyl-Z-tetradecen-1-ol acetate	C17H32O2
13	5.801	1515061	3.82	6E+06	0.28	1,2-Epoxy-5,9-cyclododecadiene	C12H18O	59	13.396	14711105	37.07	28057738	1.27	2-Heptadecanone	C17H34O
14	5.914	1074045	2.71	3E+06	0.15	2,5-Octadecadiynoic acid, methyl ester	C19H30O2	60	13.515	643358	1.62	1407740	0.06	01297107001 TETRANEURIN - A - DIOL	C15H20O5
15	6.183	16056331	40.46	4E+07	1.88	6-Tridecene, (Z)-	C13H26	61	13.875	992081	2.5	1904866	0.09	01297107001 TETRANEURIN - A - DIOL	C15H20O5
16	6.303	23592320	59.45	5E+07	2.23	Tridecane	C13H28	62	14.488	36224257	91.28	466463247	21.15	Hexadecanoic acid	C16H32O2
17	6.475	552565	1.39	2E+06	0.07	17-Octadecynoic acid	C18H32O2	63	15.087	4811322	12.12	25704943	1.17	Hexadecanoic acid, 2,3-dihydroxypropyl ester	C19H38O4
18	6.61	456670	1.15	2E+06	0.07	2,5-Octadecadiynoic acid, methyl ester	C19H30O2	64	15.356	3099171	7.81	7634538	0.35	Oleic Acid	C18H34O2
19	6.797	548663	1.38	3E+06	0.12	17-Octadecynoic acid	C18H32O2	65	16.059	31208036	78.64	309182998	14.02	Oleic Acid	C18H34O2
20	6.909	1820063	4.59	5E+06	0.22	17-Octadecynoic acid	C18H32O2	66	16.673	8919295	22.48	21404594	0.97	Oleic Acid	C18H34O2
21	7.006	1313252	3.31	4E+06	0.17	1,2-Epoxy-5,9-cyclododecadiene	C12H18O	67	16.86	4914298	12.38	23165407	1.05	Oleic Acid	C18H34O2
22	7.171	1556786	3.92	4E+06	0.18	2,5-Octadecadiynoic acid, methyl ester	C19H30O2	68	17.032	1062165	2.68	2344801	0.11	01297107001 TETRANEURIN - A - DIOL	C15H20O5
23	7.53	25557834	64.4	7E+07	3.14	1-Tetradecanol	C14H30O	69	17.503	1169115	2.95	5052291	0.23	ISOCHIAPIN B	C19H22O6
24	7.635	23588477	59.44	5E+07	2.29	Tetradecane	C14H30	70	17.705	29275720	73.77	146927909	6.66	n-Tetracosanol-1	C24H50O
25	7.844	7570774	19.08	3E+07	1.52	Decanoic acid	C10H20O2	71	18.132	2167844	5.46	5401327	0.24	ISOCHIAPIN B	C19H22O6
26	8.076	729695	1.84	1E+06	0.06	Thiosulfuric acid (H2S2O3), S-(2-aminoethyl) ester	C2H7NO3S2	72	18.319	1312236	3.31	4930403	0.22	Octadecanal, 2-bromo-	C18H35BrO
27	8.256	4702145	11.85	8E+06	0.37	Z-10-Tetradecen-1-ol acetate	C16H30O2	73	18.499	5370325	13.53	27210589	1.23	Octadecanal, 2-bromo-	C18H35BrO
28	8.338	3556483	8.96	7E+06	0.32	17-Octadecynoic acid	C18H32O2	74	18.656	495585	1.25	1654196	0.08	ISOCHIAPIN B	C19H22O6
29	8.443	693394	1.75	1E+06	0.05	trans-Traumatic acid	C12H20O4	75	19.142	12302549	31	61686822	2.8	11-Hexacosyne	C26H50
30	8.517	2427130	6.12	5E+06	0.22	17-Octadecynoic acid	C18H32O2	76	19.314	8611388	21.7	30618073	1.39	1-Hexacosene	C26H52
31	8.802	12639730	31.85	5E+07	2.15	1-Pentadecene	C15H30	77	19.404	717053	1.81	1696673	0.08	ISOCHIAPIN B	C19H22O6
32	8.951	39685385	100	2E+08	6.82	Pentadecane	C15H32	78	19.86	671619	1.69	2822681	0.13	14-.BETA.-H-PREGNA	C21H36
33	9.086	996433	2.51	2E+06	0.07	9-Octadecenoic acid (Z)-	C18H34O2	79	20.055	7782247	19.61	15051711	0.68	ISOCHIAPIN B	C19H22O6
34	9.161	1051593	2.65	3E+06	0.14	17-Octadecynoic acid	C18H32O2	80	20.646	628612	1.58	1365532	0.06	Hahnfett (stopcock grease)	
35	9.258	2636565	6.64	5E+06	0.21	17-Octadecynoic acid	C18H32O2	81	20.766	1985064	5	5510790	0.25	Hahnfett (stopcock grease)	
36	9.37	660103	1.66	2E+06	0.07	(all-Z)-methyl 5,8,11,14-eicosa-tetraen-oic acid, methyl	C21H34O2	82	21.342	899902	2.27	3391278	0.15	Hahnfett (stopcock grease)	
37	9.453	581764	1.47	1E+06	0.07	(all-Z)-methyl 5,8,11,14-eicosa-tetraen-oic acid, methyl	C21H34O2	83	21.469	1774376	4.47	3302170	0.15	4H-1-Benzopyran-4-one, 2-(3,4-dihydroxyphenyl)-6,8-	C27H30O16
38	9.55	6645645	16.75	1E+07	0.46	n-Nonylcyclohexane	C15H30	84	22.023	4809645	12.12	17516470	0.79	Hahnfett (stopcock grease)	
39	9.789	8752516	22.05	4E+07	1.78	17-Octadecynoic acid	C18H32O2	85	22.861	1463006	3.69	3008801	0.14	4H-1-Benzopyran-4-one, 2-(3,4-dihydroxyphenyl)-6,8-	C27H30O16
40	10.014	13982025	35.23	3E+07	1.21	Cyclohexadecane	C16H32	86	23.354	1110100	2.8	3454934	0.16	Hahnfett (stopcock grease)	
41	10.096	11522588	29.03	2E+07	0.83	Hexadecane	C16H34	87	24.649	8590652	21.65	25809713	1.17	16-Hentriacontanone	C31H62O
42	10.216	1481973	3.73	4E+06	0.2	9-Octadecenoic acid (Z)-	C18H34O2	88	26.467	382037	0.96	1761357	0.08	03027205002 FLAVONE 4'-OH,5-OH,7-DI-O-GLUCOSIDE	C27H30O15
43	10.403	3017677	7.6	5E+06	0.23	17-Octadecynoic acid	C18H32O2	89	26.834	3015282	7.6	19583530	0.89	Hahnfett (stopcock grease)	
44	10.47	972355	2.45	2E+06	0.09	13-Heptadecyn-1-ol	C17H32O	90	27.066	2266147	5.71	9194150	0.42	Hexadecanoic acid, 2-(octadecyloxy)ethyl ester	C36H72O3
45	10.627	1156179	2.91	4E+06	0.19	3H-Cyclodeca[b]furan-2-one, 4,9-dihydroxy-6-methyl-3,10-	C15H20O4	91	28.001	212960	0.54	988001	0.04	03027205002 FLAVONE 4'-OH,5-OH,7-DI-O-GLUCOSIDE	C27H30O15
46	10.844	2399551	6.05	8E+06	0.35	9-Octadecenoic acid (Z)-	C18H34O2	92	29.789	201437	0.51	1687777	0.08	4H-1-Benzopyran-4-one, 2-(3,4-dihydroxyphenyl)-6,8-	C27H30O16

Figure B-2

Chromatogram profile from GC-MS analysis of bio-oil obtained from WCO pyrolysis at processes temperature 400 °C with 1:40 AC:WCO ratio

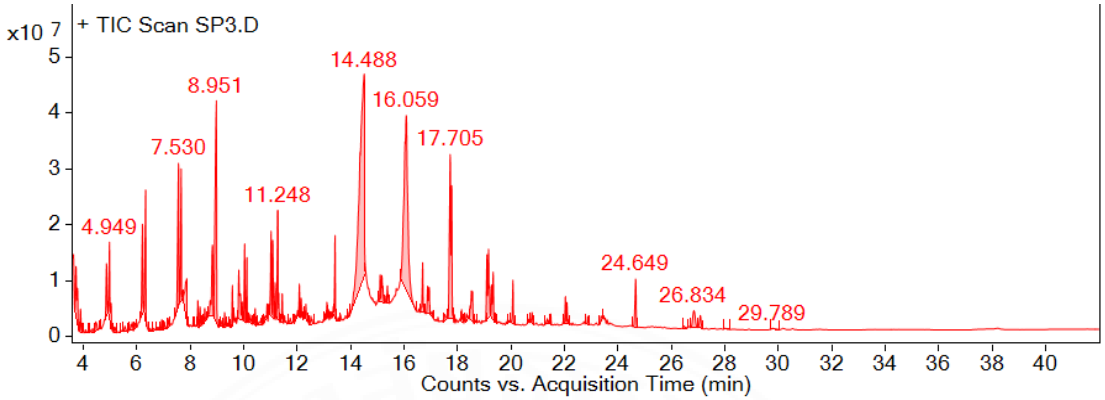

Figure B-3

TGA and DTG curves of WCO

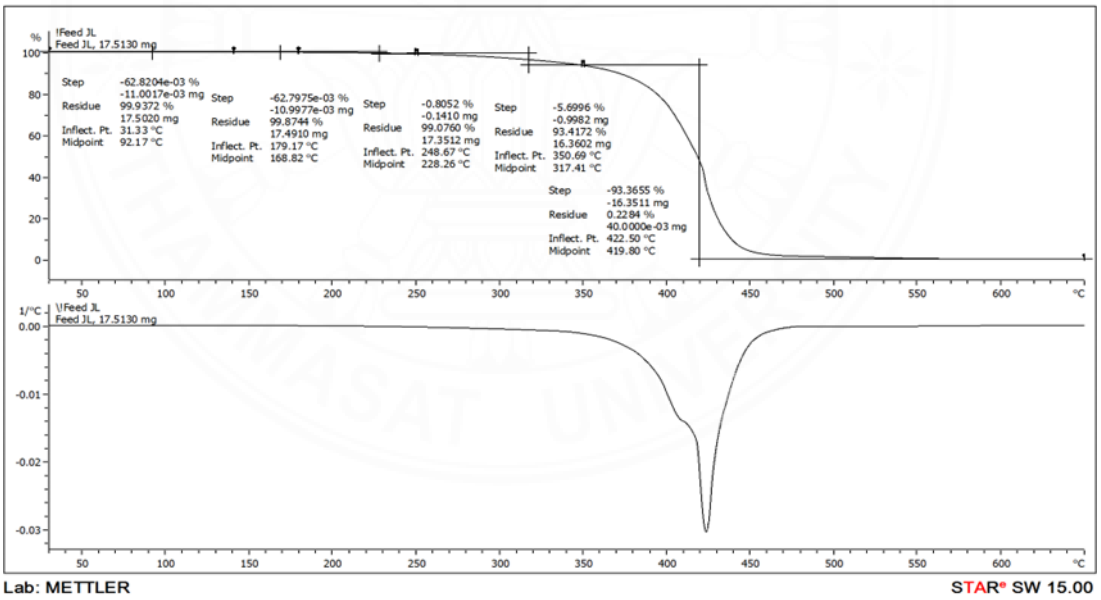

Figure B-4

Simulated distillation profile of liquid bio-oil obtained from pyrolysis of WCO at 350 °C without AC

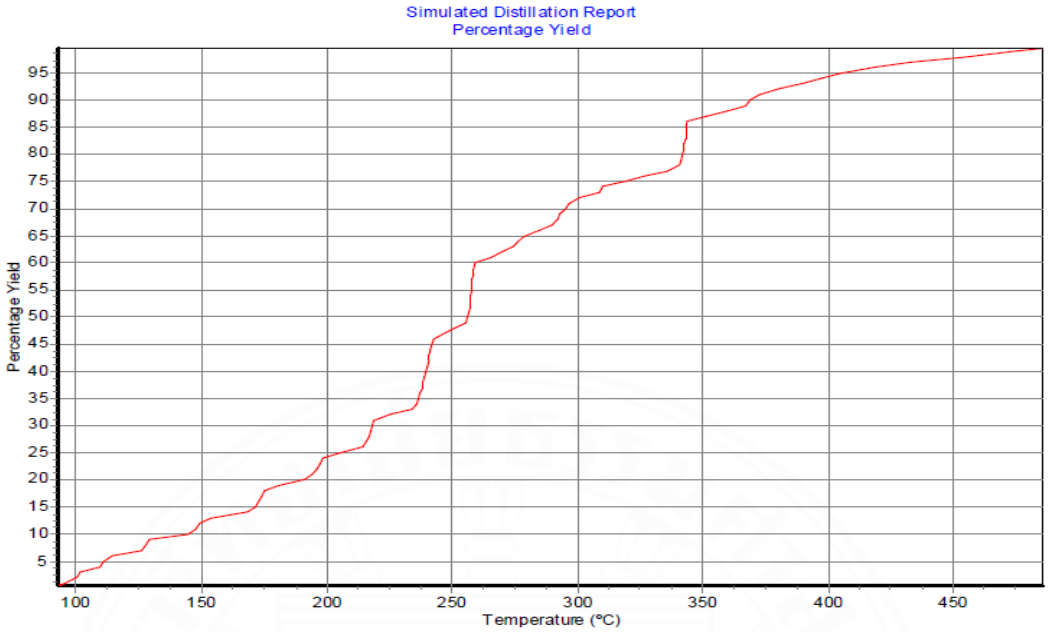

Figure B-5

Simulated distillation profile of liquid bio-oil obtained from pyrolysis of WCO at 350 °C with 1:40 AC:WCO ratio

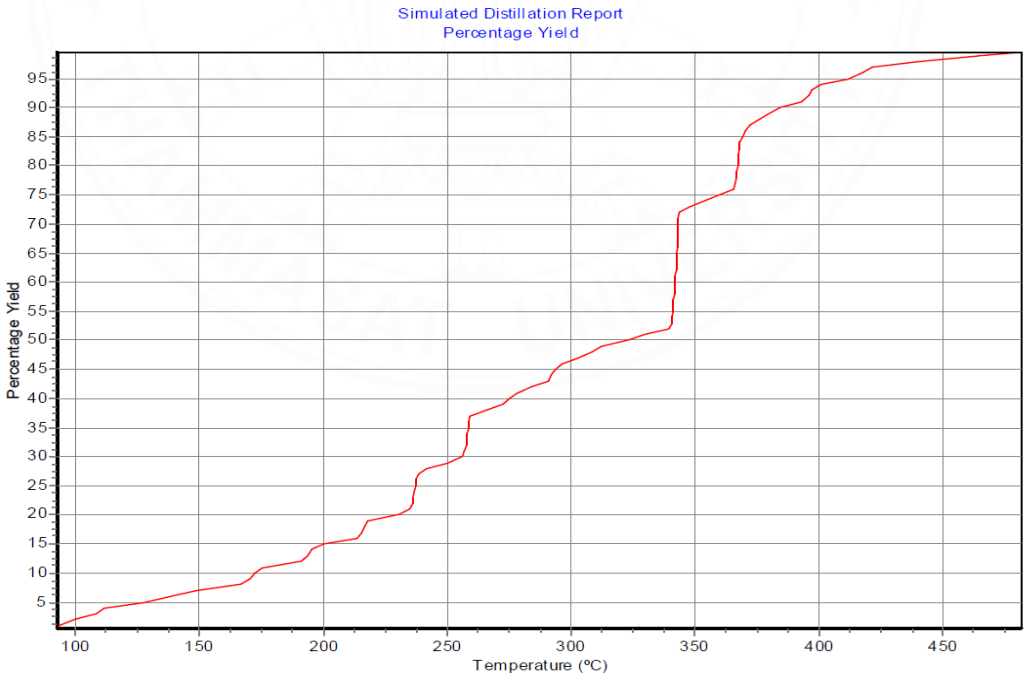

Figure B-6

Simulated distillation profile of liquid bio-oil obtained from pyrolysis of WCO at 350 °C with 1:30 AC:WCO ratio

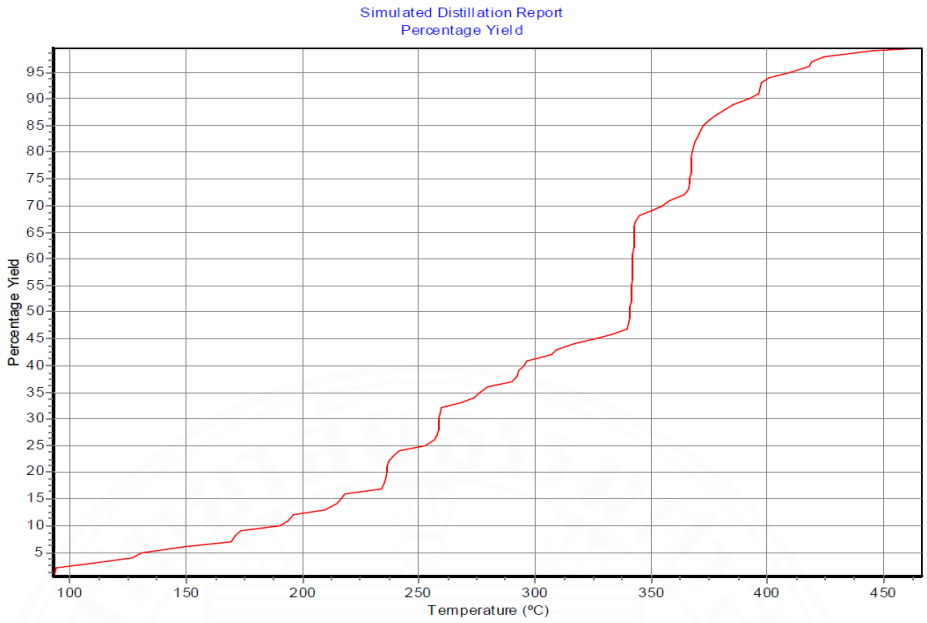

Figure B-7

Simulated distillation profile of liquid bio-oil obtained from pyrolysis of WCO at 350 °C with 1:20 AC:WCO ratio

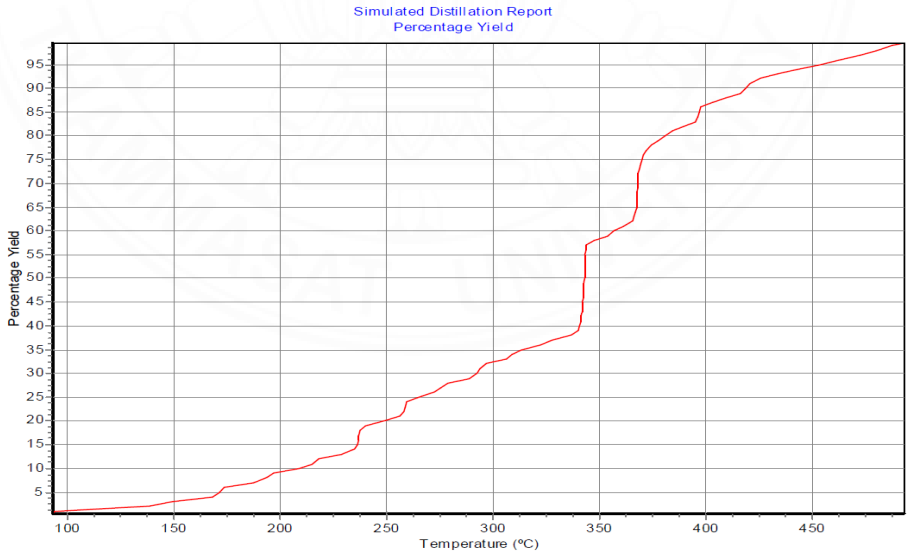

Figure B-8

Simulated distillation profile of liquid bio-oil obtained from pyrolysis of WCO at 400 °C without AC

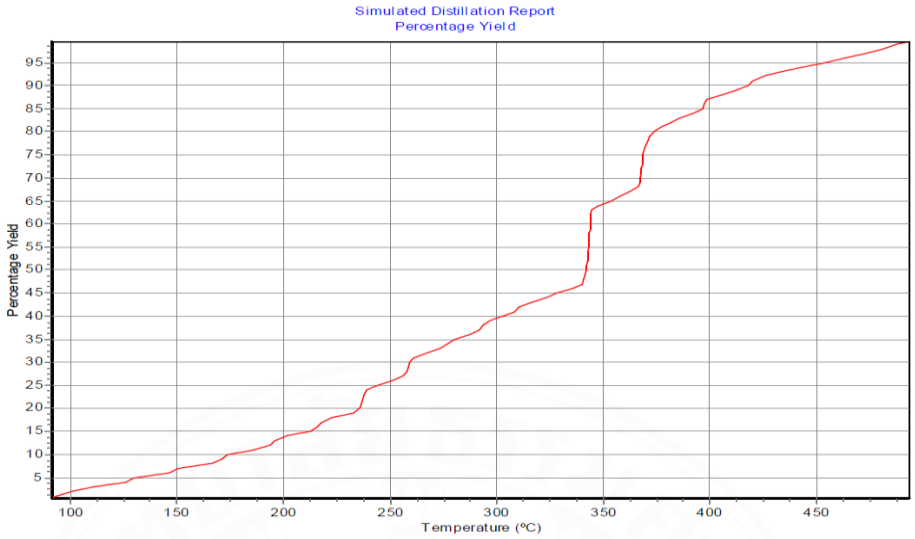

Figure B-9

Simulated distillation profile of liquid bio-oil obtained from pyrolysis of WCO at 400 °C with 1:40 AC:WCO ratio

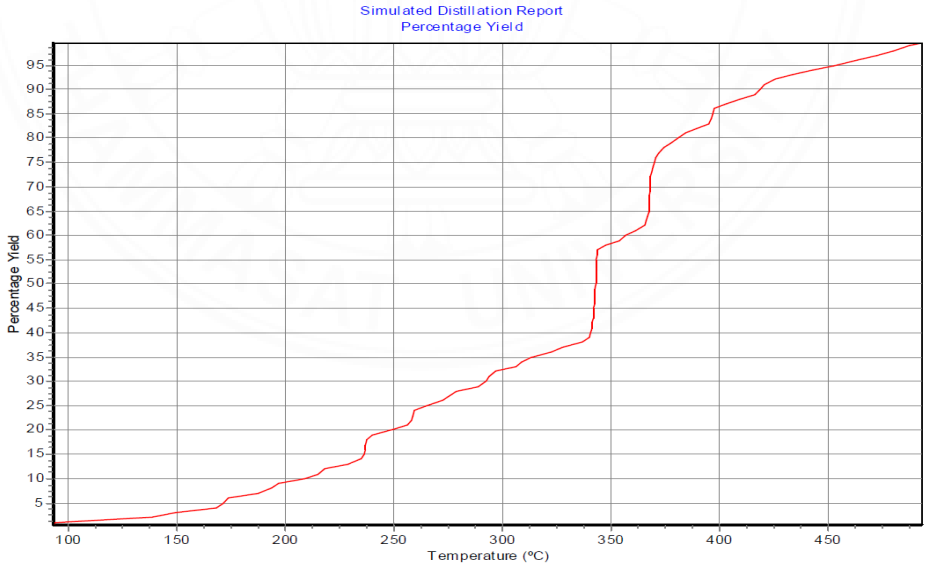

Figure B-10

Simulated distillation profile of liquid bio-oil obtained from pyrolysis of WCO at 400 °C with 1:30 AC:WCO ratio

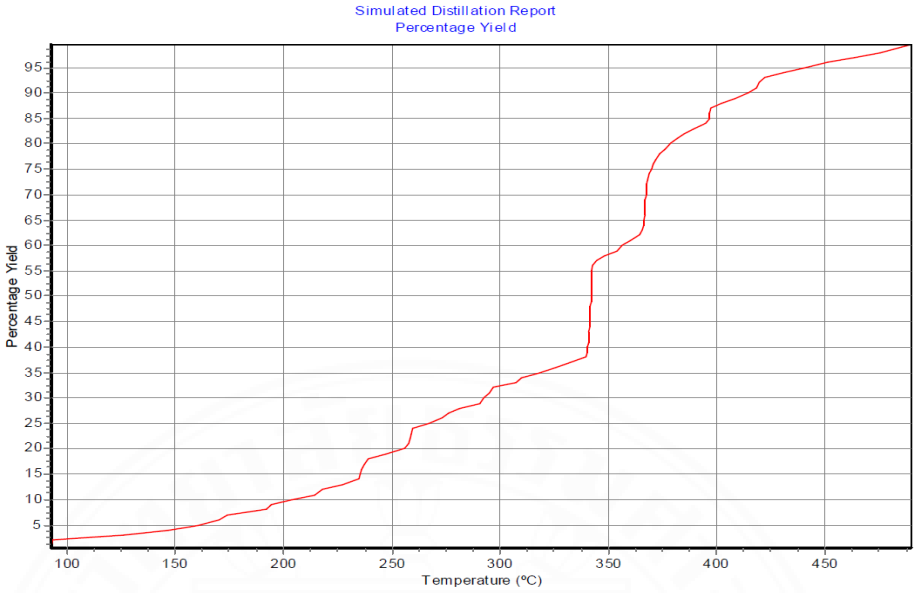

Figure B-11

Simulated distillation profile of liquid bio-oil obtained from pyrolysis of WCO at 400 °C with 1:20 AC:WCO ratio

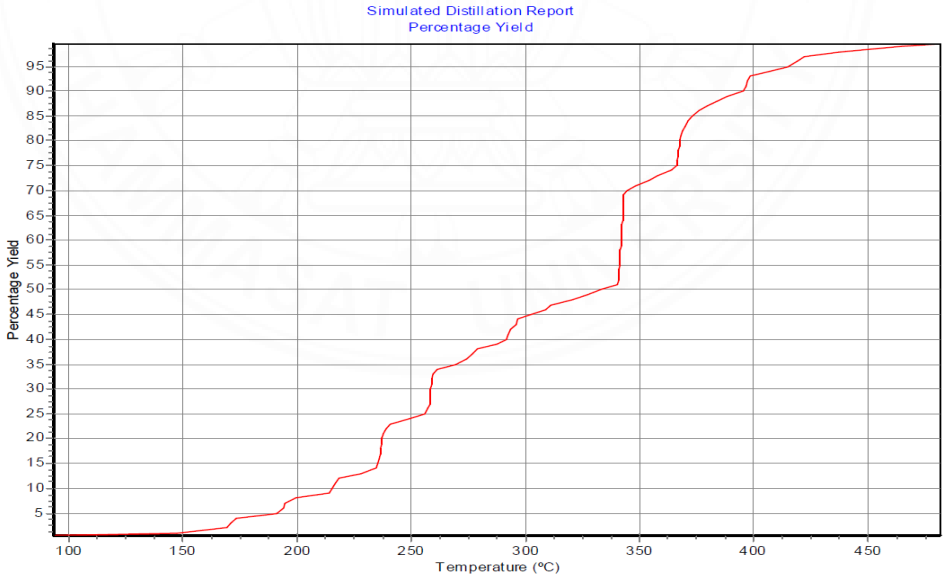

BIOGRAPHY

Name Warintorn Banchapattanasakda

Educational Attainment	Academic Year 2007: Bachelor of Engineering in Civil Engineering, Thammasat University, Thailand. Academic Year 2010: Master of Engineering in Environmental Engineering, Prince of Songkla University, Thailand. Academic Year 2011: Master of Public Administration in Management for Executive, The Graduate School of Public Administration, The National Institute of Development Administration (NIDA), Thailand.
Scholarship	Thammasat School of Engineering (TSE) Research Grant

Publications

Banchapattanasakda, W., Asavatesanupap, C., & Santikunaporn, M. (2023). Conversion of waste cooking oil into Bio-fuel via pyrolysis using activated carbon as a catalyst. *Molecules*, 28, 3590.

Banchapattanasakda, & Santikunaporn, M. (2017). Palladium Membrane for Hydrogen Separation from gas mixture [Scholarly Article]. Thai Science and Technology Journal., 25(2), 350-360.